

Dissertation zur Erlangung des Doktorgrades  
der Fakultät für Chemie und Pharmazie  
der Ludwig-Maximilians-Universität München

**Investigations on the Molecular Mechanisms of EGFR  
Signal Transactivation in Human Cancer**

vorgelegt von

Andreas Gschwind  
aus  
Straubing

2003

## Erklärung

Diese Dissertation wurde im Sinne von § 13 Abs. 3 bzw. 4 der Promotionsordnung vom 29. Januar 1998 von Herrn Prof. Dr. Horst Domdey betreut.

## Ehrenwörtliche Versicherung

Diese Dissertation wurde selbständig, ohne unerlaubte Hilfe erarbeitet.

München, den 24.02.2003

Andreas Gschwind

Dissertation eingereicht am

28.02.2003

1. Gutachter

Prof. Dr. Axel Ullrich

2. Gutachter

Prof. Dr. Horst Domdey

Mündliche Prüfung am

01.04.2003

**for my Mum and Dad**

**“The most incomprehensible thing about the world is its comprehensibility.”**

Albert Einstein

# CONTENTS

<b>1</b>	<b>INTRODUCTION</b>	<b>1</b>
<b>1.1</b>	<b>Protein tyrosine kinases</b>	<b>2</b>
1.1.1	Receptor tyrosine kinases	2
1.1.2	EGF-like ligands	3
1.1.3	Ligand-induced activation of receptor tyrosine kinases	4
1.1.4	Cytoplasmic tyrosine kinases	4
1.1.5	Recruitment of downstream signaling molecules	5
<b>1.2</b>	<b>MAP kinase pathways</b>	<b>7</b>
<b>1.3</b>	<b>G protein-coupled receptors</b>	<b>8</b>
<b>1.4</b>	<b>EGFR signal transactivation</b>	<b>10</b>
<b>1.5</b>	<b>Metalloproteases</b>	<b>14</b>
1.5.1	ADAMs	15
1.5.2	MMPs	17
<b>1.6</b>	<b>Molecular oncology</b>	<b>17</b>
<b>1.7</b>	<b>Aim of the study</b>	<b>18</b>
<b>2</b>	<b>MATERIALS AND METHODS</b>	<b>20</b>
<b>2.1</b>	<b>Materials</b>	<b>20</b>
2.1.1	Laboratory chemicals and biochemicals	20
2.1.2	Enzymes	21
2.1.3	Radiochemicals	21
2.1.4	„Kits" and other materials	21

2.1.5	Growth factors and ligands	22
2.1.6	Media and buffers	22
2.1.7	Cell culture media	22
2.1.8	Stock solutions for buffers	23
2.1.9	Bacterial strains, cell lines and antibodies	24
2.1.9.1	<i>E.coli strains</i>	24
2.1.9.2	<i>Cell lines</i>	24
2.1.9.3	<i>Antibodies</i>	25
2.1.10	Plasmids and oligonucleotides	27
2.1.10.1	<i>Primary vectors</i>	27
2.1.10.2	<i>Constructs</i>	27
2.1.10.3	<i>Important oligonucleotides</i>	29
<b>2.2</b>	<b>Methods in molecular biology</b>	<b>30</b>
2.2.1	Plasmid preparation for analytical purpose	30
2.2.2	Plasmid preparation in preparative scale	30
2.2.3	Enzymatic manipulation of DNA	30
2.2.3.1	<i>Digestion of DNA samples with restriction endonucleases</i>	30
2.2.3.2	<i>Dephosphorylation of DNA 5'-termini with calf intestine alkaline phosphatase (CIAP)</i>	30
2.2.3.3	<i>DNA insert ligation into vector DNA</i>	30
2.2.3.4	<i>Agarose gel electrophoresis</i>	31
2.2.3.5	<i>Isolation of DNA fragments using low melting temperature agarose gels</i>	31
2.2.4	Introduction of plasmid DNA into <i>E.coli</i> cells	31
2.2.4.1	<i>Preparation of competent cells</i>	31
2.2.4.2	<i>Transformation of competent cells</i>	31
2.2.5	Oligonucleotide-directed mutagenesis	31
2.2.5.1	<i>Preparation of uracil-containing, single-stranded DNA template</i>	31
2.2.5.2	<i>Primer extension</i>	32
2.2.6	Enzymatic amplification of DNA by polymerase chain reaction	32
2.2.7	DNA sequencing	33

2.2.8	cDNA array hybridization	33
<b>2.3</b>	<b>Methods in mammalian cell culture</b>	<b>33</b>
2.3.1	General cell culture techniques	33
2.3.2	Transfection of cultured cell lines	34
2.3.2.1	<i>Transfection of cells with calcium phosphate</i>	34
2.3.2.2	<i>Transfection of COS-7 cells using lipofectamine®</i>	34
2.3.3	Retroviral gene transfer in cell lines	34
<b>2.4</b>	<b>Protein analytical methods</b>	<b>35</b>
2.4.1	Lysis of cells with triton X-100	35
2.4.2	Determination of protein concentration in cell lysates	35
2.4.3	Immunoprecipitation and <i>in vitro</i> association with fusion proteins	35
2.4.4	TCA precipitation of proteins in conditioned medium	35
2.4.5	Radiolabeling	35
2.4.6	SDS-polyacrylamide-gel electrophoresis (SDS-PAGE)	35
2.4.7	Transfer of proteins on nitrocellulose membranes	36
2.4.8	Immunoblot detection	36
<b>2.5</b>	<b>Biochemical and cell biological assays</b>	<b>36</b>
2.5.1	Stimulation of cells	36
2.5.2	ERK1/2 and Akt/PKB phosphorylation	36
2.5.3	ERK/MAPK activity	36
2.5.4	Gelatin zymography	37
2.5.5	Flow cytometric analysis of cell surface proteins	37
2.5.6	AR sandwich-ELISA	37
2.5.7	Incorporation of <sup>3</sup> H-thymidine into DNA	38
2.5.8	Distribution of cell cycle phases	38
2.5.9	<i>In vitro</i> wound closure	38
2.5.10	Migration	38
<b>2.6</b>	<b>Statistical analysis</b>	<b>38</b>

<b>3</b>	<b>RESULTS</b>	<b>39</b>
<b>3.1</b>	<b>GPCR agonists stimulate EGFR tyrosine phosphorylation via a metalloprotease-dependent pathway in HNSCC.</b>	<b>39</b>
<b>3.2</b>	<b>Transactivation of HER2/neu is dependent on metalloprotease function and EGFR tyrosine kinase activity.</b>	<b>43</b>
<b>3.3</b>	<b>EGFR association and tyrosine phosphorylation of SHC and Gab1 upon LPA treatment is metalloprotease-dependent.</b>	<b>44</b>
<b>3.4</b>	<b>Activation of the ERK/MAPK pathway by LPA requires both EGFR function and metalloprotease activity.</b>	<b>45</b>
<b>3.5</b>	<b>Metalloprotease-dependent transactivation of the EGFR is required for LPA-induced DNA synthesis and S-phase progression.</b>	<b>48</b>
<b>3.6</b>	<b>LPA enhances HNSCC cell motility via transactivation of the EGFR.</b>	<b>51</b>
<b>3.7</b>	<b>LPA promotes cell-surface ectodomain processing and release of AR.</b>	<b>53</b>
<b>3.8</b>	<b>LPA-induced EGFR signal transactivation and downstream events depend on AR.</b>	<b>56</b>
<b>3.9</b>	<b>ProAR processing is required for ERK/MAPK activation and Akt/PKB phosphorylation in response to LPA.</b>	<b>58</b>
<b>3.10</b>	<b>AR bioactivity is involved in LPA stimulated DNA synthesis and cell motility.</b>	<b>60</b>
<b>3.11</b>	<b>TACE is required for proAR shedding and EGFR signal transactivation by LPA and carbachol in HNSCC cells.</b>	<b>61</b>

<b>3.12</b>	<b>TACE is involved in carbachol stimulated proHB-EGF shedding and EGFR signal transactivation in COS-7 cells.</b>	<b>65</b>
<b>3.13</b>	<b>The cytoplasmic domain of proHB-EGF is dispensible for carbachol and TPA stimulated proHB-EGF shedding in COS-7 cells.</b>	<b>68</b>
<b>4</b>	<b>DISCUSSION</b>	<b>70</b>
<b>4.1</b>	<b>Transactivation of the EGFR and HER2/neu by GPCR agonists involves a ligand-dependent mechanism in HNSCC cells.</b>	<b>70</b>
<b>4.2</b>	<b>Regulation of the proliferative and migratory behavior of HNSCC cells by GPCRs requires EGFR function and metalloprotease activity.</b>	<b>72</b>
<b>4.3</b>	<b>ProAR ectodomain cleavage is a prerequisite to EGFR activation by GPCR agonists in HNSCC cells.</b>	<b>73</b>
<b>4.4</b>	<b>TACE is the proAR sheddase in HNSCC cells.</b>	<b>75</b>
<b>4.4</b>	<b>TACE is involved in carbachol-induced proHB-EGF ectodomain processing in murine fibroblasts and COS-7 cells.</b>	<b>76</b>
<b>4.6</b>	<b>Perspectives</b>	<b>77</b>
<b>5</b>	<b>SUMMARY</b>	<b>80</b>
<b>6</b>	<b>REFERENCES</b>	<b>81</b>
<b>7</b>	<b>ABBREVIATIONS</b>	<b>95</b>

# 1 INTRODUCTION

One characteristic common to all organisms is the dynamic ability to coordinate complex physiological processes with environmental changes. The function of communicating with the environment is achieved through a number of pathways that receive and process signals, not only from the external environment but also from different regions within the cell. Individual pathways transmit signals along linear tracts resulting in regulation of discrete cell functions. This type of information transfer is an important part of the cellular repertoire of regulatory mechanisms. During normal embryonic development and in adult life, signaling needs to be precisely coordinated and integrated at all times. Deregulated signal transmission is now recognized as a cause of many human diseases (Hanahan and Weinberg, 2000; Shawver et al., 2002).

The sequencing effort of the Human Genome Project has revealed that up to 20% of the estimated 32,000 human genes encode proteins involved in signal transduction, including transmembrane receptors, G protein subunits, kinases, phosphatases and proteases (Blume-Jensen and Hunter, 2001). However, as increasingly larger numbers of cell signaling components and pathways are being identified, it has become apparent that these linear pathways are not free-standing entities but parts of larger networks (Downward, 2001).

The reversible phosphorylation of proteins is central to the regulation of most aspects of cell function (Cohen, 2002). Phosphorylation and dephosphorylation, catalyzed by protein kinases and protein phosphatases, can modify the function of a protein in almost every conceivable way; for example by increasing or decreasing its biological activity, by stabilizing it or marking it for destruction, by facilitating or inhibiting movement between subcellular compartments, or by initiating or disrupting protein–protein interactions. The simplicity, flexibility and reversibility of phosphorylation, coupled with the ready availability of ATP as a phosphoryl donor, explains its selection as the most general regulatory device adopted by eukaryotic cells.

There are more than 520 protein kinases and 130 protein phosphatases encoded in the human genome, exerting tight control on protein phosphorylation. Both of these enzyme categories can be subdivided into tyrosine- or serine/threonine-specific, based on their catalytic specificity. In addition, some possess dual specificity for both tyrosine and serine/threonine, and a few members of the phosphatidylinositol kinase family also exhibit protein-serine/threonine kinase activity.

## 1.1 Protein tyrosine kinases

Protein tyrosine kinases are important regulators of intracellular signal transduction pathways mediating aspects of multicellular communication and development in metazoans (Cohen, 2002). These enzymes catalyze transfer of the  $\gamma$ -phosphate of ATP to hydroxyl groups of tyrosines on target proteins. Tyrosine kinases play an important role in the control of most fundamental cellular processes including the cell cycle, migration, metabolism and survival, as well as proliferation and differentiation. There are currently more than 90 known tyrosine kinase genes in the human genome; 58 encode transmembrane receptor tyrosine kinases (RTKs) distributed into 20 subfamilies based on their structural characteristics (Fig. 1), and 32 encode cytoplasmic, non-receptor tyrosine kinases (NRTKs) in 10 subfamilies.

### 1.1.1 Receptor tyrosine kinases

RTKs are type I transmembrane proteins and contain an extracellular ligand-binding domain that is usually glycosylated (Hubbard and Till, 2000). The structural diversity of RTK ectodomains is due to the presence of one or several copies of immunoglobulin-like domains, fibronectin type III-like domains, EGF-like domains, cysteine-rich domains, or other domains (Fig. 1).

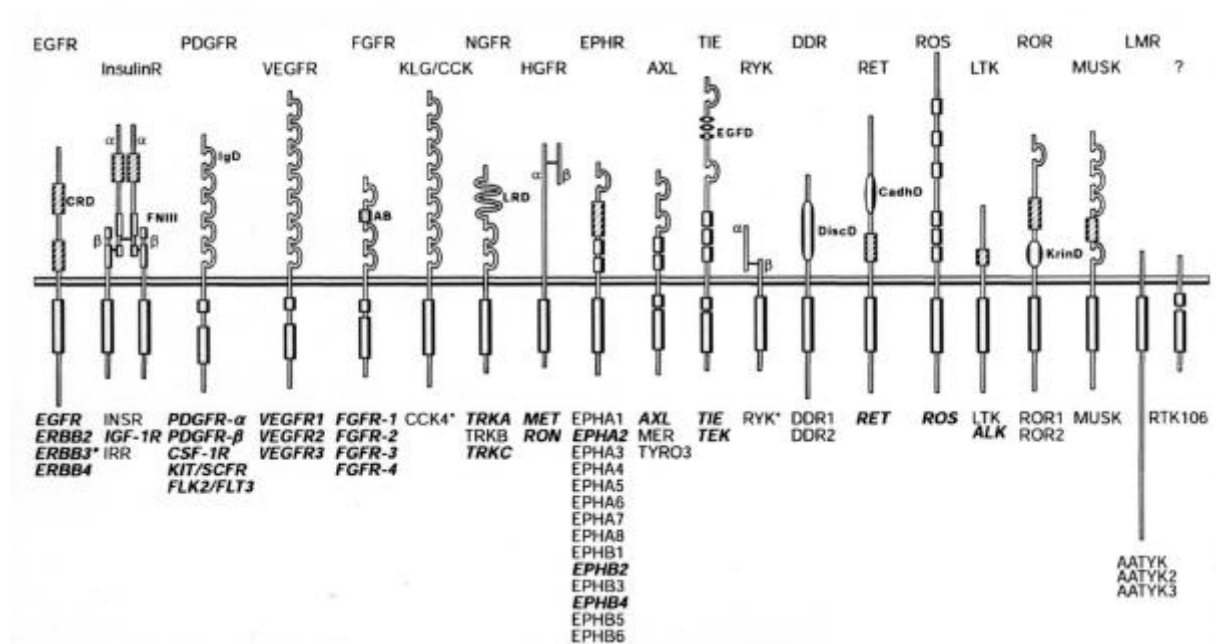


Figure 1. Subfamilies of receptor tyrosine kinases (Blume-Jensen and Hunter, 2001).

The ligand binding domain is connected to the cytoplasmic domain by a single transmembrane helix. The cytoplasmic domain contains a highly conserved protein tyrosine kinase core and additional regulatory sequences that are subjected to autophosphorylation and phosphorylation by heterologous protein kinases.

The EGFR family consists of four RTKs, EGFR, HER2/neu, HER3 which is kinase-inactive and HER4 (Ullrich and Schlessinger, 1990). The EGFR was the first cell surface signaling protein and protooncogene product to be characterized by molecular genetic methods and exemplified prototypical features of RTKs. The EGFR signaling module has been highly conserved throughout the course of evolution. The primordial signaling unit found in the nematode *Caenorhabditis elegans* consists of one receptor protein called LET-23 and a single EGF-like ligand known as LIN-3 (Yarden and Sliwkowski, 2001). In this organism, the EGFR network plays a central developmental role. A single receptor and four ligands are present in insects such as *Drosophila melanogaster* and - moving further up the evolutionary ladder - four receptors and so far ten ligands have been identified in mammals.

### 1.1.2 EGF-like ligands

Several growth factors have been shown to directly activate the EGFR: EGF, transforming growth factor alpha ( $TGF\alpha$ ), heparin-binding EGF-like growth factor (HB-EGF), amphiregulin (AR), betacellulin (BC), epiregulin (Epi) (Riese and Stern, 1998), cripto (Salomon et al., 1999) and epigen (Strachan et al., 2001). The various neuregulin (NRG) isoforms are the ligands for HER3 and HER4.

All these molecules share a common motif of 30-50 amino acids in the active peptide, the EGF structural unit, that contains six conserved cysteine residues. These cysteines form three intramolecular disulfide bonds, thereby restraining the peptide in a tertiary structure that has three disulfide bonded loops.

EGF-like ligands are synthesized as transmembrane precursors which are subject to proteolytic cleavage at the cell surface to produce the soluble and diffusible growth factors (Massague and Pandiella, 1993). Subsequently, the mature ligands activate RTKs of the EGFR family by autocrine or paracrine stimulation. In addition, several studies indicate that the membrane-anchored precursors may be biologically active (Brachmann et al., 1989; Wong et al., 1989).

### 1.1.3 Ligand-induced activation of receptor tyrosine kinases

Ligand-induced activation of receptor tyrosine kinases is mediated by intermolecular autophosphorylation of key tyrosine residues in the activation loop of the catalytic tyrosine kinase domain (Schlessinger, 2002). In the inactive state, the activation loop adopts a configuration preventing access to ATP and substrate. Upon tyrosine phosphorylation, the activation loop adopts an "open configuration" enabling access to ATP and substrate, thus resulting in enhanced tyrosine kinase activity.

Recent structural studies have revealed that receptor dimerization is mediated by receptor-receptor interactions in which a loop protruding from neighboring receptors mediates receptor dimerization and activation (Garrett et al., 2002; Ogiso et al., 2002). Dimerization of EGFR requires the binding of two molecules of monomeric EGF to two EGFR molecules in a 2:2 EGF:EGFR complex formed from stable intermediates of 1:1 EGF:EGFR complexes. Each EGF molecule is bound exclusively to a single EGFR molecule, and dimerization is mediated entirely by receptor-receptor interactions. The crystal structures are consistent with the "receptor-mediated" mechanism for dimerization (Lemmon et al., 1997), in which the binding of EGF to EGFR induces a conformational change that exposes a receptor-receptor interaction site in the extracellular domain, resulting in dimerization of two EGFR monomers only when occupied by EGF. The dimerization loop-mediated mechanism of receptor dimerization may function as a key regulatory step for control of the tyrosine kinase activity of EGFR and other members of the family.

The presence of multiple ligands and receptors imparts the EGFR signaling network with an expanded repertoire of cellular responses, as the four receptors can potentially form ten distinct homo- and heterodimers that are activated by different ligands (Olayioye et al., 2000). In the absence of a specific ligand for HER2, this RTK functions as the preferred heterodimeric partner of the other members of the EGFR family (Alroy and Yarden, 1997), and provides an additional platform for recruitment of intracellular signaling pathways.

### 1.1.4 Cytoplasmic tyrosine kinases

There are ten known subfamilies of cytoplasmic, non-receptor tyrosine kinases (NRTKs): Src, Abl, Jak, Ack, Csk, Fak, Fes, Frk, Tec and Syk (Blume-Jensen and Hunter, 2001). NRTKs lack receptor-like features such as an extracellular ligand-binding domain and a transmembrane-spanning region. Most NRTKs are localized in the cytoplasm, whereas some

are anchored to the cell membrane through amino-terminal modifications, such as myristoylation or palmitoylation. In addition to a tyrosine kinase domain, NRTKs possess domains that mediate protein-protein, protein-lipid, and protein-DNA interactions. The most common theme in NRTK regulation, as in RTK function, is tyrosine phosphorylation. In particular, phosphorylation of tyrosines in the activation loop of NRTKs leads to an increase in enzymatic activity. Activation loop phosphorylation occurs via *trans*-autophosphorylation or phosphorylation by a different NRTK (Hubbard and Till, 2000). Phosphorylation of tyrosines outside of the activation loop can negatively regulate kinase activity.

The largest subfamily of NRTKs, with nine members, is the Src family (Blume-Jensen and Hunter, 2001). Src family members participate in a variety of signaling processes, including mitogenesis, T- and B-cell activation, and cytoskeleton restructuring. Multiple *in vivo* substrates have been described for Src and include the PDGFR and EGFR, the NRTK focal adhesion kinase Fak, the adapter protein p130Cas which is involved in integrin- and growth factor-mediated signaling and cortactin, an actin-binding protein important for the proper formation of cell matrix contact sites. Regulation of Src catalytic activity has been studied extensively. Src and its family members contain a myristoylated amino terminus, a stretch of positively-charged residues that interact with phospholipid head groups, a short region with low sequence homology, an SH3 domain, an SH2 domain, a tyrosine kinase domain, and a short carboxy-terminal tail. Src possesses two important regulatory tyrosine phosphorylation sites. Phosphorylation of Tyr-527 in the carboxy-terminal tail of Src by the NRTK Csk represses kinase activity. The importance of this phosphorylation site is underscored by v-Src, an oncogenic variant of Src that is a product of the Rous sarcoma virus. Owing to a carboxy-terminal truncation, v-Src lacks the negative regulatory site Tyr-527 and is constitutively active, leading to uncontrolled growth of infected cells. A second regulatory phosphorylation site in Src is Tyr-416, an autophosphorylation site in the activation loop. Maximal stimulation of kinase activity occurs when Tyr-416 is phosphorylated. Src has also been implicated in several human carcinomas, including breast, lung, and colon cancer.

### 1.1.5 Recruitment of downstream signaling molecules

Ligand-induced receptor dimerization and autophosphorylation of RTKs, as well as, activation of NRTKs generates phosphorylated tyrosine residues on target proteins that mediate the recruitment and activation of a variety of cytoplasmic signaling proteins (Hunter, 2000). These signaling proteins are modular in nature and bring about interactions with other

proteins, with phospholipids, or with nucleic acids. Protein modules involved in cellular signaling processes downstream of RTKs and other cell surface receptors range in size from 50 to 120 amino acids (Schlessinger, 2000). SH2 domains bind specifically to distinct amino acid sequences defined by 1 to 6 residues C-terminal to the phosphotyrosine moiety, while PTB domains bind to phosphotyrosine within context of specific sequences 3 to 5 residues to its N terminus. Certain PTB domains bind to nonphosphorylated peptide sequences, while still others recognize both phosphotyrosine-containing and nonphosphorylated sequences equally well. SH3 domains bind specifically to the proline-rich sequence motif PXXP, while WW domains bind preferentially to another proline-rich motif PXPX. Pleckstrin homology (PH) domains comprise a large family of more than a hundred domains. While certain PH domains bind specifically to PtdIns(4,5)P<sub>2</sub>, another subset of PH domains binds preferentially to the products of agonist-induced phosphoinositide-3-kinases (PI-3Ks). Finally, FYVE domains comprise another family of small protein modules that specifically recognize PtdIns-3-P, and PDZ domains belong to another large family of independent protein modules that bind specifically to hydrophobic residues at the C termini of their target proteins.

A large family of SH2 domain-containing proteins possess intrinsic enzymatic activities such as protein tyrosine kinase activity (Src kinases), protein tyrosine phosphatase activity (SHP2), phospholipase C activity (PLC $\gamma$ ), or Ras-GAP activity.

Another family of proteins exclusively contains SH2 or SH3 domains. These adaptor proteins (e.g. Grb2, Nck, Crk, Shc) utilize their SH2 and SH3 domains to mediate interactions that link different proteins involved in signal transduction. For example, the adaptor protein Grb2 links a variety of surface receptors to the Ras/mitogen-activated protein (MAP) kinase signaling cascade.

Agonist-induced membrane recruitment of signaling proteins stimulated by tyrosine phosphorylation is also mediated by a family of docking proteins which all contain in their N termini a membrane targeting signal and in their C termini a large region that contains multiple binding sites for the SH2 domains of signaling proteins. Docking proteins such as Gab1 become associated with the cell membrane by binding of its PH domain to PtdIns(3,4,5)P<sub>3</sub> in response to agonist-induced stimulation of PI-3K. In addition to the membrane targeting signal, most docking proteins contain specific domains such as PTB domains that are responsible for complex formation with a particular set of cell surface receptors. Because activated receptor tyrosine kinases selectively assemble and recruit signaling complexes every RTK is not only considered as a receptor with tyrosine kinase

activity but also as a platform for the recognition and recruitment of a specific complement of signaling proteins.

## 1.2 MAP kinase pathways

The main signaling pathways linking activation of many cell surface receptors such as RTKs to the nucleus is via Ras (Schlessinger, 2000), a small membrane-bound monomeric GTP-binding protein. Both biochemical and genetic studies have demonstrated that Ras is activated by the guanine nucleotide exchange factor Sos. The adaptor protein Grb2 plays an important role in this process by forming a complex with Sos via its SH3 domains. The Grb2/Sos complex is recruited to an activated RTK through binding of the Grb2 SH2 domain to specific phosphotyrosine sites of the receptor, thus translocating Sos to the plasma membrane where it is close to Ras and can stimulate exchange of GTP for GDP. Membrane recruitment of Sos can be also accomplished by binding of Grb2/Sos to SHC, another adaptor protein that forms a complex with many receptors through its PTB domain. Alternatively, Grb2/Sos complexes can be recruited to the cell membrane by binding to membrane-linked docking proteins such as IRS1 or FRS2 which become tyrosine phosphorylated in response to activation of certain RTKs. Once in the active GTP-bound state, Ras interacts with several effector proteins such as Raf and PI-3K to stimulate numerous intracellular processes. Activated Raf stimulates MAPK kinase (MAPKK, MEK) by phosphorylating a key Ser residue in the activation loop. MAPKK then phosphorylates MAPK on Thr and Tyr residues in the activation-loop leading to its activation. Activated MAPK phosphorylates a variety of cytoplasmic and membrane linked substrates. In addition, MAPK is rapidly translocated into the nucleus where it phosphorylates and activates transcription factors. The signaling cassette composed of MAPKKK, MAPKK, and MAPK is highly conserved in evolution and plays an important role in the control of metabolic processes, cell cycle, cell migration, and cell shape as well as in cell proliferation and differentiation (Hunter, 2000).

The specificity of MAPK interactions and the effector molecules stimulated depends largely on the MAPK subtypes involved. In particular, extracellular signal-regulated kinases (ERK1/2)/MAPKs are primarily stimulated by growth factors and modulate cell growth and differentiation, whereas c-Jun N-terminal kinases (JNKs) and p38 MAPKs are most commonly activated by stress stimuli and are involved in cell growth, differentiation, survival, apoptosis, and cytokine production (Marinissen and Gutkind, 2001).

### 1.3 G protein-coupled receptors

G protein-coupled receptors (GPCRs) are the largest family of cell-surface receptors involved in the regulation of numerous physiological functions such as neurotransmission, photoreception, chemoreception, metabolism, growth and differentiation (Fukuhara et al., 2001). For signal transmission GPCRs interact with heterotrimeric G proteins which are composed of an  $\alpha$ -,  $\beta$ - and  $\gamma$ -subunit. GPCRs are also frequently referred to as heptahelical or serpentine receptors, because they contain a conserved structural motif consisting of seven  $\alpha$ -helical membrane-spanning regions. Based on certain key sequences, GPCRs can be divided into three major subfamilies, receptors related to rhodopsin (type A), receptors related to the calcitonin receptor (type B), and receptors related to the metabotropic receptors (type C) (Gether and Kobilka, 1998). All GPCRs have an extracellular N-terminal segment, seven transmembrane helices, which form the transmembrane core, three exoloops, three cytoloops, and a C-terminal segment. Each of the seven transmembrane helices is generally composed of 20-27 amino acids. On the other hand, N-terminal segments, loops, and C-terminal segments vary in size, an indication of their diverse structures and functions. Interestingly, there is a weak correlation between an N-terminal segment's length and ligand size, suggesting a role in ligand binding, in particular for large polypeptides and glycoprotein hormones. Domains critical for interaction with the G proteins have been localized to the second and third cytoplasmic loops and the C terminus (Ji et al., 1998).

The observation that muscarinic acetylcholine  $M_1$ ,  $M_3$  and  $M_5$  receptors transform murine fibroblasts provided evidence that wild-type GPCRs can be tumorigenic when exposed to an excess of agonists (Marinissen and Gutkind, 2001). Moreover, if mutated, GPCRs might be rendered transforming even in an agonist-independent fashion as shown, for example, for  $\alpha_{1B}$ -adrenoceptors, thyroid-stimulating hormone receptors and leuteinizing hormone receptors. Although activating mutations are infrequent in GPCRs, these receptors often contribute to neoplasia when persistently stimulated by agonists released from tumors in an autocrine or paracrine fashion. Interfering with the function of these receptors effectively prevents tumor growth in animal models, which raises the possibility of developing novel agents that act on GPCRs for therapeutic intervention in cancer.

Sixteen distinct mammalian G protein  $\alpha$  subunits have been cloned and are divided into four families based upon sequence similarity:  $\alpha_s$ , which activates adenylyl cyclase,  $\alpha_i$ , which inhibits adenylyl cyclase,  $\alpha_q$ , which activates phospholipase C and  $\alpha_{12}$  of unknown function. Similarly, eleven G protein  $\gamma$  subunits and five G protein  $\beta$  subunits have been identified

(Gutkind, 2000). Therefore, GPCRs are likely to represent the most diverse signal transduction systems in eukaryotic cells.

GTPase-deficient mutants of  $\alpha_i$ ,  $\alpha_q$ ,  $\alpha_{12}$ , and  $\alpha_{13}$  were found to display oncogenic properties when expressed in several cellular systems; and naturally occurring activated mutants of certain G proteins were also identified in various disease states, including cancer.

GPCR activation causes a profound change in the transmembrane helices, which affects the conformation of intracellular loops and uncovers previously masked G protein binding sites (Gutkind, 2000). The GPCR-G protein interaction in turn promotes the release of guanosine diphosphate (GDP) bound to the G protein  $\alpha$  subunit and its exchange for guanosine triphosphate (GTP), and causes a conformational change in three flexible "switch regions" of the  $G\alpha$  subunit, thus activating  $G\alpha$  and causing the dissociation and exposure of effector-interaction sites in the  $\beta\gamma$  heterodimers.

Activated G protein subunits then initiate intracellular signaling responses by acting on a variety of effector molecules (Gutkind, 2000). These include adenylyl and guanylyl cyclases, phosphodiesterases, phospholipase A<sub>2</sub> (PLA<sub>2</sub>), phospholipase C (PLC) and PI-3Ks, thereby activating or inhibiting the production of a variety of second messengers such as cAMP, cGMP, diacylglycerol, inositol (1,4,5)-trisphosphate [Ins(1,4,5)*P*<sub>3</sub>], phosphatidyl inositol (3,4,5)-trisphosphate [PtdIns(3,4,5)*P*<sub>3</sub>], arachidonic acid and phosphatidic acid, in addition to promoting increases in the intracellular concentration of Ca<sup>2+</sup> and the opening or closing of a variety of ion channels.

A myriad of extracellular agonists have been demonstrated to act through GPCRs including biogenic amines, peptide and glycoprotein hormones, neuropeptides, serine proteases, neurotransmitters, eicosanoids and phospholipids such as sphingosine-1-phosphate and lysophosphatidic acid (LPA) (Ji et al., 1998).

LPA is an extracellular lipid mediator that has been implicated in the regulation of both physiological and pathophysiological processes (Fang et al., 2000a; Moolenaar et al., 1997). LPA represents the major mitogenic activity in serum and numerous cellular responses to LPA have been documented including rapid cytoskeletal rearrangements (Gohla et al., 1998), stimulation of cell proliferation (van Corven et al., 1989), suppression of apoptosis (Fang et al., 2000b) and induction of tumor cell migration and invasion (Fishman et al., 2001; Imamura et al., 1993). LPA levels are elevated in plasma and ascites of ovarian cancer patients (Xu et al., 1995; Xu et al., 1998), and LPA is likely to play a prominent role in the pathology of other types of human cancer.

The cell-surface receptors for LPA and for the structurally related phospholipid sphingosine-1-phosphate (S1P) belong to the EDG (endothelial cell differentiation gene) subfamily of GPCRs (Kranenburg and Moolenaar, 2001; Pyne and Pyne, 2000). To date, three functional LPA receptors have been described (EDG2, EDG4 and EDG7) which couple to  $G_i$ ,  $G_q$  and  $G_{13}$  subtypes of G proteins and show distinct properties in ligand specificity and activation of intracellular signaling pathways. According to the cellular context, LPA was shown to be involved in the modulation of adenylate cyclase, stimulation of phospholipase C (PLC) and subsequent  $Ca^{2+}$  mobilization, activation of the Ras/MAPK pathway, phosphorylation of the survival mediator Akt/protein kinase B (PKB) by PI-3K and transcriptional regulation of immediate-early genes (Kranenburg and Moolenaar, 2001; Moolenaar, 1999; Moolenaar et al., 1997).

#### 1.4 EGFR signal transactivation

Various studies have revealed that cellular responses to LPA and other GPCR agonists depend on the function of the EGFR in several cell systems, a phenomenon that was termed inter-receptor cross-talk or EGFR signal transactivation (Daub et al., 1996; Luttrell et al., 1999a; Marinissen and Gutkind, 2001; Zwick et al., 1999a). The pioneer studies of H. Daub and colleagues described a critical role of the EGFR in GPCR-induced mitogenesis of rat fibroblasts (Daub et al., 1996). They demonstrated that the EGFR and HER2/neu were rapidly tyrosine phosphorylated after stimulation of Rat-1 cells with the GPCR agonists endothelin-1 (ET-1), LPA or thrombin (Fig. 2). This transactivation of a receptor tyrosine kinase coupled GPCR-ligand engagement to ERK activation, induction of *fos* gene expression and DNA synthesis, which were abrogated either by the selective EGFR inhibitor tyrphostin AG1478 or by expression of a dominant-negative EGFR mutant.

Further investigations revealed that the GPCR-EGFR cross-talk mechanism is installed in a variety of other cell types such as human keratinocytes, primary mouse astrocytes, PC-12 cells and vascular smooth muscle cells (Daub et al., 1997; Eguchi et al., 1998; Zwick et al., 1997) and established it as a widely relevant pathway towards the activation of the MAP kinase signal.

A number of reports have demonstrated that various extracellular stimuli, unrelated to EGF-like ligands and GPCR agonists can also activate the EGF receptor (Zwick et al., 1999a). These diverse stimuli include agonists for cytokine receptors (prolactin, growth hormone),

adhesion receptors (integrins), membrane-depolarizing agents (KCl), and environmental stress factors (ultraviolet and gamma irradiation, oxidants, heat shock, hyperosmotic shock).

In addition to EGFR transactivation, other RTKs have been shown to be activated by GPCR ligands (Fig. 2B). For example, in primary rat smooth muscle cells the insulin-like growth factor receptor (IGF-1R) phosphorylation is induced by thrombin (Weiss et al., 1997) while the VEGFR-2 is transactivated by S1P in human umbilical vein endothelial cells (HUVECs) (Endo et al., 2002). Moreover, it was reported that LPA induces PDGFR tyrosine phosphorylation in L cells (Herrlich et al., 1998) and that opioid receptor agonists transactivate the fibroblast growth factor receptor (FGFR)-1 in rat C6 glioma cells that lack the EGFR (Belcheva et al., 2002) suggesting that transactivation of distinct RTKs can contribute to GPCR signaling in a cell-type-specific manner.

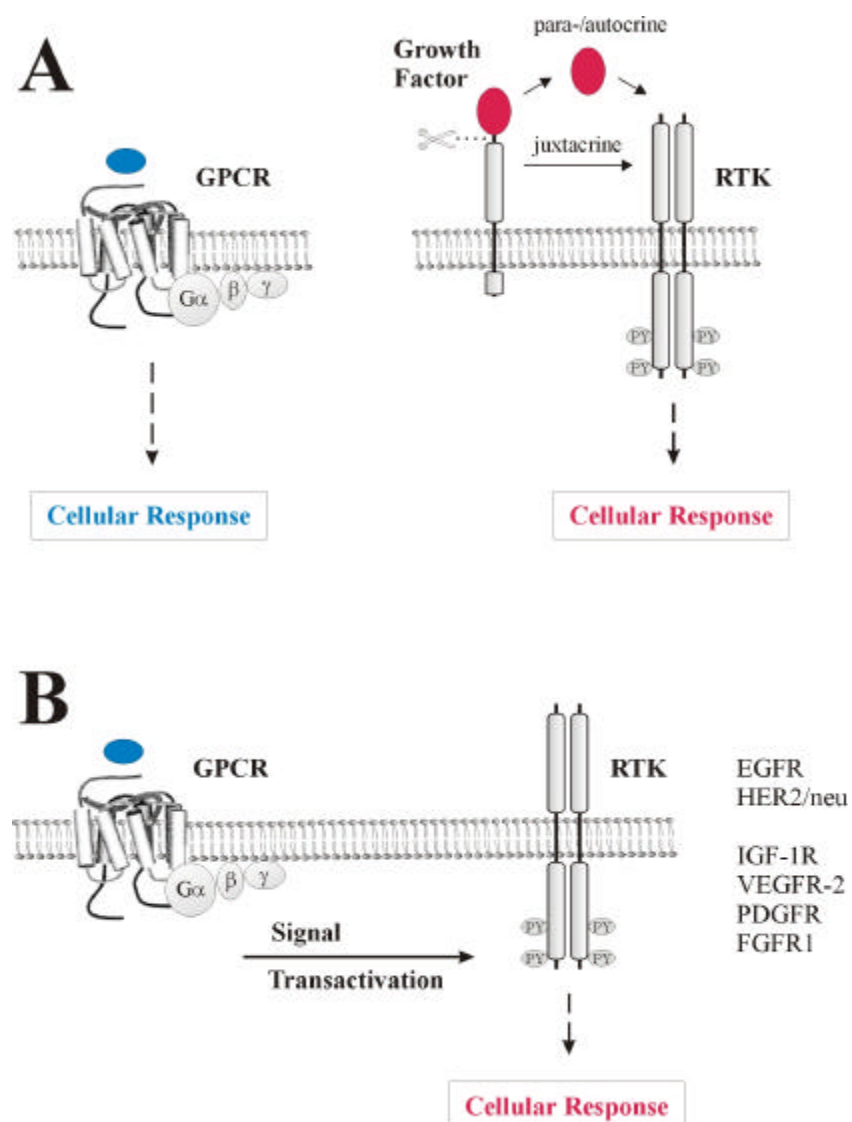


**Figure 2. GPCR and RTK signaling systems.** A) Individual pathways transmit signals along linear tracts resulting in regulation of discrete cell functions. B) RTK signal transactivation leads to RTK-characteristic cellular responses upon GPCR stimulation.

Subsequent work provided evidence for widespread use of EGFR signal transactivation by diverse GPCRs and the capacity of different G-proteins to generate the necessary connections (Table 1). Interestingly, LPA-induced transactivation of the EGFR in COS-7 cells was attenuated by pertussis toxin (PTX) which inactivates  $G\alpha$  subunits of the  $G_{i/o}$  family of G proteins. In contrast, thrombin stimulated EGFR tyrosine phosphorylation and downstream signaling was not affected (Daub et al., 1997). Furthermore, agonist stimulation of ectopically expressed  $G_q$ -coupled bombesin (BombR) or  $G_i$ -coupled  $M_2$  muscarinic acetylcholine receptor ( $M_2R$ ) triggered EGFR transactivation followed by tyrosine phosphorylation of SHC and formation of SHC-Grb2 complexes. These results demonstrated that EGFR transactivation occurs via both PTX-insensitive and -sensitive pathways and that the EGFR mediates MAP kinase activation by  $G_q$ - and  $G_i$ -coupled receptors in COS-7 cells. More recent studies showed that  $G\alpha_{13}$  subunits mediate LPA-induced actin polymerization and actin stress fiber formation in Swiss 3T3 cells and mouse fibroblasts via EGFR transactivation (Gohla et al., 1998; Gohla et al., 1999).

GPCR ligand	G proteins involved	Cell type/ tissue	Cellular response	Reference
Endothelin-1, LPA, Thrombin	?	Rat-1	ERK activation, FOS transcription	(Daub et al., 1996)
Bradykinin	$G_q$	PC-12	ERK activation	(Zwick et al., 1997)
Bombesin, Carbachol, LPA	$G_q, G_i$	COS-7	ERK activation	(Daub et al., 1997)
Angiotensin II	$G_q$	vascular smooth muscle	ERK activation	(Eguchi et al., 1998)
Thrombin, LPA	?	HaCaT	ERK activation	(Daub et al., 1997)
Thrombin	?	primary astrocytes	ERK activation	(Daub et al., 1997)
Carbachol	$G_q$	HEK 293	Modulation of Kv1.2 ion channel activity	(Tsai et al., 1997)
Carbachol	$G_q$	T84	ERK activation, inhibition of $Cl^-$ secretion	(Keely et al., 1998)
LPA	$G_{13}$	Swiss 3T3	stress fiber formation	(Gohla et al., 1998)
LPA	?	HeLa	ERK activation	(Cunnick et al., 1998)
LPA	?	NIH 3T3	MKK1/2 activation, DNA synthesis	(Cunnick et al., 1998)
Bombesin	?	PC3	EGFR tyrosine phosphorylation	(Prenzel et al., 1999)
Substance P	$G_i$	U-373 MG	ERK activation, DNA synthesis	(Castagliuolo et al., 2000)
Interleukin-8	$G_q$	SK-OV-3	ERK activation, morphology changes	(Venkatakrishnan et al., 2000)

**Table 1: Cross-talk between GPCRs and the EGFR (Gschwind et al., 2001)**

In summary,  $G_i$ -,  $G_q$ - as well as  $G_{13}$ -coupled receptors have been reported to transactivate the EGFR after agonist stimulation in diverse cell systems, whereas up to now there is no data available concerning an analogous function of  $G_s$ -coupled receptors.

Several studies indicate that the EGFR transactivation mechanism is subject to different cell type-characteristic regulatory influences. In PC-12, vascular smooth muscle cells and intestinal epithelial cells intracellular  $\text{Ca}^{2+}$  concentration has been demonstrated to be a critical parameter in  $\text{G}_q$ -coupled receptor-mediated EGFR transactivation (Eguchi et al., 1998; Iwasaki et al., 1999; Murasawa et al., 1998; Soltoff, 1998; Zwick et al., 1997). Activation of the Ser/Thr protein kinase C (PKC) was shown to be required for  $\text{G}_q$ -coupled receptors to induce EGFR transactivation in cell lines such as HEK-293 and PC-12 cells (Grosse et al., 2000; Soltoff, 1998; Tsai et al., 1997).

Besides the function of PKC in GPCR-mediated EGFR transactivation Matsubara and coworkers reported  $\text{Ca}^{2+}$ /calmodulin-dependent receptor activation in Ang II-stimulated cardiac fibroblasts (Murasawa et al., 1998). Similarly in PC-12 cells, Zwick and colleagues (Zwick et al., 1999b) demonstrated the involvement of an  $\text{Ca}^{2+}$ -calmodulin-dependent kinase II (CaMK II) activity in  $\text{K}^+$ - but not bradykinin-induced EGFR signal transactivation. The role of another  $\text{Ca}^{2+}$ -dependent kinase, PYK2, in the transmission of mitogenic signals is controversial. While several reports suggested a role of this tyrosine kinase in  $\text{G}_q$ -mediated EGFR tyrosine phosphorylation in PC-12 (Soltoff, 1998) and intestinal epithelial cells (Keely et al., 2000) respectively, Zwick *et al.* reported  $\text{Ca}^{2+}$ -dependent, but PYK2-independent EGFR transactivation in response to bradykinin in PC-12 cells (Zwick et al., 1999b). Furthermore, tyrosine phosphorylated Src is often found in association with the EGFR (Luttrell et al., 1999b) or with PYK2 (Keely et al., 2000; Soltoff, 1998) upon stimulation of  $\text{G}_q$ -coupled receptors and has therefore been proposed to function as a mediator of EGFR transactivation. Since other reports have demonstrated Src-independent EGFR transactivation, but Src-dependent SHC tyrosine phosphorylation and ERK activation (Adomeit et al., 1999; Daub et al., 1997; Slack, 2000) it seems likely that Src is recruited by the transactivated EGFR and thereby contributes to activation of the Ras signaling pathway.

Due to the rapid kinetics of EGFR signal transactivation and the fact that release of EGFR-ligands was not detectable after GPCR stimulation, the mechanism of EGFR transactivation was proposed not to involve the interaction of the EGFR with a ligand. Hence, EGFR activation by GPCR agonists was assumed to exclusively rely on intracellular elements such as  $\text{Ca}^{2+}$ , PKC and Src (Carpenter, 1999).

Very recently, a new mechanistic concept of strictly ligand-dependent EGFR transactivation by GPCRs has been presented and summarizes experimental data obtained from Rat-1, COS-7 and HEK-293 cells (Prenzel et al., 1999). The GPCR ligands LPA, carbachol and bombesin were shown to induce the proteolytic processing of the transmembrane proHB-EGF precursor

to yield the mature ligand. Blocking of this process either with the metalloprotease inhibitor batimastat or the HB-EGF antagonistic diphtheria toxin mutant CRM197 completely abrogated GPCR-induced EGFR transactivation and SHC tyrosine phosphorylation. The so-called triple-membrane-passing signal (TMPS) model includes the G protein-mediated activation of a metalloprotease via an unknown mechanism (Gschwind et al., 2001). The TMPS mechanism also allows the transactivation of EGFRs on neighboring cells but only over short distances and under participation of the heparan sulfate proteoglycan matrix which in retrospect explains the failure of Daub and colleagues (Daub et al., 1996) to detect EGF-like activity in conditioned medium of GPCR-ligand-stimulated Rat1 cell cultures. In this context, growing evidence points to transmembrane metalloproteases as the key enzymes of growth factor precursor shedding.

## 1.5 Metalloproteases

Metalloproteases are important in many aspects of biology, ranging from cell proliferation, differentiation and remodeling of the extracellular matrix (ECM) to vascularization and cell migration. These events occur several times during organogenesis in both normal development and during tumor progression. Mechanisms of metalloprotease action underlying these events include the proteolytic cleavage of growth factors so that they can become available to cells not in direct physical contact, degradation of the ECM so that founder cells can move across tissues into nearby stroma, and regulated receptor cleavage to terminate migratory signaling. Most of these processes require a delicate balance between the functions of matrix metalloproteases (MMPs) or metalloprotease-disintegrins (ADAMs) and natural tissue inhibitors of metalloproteases (TIMPs).

Metalloproteases are generally characterized by a catalytically indispensable zinc ion in their active site. Many of these enzymes contain a conserved HEXXH (X is any amino acid residue) consensus sequence (Hooper, 1994). Due to the presence of an extended zinc-binding motif, HEXXHXXGXXH and a methionine-containing turn of similar conformation close to the active site, the astacins, the serralsins, the MMPs and the adamalysins (ADAMs) are grouped into the metzincin superfamily of metalloproteases (Bode et al., 1993). The three histidines of the extended HEXXH sequence serve as ligands to the zinc, whereas the glutamic acid is believed to transfer hydrogen atoms and to polarize a zinc-bound water molecule for nucleophilic attack on the scissile peptide bond of bound substrate (Stocker and Bode, 1995).

Many metalloproteases are synthesized as inactive precursors in which the prodomain is responsible for maintaining latency of the protease via a cysteine switch mechanism: In particular, the free sulfhydryl group a cysteine residue in the prodomain provides a fourth coordination site keeping the protease inactive until the prodomain is removed (Bode et al., 1993). Besides its role as an inhibitor of the protease domain, the prodomain appears to be important for the proper maturation and intracellular transport of metalloproteases. Although prodomain removal is probably a prerequisite for protease activity, this processing appears to be mediated constitutively by a furin-type proprotein convertase in the trans-Golgi network.

### 1.5.1 ADAMs

Metalloprotease-disintegrins are transmembrane glycoproteins that play roles in cell-cell interaction and in the processing of the ectodomains of proteins (Wolfsberg et al., 1995). They combine features of both cell surface adhesion molecules and proteinases and are characterized by a conserved domain structure consisting of N-terminal signal sequence followed by a prodomain, metalloprotease and disintegrin domains, a cysteine-rich region and finally a transmembrane domain and cytoplasmic tail (Fig. 3). Thus family members are referred to as ADAM (a disintegrin and metalloprotease domain) or as MDCs (metalloprotease, disintegrin, cysteine-rich proteins).

More than 30 ADAM cDNA sequences have been identified to date in organisms ranging from *S. pombe* to humans (Primakoff and Myles, 2000). Interestingly, although all ADAMs have a relatively well-conserved metalloprotease domain, only 15 of those identified contain the zinc-binding catalytic-site consensus sequence (HEXXH). Thus, only half of the known ADAMs are predicted to be catalytically active, whereas the others most likely lack metalloprotease activity. ADAMs have been implicated in diverse processes, including sperm-egg binding and fusion, myoblast fusion, protein-ectodomain processing or shedding of cytokines, cytokine receptors, adhesion proteins and other extracellular protein domains (Schlondorff and Blobel, 1999). The regulation of ADAM metalloprotease activity after prodomain removal is only poorly understood. Processing of membrane proteins by ADAMs requires both the membrane-anchored enzyme and its substrate to be present in cis on the same cell, probably anchored in distinct domains of the plasma membrane through cytoskeletal interactions (Fig. 3).

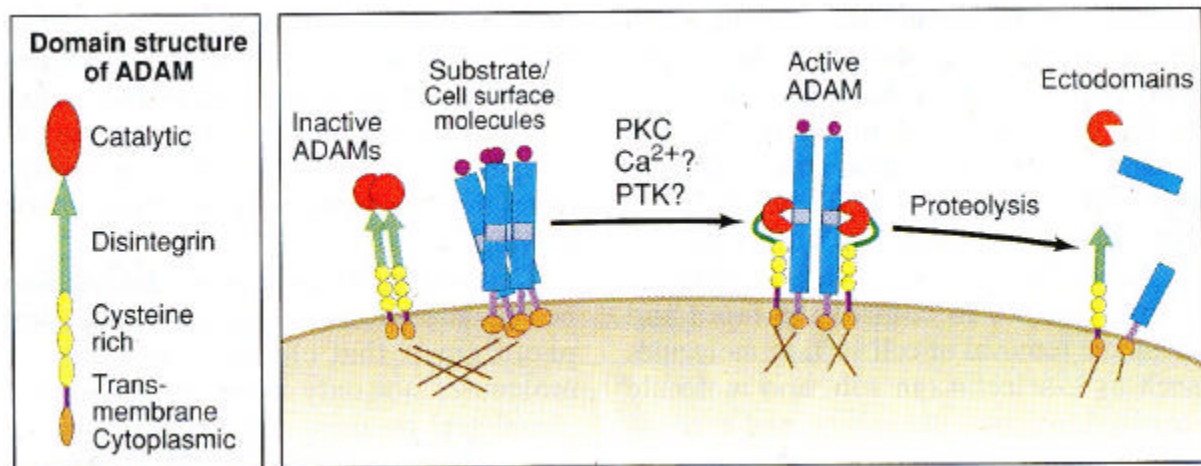


**Figure 3. Structure of ADAM family metalloproteases and their involvement in cell surface ectodomain shedding of multiple substrates (PTK, protein tyrosine kinase; PKC, protein kinase C) (Werb and Yan, 1998).**

Upon cell activation (for example, by PKC agonists, increases in cytoplasmic  $\text{Ca}^{2+}$  levels or tyrosine kinase stimulation), the attachments change and the proteinases and substrates become co-clustered and can interact. Alternatively, the signaling cascade could modify the cytoplasmic domains of the proteinases or substrate, producing a conformational change that either activates the enzyme or makes the cleavage site available (Schlondorff and Blobel, 1999).

For most processing reactions there appears to be a constitutive level of ectodomain shedding. Processing is necessary to make available paracrine growth and survival factors including EGF-like ligands allowing for the consistent supply of EGFR agonists.

The first and best-characterised “sheddase” is TACE (tumour necrosis factor alpha converting enzyme, ADAM17) (Black et al., 1997; Moss et al., 1997). Besides  $\text{TNF}\alpha$ , TACE mediates cleavage of several other unrelated membrane proteins, such as  $\text{TGF}\alpha$ , L-selectin, p75 TNFR and HER4 (Black, 2002). Surprisingly, mice lacking functional TACE display multiple defects in epithelial cell maturation and organization in multiple organs such as the eye, hair and skin. This phenotype is similar in animals engineered to lack the EGFR (Peschon et al., 1998). In addition, targeted disruption of the TACE genes causes a phenotype that is much more severe than knock-out of  $\text{TGF}\alpha$  alone, suggesting the involvement of TACE not only in pro $\text{TGF}\alpha$  shedding, but also in the membrane cleavage of other EGF-like ligand precursors.

### 1.5.2 MMPs

The matrix metalloproteinases (MMPs) which are closely related to the ADAM family of metalloproteases play a central role in the timely breakdown of virtually any component of the extracellular matrix (ECM) (Shapiro, 1998). Matrix remodelling is essential for embryonic development, morphogenesis, reproduction, and tissue resorption.

MMPs were historically divided into collagenases, gelatinases, stromelysins and matrilysins on the basis of their specificity for ECM components. However, a sequential numbering system for the more than 20 known human MMPs has been adapted, and the MMPs are now grouped according to their structure (Nagase and Woessner, 1999). There are eight distinct classes of MMPs: five are secreted and three are membrane-type MMPs (MT-MMPs). All MMPs are synthesized as prepro-enzymes and secreted as inactive pro-MMPs in most cases. The prodomain has a conserved unique PRCG(V/N)PD sequence. The cysteine within this sequence ligates the catalytic zinc to maintain the latency of pro-MMPs. The catalytic domains of MMPs have an additional structural zinc ion and 2-3 calcium ions, which are required for the stability and the expression of enzymic activity. The gelatinases MMP-2 and MMP-9 have three repeats of fibronectin-type II domain inserted in the catalytic domain. These repeats interact with collagens and gelatins. Most of the MMPs are activated outside the cell by other activated MMPs or furin-like serine proteases. The proteolytic activities of MMPs are tightly controlled by endogenous inhibitors such as  $\alpha$ -macroglobulins, and TIMPs. The expression of many MMPs is transcriptionally regulated by growth factors, hormones, cytokines, and cellular transformation (Brinckerhoff and Matrisian, 2002).

## 1.6 Molecular oncology

Tumorigenesis is a multistep process involving genetic alterations that drive the progressive transformation of normal human cells into highly malignant derivatives (Hanahan and Weinberg, 2000). Cancer is the most common genetic disease: one in three people in the western world develop cancer, and one in five die from it. The genomes of tumor cells are altered at multiple sites, having suffered disruption through lesions as subtle as point mutations and as obvious as changes in chromosome complement (Blume-Jensen and Hunter, 2001). Many types of cancers are diagnosed in the human population with an age-dependent incidence implicating four to seven rate-limiting, stochastic events.

Observations of human cancers and animal models argue that tumor development proceeds via a process formally analogous to Darwinian evolution, in which a succession of genetic changes, each conferring one or another type of growth advantage, leads to the progressive conversion of normal human cells into cancer cells.

The vast catalog of cancer cell genotypes is a manifestation of six essential alterations in cell physiology that collectively dictate malignant growth and which are now recognized as the six hallmarks of cancer: self-sufficiency in growth signals, insensitivity to growth-inhibitory (anti-growth) signals, evasion of programmed cell death (apoptosis), limitless replicative potential, sustained angiogenesis, and tissue invasion and metastasis. It is assumed that these six capabilities are shared in common by most and perhaps all types of human tumors (Hanahan and Weinberg, 2000).

Cancers of the oral cavity, salivary glands, larynx, and pharynx, collectively referred to as squamous cell carcinomas of the head and neck (HNSCC), are one of the most common malignancies and a major cause of cancer mortality worldwide. The 5-year survival rate for this disease is about 50% (Greenlee et al., 2001). The poor prognosis of HNSCC patients reflects the fact that although the risk factors for HNSCC are well-recognized, very little is known about the molecular mechanisms responsible for this malignancy.

High expression levels of the EGFR and HER2/neu have been proposed as prognostic markers for HNSCC that correlate with poor clinical outcome (Quon et al., 2001; Shiga et al., 2000). Therefore, these RTKs serve as molecular targets for recently developed target-directed HNSCC therapies (Azemar et al., 2000; Shin et al., 2001). Interestingly, overexpression of the EGFR and TGF $\alpha$  have been connected to high levels of activated ERK/MAPK in HNSCC tumors (Albanell et al., 2001) which led to considerable interest in understanding the EGFR-directed mitogenic signaling pathways in this type of cancer.

## 1.7 Aim of the study

The traditional view of growth factor receptors and hormone receptors in general is that a specific ligand directly recognizes a highly selective binding site on its cognate receptor and, thereby, activates receptor-dependent signaling and biological responses (Fig. 2A). It has become apparent in recent years, however, that the EGFR is also part of signaling networks activated by heterologous stimuli. Most importantly, agonists for GPCRs which comprise the largest family of cell-surface receptors have been recognized as potent inducers of EGFR activation (Fig. 2B).

Following the early observation by Faure and colleagues that agonist stimulation of COS-7 cells transiently expressing Gq-, or Gi-coupled receptors results in ERK1/2 activation (Faure et al., 1994), in 1996, Daub *et al.* described a critical role of the EGFR in GPCR-triggered ERK stimulation and proliferation of rat fibroblasts (Daub et al., 1996). This was the first demonstration that GPCR-dependent mitogenic activity involves receptor networking that couples GPCRs to a growth factor receptor tyrosine kinase. Subsequent studies further established the EGFR as an essential element in GPCR mitogenic signaling in a variety of other cell systems including COS-7, HaCaT, PC-12 and HEK-293 cells (Carpenter, 1999; Gschwind et al., 2001; Zwick et al., 1999a).

Because of the very rapid kinetics of the EGFR transactivation response to GPCR ligand stimulation, a mechanism that bypasses extracellular interaction with an EGFR ligand and involves an intracellular pathway was proposed. In contrast to this concept, recent experimental data support the view of a strictly ligand-dependent mechanism of EGFR signal transactivation. Most importantly, the GPCR agonists LPA, carbachol and bombesin were shown to induce the proteolytic processing of the transmembrane proHB-EGF precursor to yield the mature ligand in COS-7 cells (Prenzel et al., 1999). Blockade of this process either with the metalloprotease inhibitor batimastat or the HB-EGF antagonistic diphtheria toxin mutant CRM197 completely abrogated GPCR-induced EGFR transactivation. These experimental findings led to the establishment of the TMPS model of EGFR signal transactivation (see 1.4).

On the basis of these findings and the fact that deregulation of both GPCR and EGFR signaling systems has been recognized as a major cause of hyperproliferative diseases, the aim of this study was to investigate the molecular mechanisms and the pathophysiological significance of EGFR signal transactivation in human cancer. Since the EGFR has been identified as a critical determinant of disease development and progression in HNSCC (see 1.6), cancer cells derived from this tumor type served as an experimental model system. Three questions were of special interest:

1. Are GPCR-EGFR cross-talk pathways broadly installed in HNSCC cells?
2. Is the EGFR signal transactivation pathway critical for the manifestation of hallmark cancer cell characteristics such as self-sufficiency of growth signals, replicative potential, migration and invasion of cancer cells (see 1.6)?
3. What are the elements involved in signal transmission from agonist-treated GPCRs to the EGFR?

## 2 MATERIALS AND METHODS

### 2.1 Materials

#### 2.1.1 Laboratory chemicals and biochemicals

Acrylamide	Serva, Heidelberg
Agar	Difco, Detroit, USA
Agarose	BRL, Eggenstein
Ampicillin	Roche, Mannheim
Aprotinin	Sigma, Taufkirchen
APS (Ammonium peroxodisulfate)	Bio-Rad, München
ATP (Adenosine 3'-triphosphate)	Pharmacia, Freiburg
Batimastat	British Biotech, Oxford, UK
Bisacrylamide	Roth, Karlsruhe
Bromphenol blue	Sigma, Taufkirchen
BSA (Bovine serum albumin)	Sigma, Taufkirchen
Coomassie G250	Serva, Heidelberg
Deoxynucleotides (dG/A/T/CTP)	Roche, Mannheim
Dideoxynucleotides (ddG/A/T/CTP)	Pharmacia, Freiburg
DTT (Dithiothreitol)	Sigma, Taufkirchen
Ethidium bromide	Sigma, Taufkirchen
Fibronectin	Calbiochem, Bad Soden
FN-439 (4-(2-aminobenzoyl)-Gly-Pro-D-Leu-D-Ala-NH-OH))	Calbiochem, Bad Soden
Heparin	Sigma, Taufkirchen
HEPES (N-(2-Hydroxyethyl)piperazine-N`-(2-ethanesulfonic acid))	Serva, Heidelberg
IPTG (Isopropyl $\beta$ -D-1-thiogalactopyranoside)	Biomol, Hamburg
L-Glutamine	Gibco, Eggenstein
Leupeptin	Sigma, Taufkirchen
Lipofectamine®	Gibco, Eggenstein
Lysozyme	Sigma, Taufkirchen
Marimastat	Sugen Inc., CA, USA
MBP (Myelin basic protein)	Sigma, Taufkirchen
Mineral oil	Sigma, Taufkirchen
MOPS (3-Morpholinopropanesulfonic acid)	Biomol, Haub
PMSF (Phenylmethanesulfonyl fluoride)	Sigma, Taufkirchen
pNPP (p-Nitrophenyl phosphate)	Sigma, Taufkirchen
Polybrene (Hexadimethrine bromide)	Sigma, Taufkirchen
PD98059	Alexis, Grünberg
PEG (Polyethylene glycol) 4000, 6000	Serva, Heidelberg
Ponceau S	Sigma, Taufkirchen
PP2	Calbiochem, Bad Soden
PTX (Pertussis toxin)	List, Campbell, USA
Salmon sperm DNA	Sigma, Taufkirchen
SDS (Sodium dodecyl sulfate)	Roth, Karlsruhe
Sodium azide	Serva, Heidelberg
Sodium fluoride	Sigma, Taufkirchen
Sodium orthovanadate	Aldrich, Steinheim
Scintillation cocktail (Rotiszint®ecoplus)	Roth, Karlsruhe

TEMED (N,N,N',N'-Tetramethylethylenediamine)	Serva, Heidelberg
TPA (Tetradecanoyl-phorbol-13-acetate)	Sigma, Taufkirchen
Triton X-100	Serva, Heidelberg
Tween 20, 40	Sigma, Taufkirchen
Tyrphostin AG1478	Alexis, Grünberg

All other chemicals were purchased from Merck (Darmstadt).

### 2.1.2 Enzymes

Alkaline Phosphatase	Roche, Mannheim
Restriction Endonucleases	Pharmacia, Freiburg
	Roche, Mannheim
	NEB, Frankfurt/ Main
	MBI Fermentas, St. Leon-Rot
T4-DNA Ligase	Roche, Mannheim
T7-DNA Polymerase	Pharmacia, Freiburg
Taq-DNA Polymerase	Roche, Mannheim
	Takara, Japan
Trypsin	Gibco, Eggenstein

### 2.1.3 Radiochemicals

[ $\gamma$ - <sup>32</sup> P] ATP	>5000 Ci/mmol
[ $\alpha$ - <sup>33</sup> P] dATP	2500 Ci/mmol
L-[ <sup>35</sup> S] Methionine	>1000 Ci/mmol

All radiochemicals were obtained from PerkinElmer Life Sciences, Köln.

### 2.1.4 „Kits" and other materials

Cell culture materials	Greiner, Solingen
	Nunclon, Dänemark
	Falcon, U.K.
Cellulose nitrate 0.45 $\mu$ m	Schleicher & Schüll, Dassel
Dowex AG1-X8	Bio-Rad, München
ECL Kit	PerkinElmer, Köln
Glutathione-Sepharose	Pharmacia, Freiburg
Hyperfilm MP	Amersham, USA
Micro BCA Protein Assay Kit	Pierce, Sankt Augustin
Parafilm	Dynatech, Denkendorf
Poly Prep <sup>®</sup> Chromatography columns	Bio-Rad, München
Protein A-Sepharose	Pharmacia, Freiburg
Protein G-Sepharose	Pharmacia, Freiburg
QIAquick Gel Extraction Kit (50)	Qiagen, Hilden
QIAquick PCR Purification Kit	Qiagen, Hilden
QIAGEN Plasmid Maxi Kit	Qiagen, Hilden
Random-Primed DNA Labeling Kit	Pharmacia, Freiburg
Sephadex G-50 (DNA Quality)	Pharmacia, Freiburg
Sterile filter 0.22 $\mu$ m, cellulose acetate	Nalge Company, USA
Sterile filter 0.45 $\mu$ m, cellulose acetate	Nalge Company, USA

Transwells	Corning, New York, USA
Whatman 3MM	Whatman, USA

### 2.1.5 Growth factors and ligands

Anisomycin	Calbiochem
Amphiregulin	R&D Systems
Bradykinin	Calbiochem
EGF (murine)	Toyoba, Japan

All other growth factors and ligands were purchased from Sigma.

### 2.1.6 Media and buffers

Medium for *E.coli*

LB-Medium	1.0	%	Tryptone
	0.5	%	Yeast Extract
	1.0	%	NaCl
			pH 7.2
2xYT-Medium	1.6	%	Tryptone
	1.0	%	Yeast Extract
	1.0	%	NaCl
			pH 7.2

When necessary the following antibiotics were added to the media after autoclavation:

Ampicillin	100	µg/mL
Kanamycin	100	µg/mL
Chloramphenicol	30	µg/mL

LB-plates additionally contained 1.5% Agar.

### 2.1.7 Cell culture media

All cell culture media and additives were from Gibco (Eggenstein), fetal calf serum (FCS) was purchased from Sigma.

Dulbecco's modified eagle medium (DMEM) with 4.5 mg/mL glucose, 2 mM L-glutamine, 1 mM sodium pyruvate.

Eagle's minimum essential medium (EMEM) supplemented with 2 mM L-glutamine, 0.1 mM non-essential amino acids and 1 mM sodium pyruvate.

Nutrient mixture F12 (HAM) with L-glutamine.

Freeze medium: 90% heat-inactivated FCS, 10% DMSO.

## 2.1.8 Stock solutions for buffers

BBS (2x)	50	mM	BES
	280	mM	NaCl
	1.5	mM	Na <sub>2</sub> HPO <sub>4</sub>
			pH 6.96 (NaOH)
HBS (2x)	46	mM	HEPES pH 7.5
	274	mM	NaCl
	1.5	mM	Na <sub>2</sub> HPO <sub>4</sub>
			pH 7.0
Denhardt (100x)	2.0	%	Polyvinylpyrrolidone
	2.0	%	Ficoll
	2.0	%	BSA
DNA loading buffer (6x)	0.25	%	Bromphenol blue
	0.25	%	Xylencyanol
	30.0	%	Glycerol
	100.0	mM	EDTA pH 8.0
Laemmli buffer (2x)	187.5	mM	Tris/HCl pH 6.8
	6.0	%	SDS
	30.0	%	Glycerol
	0.01	%	Bromphenol blue
	5.0	%	β-Mercaptoethanol
NET (1x)	150.0	mM	NaCl
	5	mM	EDTA
	50	mM	Tris
	0.05	%	Triton X-100 pH 7.4 (HCl)
PBS	13.7	mM	NaCl
	2.7	mM	KCl
	80.9	mM	Na <sub>2</sub> HPO <sub>4</sub>
	1.5	mM	KH <sub>2</sub> PO <sub>4</sub> , pH 7.4 (HCl)
SD-Transblot	50.0	mM	Tris/HCl pH 7.5
	40.0	mM	Glycine
	20.0	%	Methanol
	0.004	%	SDS
“Strip” buffer	62.5	mM	Tris/HCl pH 6.8
	2.0	%	SDS
	100	mM	β-Mercaptoethanol
SSC (20x)	3.0	M	NaCl
	0.3	M	Sodium citrate
TAE (10x)	400	mM	Tris/Acetate

	10	mM	EDTA pH 8.0 (Acetic acid)
TE10/0.1	10.0	mM	Tris/HCl pH 8.0
	0.1	mM	EDTA pH 8.0
Tris-Glycine-SDS (10x)	248.0	mM	Tris/HCl pH 7.5
	1918.0	mM	Glycine
	1.0	%	SDS

## 2.1.9 Bacterial strains, cell lines and antibodies

### 2.1.9.1 *E. coli* strains

<i>E. coli</i>	Description	Origin/ Reference
DH5aF'	F'/endA1 hsd17 (rk-mk-),supE44,recA1, gyrA (Nal), thi-1, (lacZYA-argF	Genentech, San Francisco, USA
CJ236	dut-, ung-, thi-, relA-	(Kunkel, 1985)

### 2.1.9.2 Cell lines

Cell Line	Description	Origin/ Reference
COS-7	African green monkey, SV40-transformed kidney fibroblasts	Genentech
SCC-4	Human squamous cell carcinoma of the tongue	ATCC CRL-1624
SCC-9	Human squamous cell carcinoma of the tongue	ATCC CRL-1629
SCC-15	Human squamous cell carcinoma of the tongue	ATCC CRL-1623
SCC-25	Human squamous cell carcinoma of the tongue	ATCC CRL-1628
FaDu	Human squamous cell carcinoma of the pharynx	ATCC HTB-43
Detroit 562	Human squamous cell carcinoma of the pharynx	ATCC CCL-138
HEK-293 T	Human embryonic kidney fibroblasts, transformed with adenovirus Typ V DNA	ATCC CRL-1573
Phoenix E, A	Retrovirus producer cell lines for the generation of helper free ecotropic and amphotropic retroviruses based on HEK-293	Nolan, Stanford
EC-2	Murine clonal fibroblast cell line, <i>tace</i> <sup><math>\Delta</math>Zn/<math>\Delta</math>Zn</sup>	(Reddy et al., 2000) R. Black (Immunex)
EC-4	Murine clonal fibroblast cell line, wild-type	(Reddy et al., 2000)

R. Black (Immunex)

All other cell lines were obtained from the American Type Culture Collection (ATCC, Manassas, USA) and grown as recommended by the supplier.

### 2.1.9.3 *Antibodies*

The following antibodies were used in immunoprecipitation experiments, as primary antibodies in immunoblot analysis or for staining of cell surface proteins in FACS analysis.

Antibody	Description/ Immunogen	Origin/ Reference
P-Tyr (4G10)	Mouse, monoclonal; recognizes phospho-(3)-tyrosine residues	UBI, Lake Placid
EGFR	Sheep, polyclonal/ part of cytoplasmic domain of the human EGFR	UBI
EGFR (108.1)	Mouse, monoclonal/ ectodomain of the human EGFR	(Daub et al., 1997)
HER2/neu	Rabbit, polyclonal/ C-terminal peptide of human HER2/neu	(Daub et al., 1996)
Akt1/2	Rabbit, polyclonal/ AA 345-480 of human Akt1	Santa Cruz, USA
SHC	Mouse, monoclonal	Santa Cruz
SHC	Rabbit, polyclonal/ 220 AA at C-terminus of human SHC	(Daub et al., 1997)
Gab1	Rabbit, polyclonal/ AA 23-189 of human Gab1	(Daub et al., 1997)
P-ERK	Rabbit, polyclonal; recognizes phospho-p44/p42 (Thr-202/ Tyr-204) MAPK	NEB, Frankfurt/M.
P-p38	Rabbit, polyclonal; recognizes phospho-p38 (Thr-180/Tyr-182) MAPK	NEB
P-Akt/PKB	Rabbit, polyclonal; recognizes phospho-Akt (Ser-473)	NEB
ADAM17/TACE	Rabbit, polyclonal/ AA 807-823 of human TACE	Chemicon, Hofheim
ADAM17/TACE	(M220) Mouse, monoclonal; recognizes the Disintegrin and cystein-rich domains of human TACE	(Doedens and Black, 2000)

$\beta$ PDGFR	Mouse, monoclonal/ 187 AA at N-terminus of the human $\beta$ PDGFR	Transduction Lab., Lexington
$\beta$ PDGFR (128D4C10)	Mouse, monoclonal/ ectodomain of human $\beta$ PDGFR	(Daub et al., 1997)
HB-EGF	Goat, polyclonal/ recombinant, human HB-EGF	R&D Systems, Wiesbaden
AR	Goat, polyclonal/ recombinant, human AR	R&D Systems
AR	Goat, polyclonal, biotinylated/ recombinant, human AR	R&D Systems
AR	Mouse, monoclonal/ recombinant, human AR	R&D Systems
TGF $\alpha$ ?	Mouse, monoclonal/ recombinant, human TGF $\alpha$ ?	Oncogene, Bad Soden
ERK2 (C-14)	Rabbit, polyclonal/ peptide at C-terminus of rat ERK2	Santa Cruz
ERK2 (K-23)	Rabbit, polyclonal/ peptide from sub-domain XI of rat ERK2	Santa Cruz
Pan-ERK	Mouse monoclonal/ AA 219-358 of human ERK2	Transduction Lab.
HA	Mouse, monoclonal; recognizes the influenza hemagglutinin epitope	Babco, California, USA
VSV (P5D4)	Mouse, monoclonal; recognizes an epitope of eleven AA derived from the vesicular stomatitis virus glycoprotein VSV-G	Roche, Mannheim
p38 (C-20)	Rabbit, polyclonal/ peptide at C-terminus of murine p38	Santa Cruz

For western blot secondary antibodies conjugated with horseradish peroxidase (HRP) were utilized.

Antibody	Dilution	Origin
Goat anti-mouse	1 : 10,000	Sigma
Goat anti-sheep	1 : 25,000	Dianova, Hamburg
Goat anti-rabbit	1 : 25,000	BioRad, München

The FITC-conjugated rabbit anti-goat and FITC-conjugated goat anti-mouse secondary antibodies for flow cytometry were obtained from Sigma.

## 2.1.10 Plasmids and oligonucleotides

## 2.1.10.1 Primary vectors

Vector	Description	Origin/ Reference
pcDNA3	Mammalian expression vector, Amp <sup>r</sup> , CMV promotor, BGH poly A, high copy number plasmid	Invitrogen, USA
pLXSN	Expression vector for retroviral gene transfer, Amp <sup>r</sup> , Neo <sup>r</sup> , ori from pBR322, 5'-LTR and 3'-LTR from MoMuLV, SV40 promotor	Clontech, Palo Alto, USA
pLXSN-ESK	Modified pLXSN vector with multiple cloning site from pBluescript	J. Ruhe
pRK5	Expression vector, Amp <sup>r</sup> , CMV Promoter, SV 40 poly A, high copy number plasmid	Genentech

## 2.1.10.2 Constructs

Vector	Description	Reference
pcDNA3-HA-ERK2	cDNA of ERK2 in pcDNA3, HA-Tag	(Daub et al., 1997)
pRK5-HER-CD533	cDNA of the dominant negative EGFR mutant HER-CD533 in pRK5	(Daub et al., 1997)
pRK5-βPDGFR-CD504	cDNA of the dominant negative βPDGFR mutant βPDGFR-CD504 in pRK5	(Daub et al., 1997)
pLXSN-ESK-Timp-1-VSV	cDNA of human Timp-1 in pLXSN-ESK; C-terminal VSV-tag	this study
pLXSN-ESK-Timp-3-VSV	cDNA of human Timp-3 in pLXSN-ESK; C-terminal VSV-tag	this study
pcDNA3-hADAM10-HA	cDNA of human ADAM10 in pcDNA3; C-terminal HA-tag	this study
pLXSN-ESK-Δ(Pro-MP)-hADAM10-HA	cDNA of ADAM10 lacking the prodomain and metalloprotease domain Δ(AA19-455);	this study

	pLXSN-ESK; HA-tag	
pcDNA3- $\Delta$ (Pro-MP)- -hADAM12-HA	cDNA of ADAM12 lacking the prodomain and metalloprotease domain $\Delta$ (AA29-416); in pcDNA3; C-terminal HA-tag	S. Hart
pLXSN-ESK- $\Delta$ (Pro-MP)- -hADAM12-HA	cDNA of ADAM12 lacking the prodomain and metalloprotease domain in pLXSN-ESK; HA-tag	S. Hart
pLXSN-ESK- $\Delta$ (Pro-MP)- -hADAM15-HA	cDNA of ADAM15 lacking the prodomain and metalloprotease domain $\Delta$ (AA29-419) in pLXSN-ESK; C-terminal HA-tag	S. Hart
pcDNA3-mADAM17/TACE	cDNA of murine TACE in pcDNA3	(Black et al., 1997)
pLXSN-ESK-mADAM17/TACE	cDNA of murine TACE in pLXSN-ESK	this study
pcDNA3-hADAM17/TACE-HA	cDNA of human TACE in pcDNA3; C-terminal HA-tag	this study
pLXSN-ESK-hADAM17/ TACE-HA	cDNA of human TACE in pLXSN-ESK; C-terminal HA-tag	this study
pcDNA3- $\Delta$ (Pro-MP)- -hADAM17/TACE-HA	cDNA of TACE lacking the prodomain and metalloprotease domain $\Delta$ (AA18-473) in pcDNA3; C-terminal HA-tag	this study
pLXSN-ESK- $\Delta$ (Pro-MP)- -hADAM17/TACE-HA	cDNA of TACE lacking the prodomain and metalloprotease domain in pLXSN-ESK; C-terminal HA-tag	this study
pcDNA3-M1R	cDNA of human M1R in pcDNA3	(Daub et al., 1997)
pLXSN-M1R	cDNA of human M1R in pLXSN	(Prenzel et al., 1999)
pcDNA3-proHB-EGF-VSV	cDNA of human proHB-EGF in pcDNA3, C-terminal VSV-tag	(Prenzel et al., 1999)
pcDNA3- $\Delta$ (Cyto)- -proHB-EGF-VSV	cDNA of proHB-EGF lacking the cytoplasmic domain $\Delta$ (AA185-208) in pcDNA3; C-terminal VSV-tag	this study

### 2.1.10.3 Important oligonucleotides

Sequence (description)	Name
ACAGAATTCTGCCGCATCGCCGAGATC (cloning of human Timp-1 cDNA; forward primer)	Timp-1/1
ACATCTAGAGGCTATCTGGGACCGCAG (cloning of human Timp-1 cDNA; reverse primer)	Timp-1/2
ACAGAATTCGCCACCATGACCCCTTGGCTCGGGCTC (cloning of human Timp-3 cDNA; forward primer)	Timp-3/1
ACATCTAGAGGGGTCTGTGGCATTGATGA (cloning of human Timp-3 cDNA; reverse primer)	Timp-3/2
GGGGTA CCG CCA CCA TGG TCT TGC TGA GAG TGT TA (cloning of human ADAM10 cDNA; forward primer)	ADAM10/1
TCTGGG CCC TCC TCC GCG TCT CAT GTG TCC CAT TT (cloning of human ADAM10 cDNA; reverse primer)	ADAM10/2
ACAGAATTCGCCACCATGAGGCAGTCTCTCCTATTC (cloning of human ADAM17 cDNA; forward primer)	ADAM17/1
TGCTCTAGATCCTCCGCACTCTGTTTCTTTGCTGTC (cloning of human ADAM17 cDNA; reverse primer)	ADAM17/2
AGGATTCCCATACTGACCGAATTCTCCCATCCCC GCCGCCCA (cloning of $\Delta$ Pro-MP-ADAM10 lacking the prodomain and metalloprotease domain; creation of EcoRI-site between signal peptide and prodomain)	$\Delta$ Pro-MP-10/1
TCCACAAATAGGTTGGCCGAATTCAACAAAACAG TTGTT (cloning of $\Delta$ Pro-MP-ADAM10 lacking the prodomain and metalloprotease domain; creation of EcoRI-site between the metalloprotease and the disintegrin domain)	$\Delta$ Pro-MP-10/2
GTCATCCGGAGGTCGCGGGATATCCGCCAGCACGA AAGGAAC (cloning of $\Delta$ Pro-MP-ADAM17/TACE lacking the prodomain and metalloprotease domain; creation of EcoRV-site between signal peptide and prodomain)	$\Delta$ Pro-MP-TACE/1
CCCACAACTTTATTGCTGATATCGCGTTCTTGAAA ACACTC (cloning of $\Delta$ Pro-MP-ADAM17/TACE lacking the prodomain and metalloprotease domain; creation of EcoRV-site between the metalloprotease and the disintegrin domain)	$\Delta$ Pro-MP-TACE/2

GTCGGTGTAGGGCCCTCTAGAGAATTCATTAGTC  $\Delta$ Cyto-HB- EGF/1  
ATGCCCAACTTCAC

(cloning of  $\Delta$ Cyto-proHB-EGF lacking the cytoplasmic domain;  
forward primer)

CACATCATAACCTCCTCTCCTGAATTCCTAAAC  $\Delta$ Cyto-HB- EGF/2  
ATGAGAAGCCCCAC

(cloning of  $\Delta$ Cyto-proHB-EGF lacking the cytoplasmic domain;  
reverse primer)

## 2.2 Methods in molecular biology

### 2.2.1 Plasmid preparation for analytical purpose

Small amounts of plasmid DNA were prepared as described previously (Lee and Rasheed, 1990).

### 2.2.2 Plasmid preparation in preparative scale

For transfection experiments of mammalian cells DNA of high quality was prepared using Qiagen Maxi-Kits (Qiagen, Hilden) according to the manufacturers' recommendations.

### 2.2.3 Enzymatic manipulation of DNA

#### 2.2.3.1 Digestion of DNA samples with restriction endonucleases

Restriction endonuclease cleavage was accomplished by incubating the enzyme(s) with the DNA in appropriate reaction conditions. The amounts of enzyme and DNA, the buffer and ionic concentrations, and the temperature and duration of the reaction was adjusted to the specific application according to the manufacturers' recommendations.

#### 2.2.3.2 Dephosphorylation of DNA 5'-termini with calf intestine alkaline phosphatase (CIAP)

Dephosphorylation of 5'-termini of vector DNA in order to prevent self-ligation of vector termini. CIP catalyzes the hydrolysis of 5'-phosphate residues from DNA, RNA, and ribo- and deoxyribonucleoside triphosphates. The dephosphorylated products possess 5'-hydroxyl termini.

For dephosphorylation 1-20 picomoles of DNA termini were dissolved in 44  $\mu$ L deionized water, 5  $\mu$ L 10x reaction buffer (500 mM Tris/HCl pH 8.0, 1 mM EDTA pH 8.5) and 1  $\mu$ L CIP (1 U/ $\mu$ L). The reaction was incubated 30 min at 37°C and stopped by heating at 85°C for 15 minutes.

#### 2.2.3.3 DNA insert ligation into vector DNA

T4 DNA Ligase catalyzes the formation of a phosphodiester bond between juxtaposed 5'-phosphate and 3'-hydroxyl termini in duplex DNA. T4 DNA Ligase thereby joins double-stranded DNA with cohesive or blunt termini.

In a total volume of 10  $\mu$ L the digested, dephosphorylated and purified vector DNA (200 ng), the foreign DNA to be inserted, 1  $\mu$ L 10x T4 DNA Ligase buffer (0.66 M Tris/HCl pH 7.5, 50 mM MgCl<sub>2</sub>, 50 mM DTT, 10 mM ATP) and 1  $\mu$ L T4 DNA Ligase (2 U for sticky ends and 4 U for blunt ends) were mixed. The reaction was incubated at 15°C overnight. T4 DNA Ligase was inactivated by heating the reaction mixture at 65°C for 10 minutes. The resulting ligation reaction mixture was directly used for bacterial transformation.

#### 2.2.3.4 Agarose gel electrophoresis

Agarose gel electrophoresis is a simple and highly effective method for separating, identifying, and purifying 0.5- to 25 kb DNA fragments. 0.6-2%, horizontal agarose gels with 1x TAE electrophoresis buffer were used for separation. The voltage was set typically to 1-10 V/cm of gel. Gels were stained by covering the gel in a dilute solution of ethidium bromide (0.5  $\mu$ g/mL in water) and gently agitating for 30 min and destained by shaking in water for an additional 30 min.

#### 2.2.3.5 Isolation of DNA fragments using low melting temperature agarose gels

Following preparative gel electrophoresis using low melting temperature agarose, the gel slice containing the band of interest was removed from the gel. This agarose slice was then melted and subjected to isolation using the QIAquick Gel Extraction Kit (Qiagen).

### 2.2.4 Introduction of plasmid DNA into *E.coli* cells

#### 2.2.4.1 Preparation of competent cells

Competent cells were made according to the procedure described before (Chung and Miller, 1988). For long-term storage competent cells were directly frozen at -70°C. Transformation frequency ranged between 10<sup>6</sup> and 10<sup>7</sup> colonies/ $\mu$ g DNA.

#### 2.2.4.2 Transformation of competent cells

100  $\mu$ L competent cells were added to 10  $\mu$ L ligation mix and 20  $\mu$ L 5x KCM (500 mM KCl, 150 mM CaCl<sub>2</sub>, 250 mM MgCl<sub>2</sub>) in 70  $\mu$ L H<sub>2</sub>O and incubated on ice for 20 min. Upon incubation at room temperature for 10 min 1 mL LB medium was added and incubated 45 min at 37°C with mild shaking to allow expression of the antibiotic resistance gene. Transformants were selected on appropriate plates.

### 2.2.5 Oligonucleotide-directed mutagenesis

A DNA sequence can be specifically altered by synthesizing the desired sequence change within an oligonucleotide, and then converting this into a biologically active circular DNA strand by using the oligonucleotide to prime *in vitro* synthesis on a single-stranded circular template. This protocol (Kunkel, 1985; Messing, 1983) uses a DNA template containing a small number of uracil residues in place of thymine. Use of the uracil-containing template allows rapid and efficient recovery of mutants.

#### 2.2.5.1 Preparation of uracil-containing, single-stranded DNA template

CJ236 bacteria were transformed with the DNA of interest (typically pcDNA3 constructs). 2 mL 2xYT-medium were inoculated with several colonies of transformed CJ236 at 37°C until

the early log-phase was reached. Cultures were infected with  $2 \times 10^7$  M13K07 phages/mL (Amersham) and incubated for further 1.5 h. Next, kanamycin was added (70  $\mu\text{g}/\text{mL}$  final concentration) and the culture was incubated with vigorous shaking at 37 °C overnight. Cells were pelleted twice by centrifugation (13000 rpm, 5 min) to clear the supernatant. Phage was then precipitated by adding 200  $\mu\text{L}$  2.5 M NaCl/ 20% PEG 6000 and incubation for 15 min at room temperature. Precipitated phage was collected by centrifugation. The phage sediment was resuspended in 100  $\mu\text{L}$  TE10/0.1 buffer and subjected to phenol extraction/ ethanol precipitation in order to purify the single-stranded phage DNA. Quality and concentration of DNA was determined spectrophotometrically at 260 nm. For visual examination and documentation an aliquot of the single-stranded DNA was run on a 1% agarose gel.

### 2.2.5.2 Primer extension

The uracil-containing DNA was used as a template in oligonucleotide-directed mutagenesis experiments: 200 ng single-stranded template DNA, 2-3 pmol phosphorylated oligonucleotide, 1  $\mu\text{L}$  10x hybridization buffer (20 mM Tris/HCl pH 7.4, 2 mM  $\text{MgCl}_2$ , 50 mM NaCl) in a total volume of 10  $\mu\text{L}$  were incubated for 2 min at 90°C and allowed to cool to room temperature. To the hybridization mixture 1  $\mu\text{L}$  10x synthesis buffer (5 mM dNTP-mix, 100 mM Tris/HCl pH 7.5, 50 mM  $\text{MgCl}_2$ , 20 mM DTT), 5 U T4-DNA Ligase (1  $\mu\text{L}$ ), 1  $\mu\text{g}$  T4-Gen 32 Protein (0.5  $\mu\text{L}$ ) and 3 U T4-DNA Polymerase (1  $\mu\text{L}$ ) were added. The reaction was incubated for 5 min on ice, 5 min at 25 °C and finally for 90 min at 37°C. The reaction was stopped by adding 66  $\mu\text{L}$  TE. 100 ng of double-stranded DNA product were used for transformation of *E. coli*. Resulting clones were chosen randomly for isolation of plasmid DNA which was analysed by sequencing.

### 2.2.6 Enzymatic amplification of DNA by polymerase chain reaction (PCR)

The polymerase chain reaction (PCR) is a rapid procedure for *in vitro* enzymatic amplification of a specific segment of DNA (Mullis and Faloona, 1987). A multitude of applications have been developed including direct cloning from cDNA, *in vitro* mutagenesis and engineering of DNA, genetic fingerprinting of forensic samples, assays for the presence of infectious agents and analysis of allelic sequence variations. For long and accurate cDNA amplification LA-Taq™ polymerase (TaKaRa) was used:

0.5 $\mu\text{L}$	template cDNA
2 $\mu\text{L}$	"sense" oligonucleotide, 10 pmol/ $\mu\text{L}$
2 $\mu\text{L}$	"antisense" oligonucleotide, 10 pmol/ $\mu\text{L}$
5 $\mu\text{L}$	10x LA PCR buffer II (w/o $\text{MgCl}_2$ )
5 $\mu\text{L}$	$\text{MgCl}_2$ , 25 mM
8 $\mu\text{L}$	dNTP-Mix, 2.5 mM each
0.5 $\mu\text{L}$	LA-Taq™ (5 U/ $\mu\text{L}$ )
ad 50 $\mu\text{L}$	$\text{H}_2\text{O}$

PCR reactions were performed in a automated thermal cycler („Progene“, Techne). The following standard protocol was adjusted to the specific application:

first denaturation:	3 min	94°C
amplification 25-30 cycles:	1 min	94°C (denaturation)
	1 min	58°C (hybridization)
	1 min/ kb product	72°C (extension)

last extension: 7 min 72°C

10 µL from each reaction were electrophoresed on an agarose gel appropriate for the PCR product size expected. PCR products were subjected to isolation using the PCR purification kit (Qiagen).

### 2.2.7 DNA sequencing

DNA sequencing was performed according to the “Big Dye Terminator Cycle Sequencing Protocol” (ABI). The following mix was subjected to a sequencing-PCR run:

	0.5 µg	DNA of interest
	10 pmol	oligonucleotide
	4 µL	Terminator Ready Reaction Mix
	ad 20 µL	H <sub>2</sub> O
25 cycles:	30 sec	94°C
	15 sec	45-60°C
	4 min	60°C

The sequencing products were purified by sodium acetate/ EtOH precipitation, dissolved in 20 µL template suppression reagent, denatured for 2 min at 90°C and analyzed on a 310-Genetic Analyzer (ABI Prism).

### 2.2.8 cDNA array hybridization

Filters spotted with genes of interest (cloned into pBluescript SKII+) were a generous gift from J. Ruhe, cDNA probes of the HNSCC cell lines SCC-9, SCC-15 and SCC-25 were from T. Knyazeva and generated according to standard molecular biology methods. Labeling of 3–5 µL of cDNA was performed with the Megaprime kit (Amersham) in the presence of 50 µCi of [ $\alpha$ -<sup>32</sup>P]dATP. The prehybridization solution was replaced from filters by the hybridization solution containing 5x SSC, 0.5% (v/v) SDS, 100 µg/mL baker yeast tRNA (Roche), and the labeled cDNA probe (2–5 x 10<sup>6</sup> cpm/mL) and incubated at 68°C for 16 h. Filters were washed under stringent conditions. A phosphorimager system (Fuji BAS 1000; Fuji) was used to quantify the hybridization signals. Average values for each slot were calculated using the formula:  $A = (AB - B) \times 100/B$ ; [A, final volume; AB, intensity of each slot signal (pixel/mm<sup>2</sup>); B, background (pixel/mm<sup>2</sup>)].

## 2.3 Methods in mammalian cell culture

### 2.3.1 General cell culture techniques

HNSCC cell lines were grown in a humidified 93% air, 7% CO<sub>2</sub> incubator (Heraeus, B5060 Ek/CO<sub>2</sub>) at 37°C and routinely assayed for mykoplasma contamination using a bisbenzimidazole-staining kit (Sigma). Before seeding cells were counted with a Coulter Counter (Coulter Electronics). SCC-4, SCC-9, SCC-15 and SCC-25 were cultured in Dulbecco's modified Eagle's medium (DMEM) : Ham's F12 medium (1:1) containing 400 ng/mL hydrocortisone and 10% FCS. FaDu and Detroit-562 were cultured in Eagle's Minimum essential medium (EMEM) supplemented with 2 mM L-glutamine, 0.1 mM non-essential amino acids and 1.0 mM sodium pyruvate and 10% FCS. EC-4 and *tace*<sup>ΔZn/ΔZn</sup> EC-2 were maintained in

Dulbecco's modified Eagle's medium-Ham's F-12 medium supplemented with 1% heat-inactivated fetal bovine serum and glutamine.

### 2.3.2 Transfection of cultured cell lines

#### 2.3.2.1 Transfection of cells with calcium phosphate

SCC-9 cells or HEK-293 cells in six-well dishes were transfected transiently at about 70% confluency with a total of 2  $\mu\text{g}$  DNA by using a modified calcium phosphate precipitation method as described previously (Chen and Okayama, 1987). In this protocol, a calcium phosphate-DNA complex is formed gradually in the medium during incubation with cells. The transfection mix of DNA and  $\text{CaCl}_2$  in water was prepared as follows:

dish	6-well	6 cm	10 cm
area	10 $\text{cm}^2$	21 $\text{cm}^2$	57 $\text{cm}^2$
Volume of medium	1 mL	2 mL	4 mL
DNA in $\text{H}_2\text{O}_{\text{bidest}}$	2 $\mu\text{g}$ in 90 $\mu\text{L}$	5 $\mu\text{g}$ in 180 $\mu\text{L}$	10 $\mu\text{g}$ in 360 $\mu\text{L}$
2.5 M $\text{CaCl}_2$	10 $\mu\text{L}$	20 $\mu\text{L}$	40 $\mu\text{L}$
2 x BBS (pH 6.96)	100 $\mu\text{L}$	200 $\mu\text{L}$	400 $\mu\text{L}$
Total volume	200 $\mu\text{L}$	400 $\mu\text{L}$	800 $\mu\text{L}$

To initiate the precipitation reaction the adequate volume of 2x BBS was added and mixed by vortexing. The reaction was incubated for 10 min at room temperature before being added to each well. Plates were placed in a humidified container at 3%  $\text{CO}_2$  overnight. One day following transfection, cells were serum-starved for 24 hours in standard cell culture medium without FCS. Transfection efficiency of SCC-9 cells was typically about 50% as determined by LacZ staining after transfection of a LacZ-containing expression plasmid. For transfection of Phoenix cells HBS was used instead of BBS.

#### 2.3.2.2 Transfection of COS-7 cells using lipofectamine®

COS-7 cells were transiently transfected using Lipofectamine® (Gibco-BRL) essentially as described (Daub et al., 1997). For transfections in 6-well dishes, 1.0 mL of serum-free medium containing 10  $\mu\text{L}$  of Lipofectamine and 1.5  $\mu\text{g}$  of total plasmid DNA per well were used. After 4 h the transfection mixture was supplemented with an equal volume of medium containing 20% FCS and, 20 h later, cells were washed and cultured for a further 24 h in serum-free medium until lysis.

### 2.3.3 Retroviral gene transfer in cell lines

High titer retrovirus was prepared as described previously (Pear et al., 1993). The packaging cell lines Phoenix A and Phoenix E were transfected with pLXSN-ESK expression vectors using calcium phosphate. Target cell lines SCC-9 ( $8 \times 10^4$ ) and murine fibroblasts wt EC-4 and *tace* <sup>$\Delta\text{Zn}/\Delta\text{Zn}$</sup>  EC-2 ( $4 \times 10^4$ ) were seeded into 6-well dishes 24 h prior to infection. The supernatant of transfected Phoenix A and Phoenix E cells was collected and filtered through a 0.45  $\mu\text{m}$  filter. Target cells were incubated with virus supernatant for 12 h in the presence of 4  $\mu\text{g}/\text{mL}$  polybrene. Retroviral supernatant was then replaced with fresh medium. 2 d following infection, target protein expression was monitored by western blot.

## 2.4 Protein analytical methods

### 2.4.1 Lysis of cells with triton X-100

Prior to lysis, cells grown to 80% confluence were treated with inhibitors and agonists as indicated in the figure legends. Cells were washed with cold PBS and then lysed for 10 min on ice in buffer containing 50 mM HEPES, pH 7.5, 150 mM NaCl, 1% Triton X-100, 1 mM EDTA, 10% glycerol, 10 mM sodium pyrophosphate, 2 mM sodium orthovanadate, 10 mM sodium fluoride, 1 mM phenylmethylsulfonyl fluoride, and 10 µg/mL aprotinin. Lysates were precleared by centrifugation at 13000 rpm for 10 min at 4°C.

### 2.4.2 Determination of protein concentration in cell lysates

The „Micro BCA Protein Assay Kit” (Pierce, Sankt Augustin) was used according to the manufacturers’ recommendations.

### 2.4.3 Immunoprecipitation and *in vitro* association with fusion proteins

An equal volume of HNTG buffer was added to the precleared cell lysates that had been adjusted for equal protein concentration. Proteins of interest were immunoprecipitated using the respective antibodies and 20 µL of protein A-Sepharose for 4 h at 4°C. Alternatively, lysates were subjected to *in vitro* associations with either 3 µg of GST-Grb2 (Daub et al., 1997) or 2 µg of GST as control pre-bound to 30 µL of glutathione-agarose beads. Precipitates were washed three times with 0.5 mL of HNTG buffer, suspended in 2× SDS sample buffer, boiled for 3 min, and subjected to SDS-PAGE.

### 2.4.4 TCA precipitation of proteins in conditioned medium

Phenylmethylsulfonyl fluoride (1 mM final concentration) was added to cell culture medium of stimulated and control treated cells and precleared by centrifugation at 13000 rpm for 10 min at 4°C. For TCA precipitation, proteins were incubated in 0.1 mg/mL sodium deoxycholate, 0.6 M TCA for 30 min on ice.

### 2.4.5 Radiolabeling

For [<sup>35</sup>S]Methionine labeling, cells were incubated in methionine-free DMEM during starvation, and 50 µCi/mL L-[<sup>35</sup>S]Methionine were added 16 h prior to lysis.

### 2.4.6 SDS-polyacrylamide-gelelectrophoresis (SDS-PAGE)

SDS-PAGE was conducted as described previously (Sambrook, 1990). The following proteins were used as molecular weight standards:

Protein	MW (kD)	Protein	MW (kD)
Myosin	205.0	Ovalbumin	42.7
β-Galaktosidase	116.25	Carboanhydrase	29.0
Phosphorylase b	97.4	Trypsin-Inhibitor	21.5
BSA	66.2	Lysozym	14.4

Because of the small size of pro-HB-EGF and the processed form of HB-EGF, the tricine SDS-PAGE system was used as described (Schagger and von Jagow, 1987).

#### 2.4.7 Transfer of proteins on nitrocellulose membranes

For immunoblot analysis proteins were transferred to nitrocellulose membranes (Gershoni and Palade, 1982) for 2 h at 0.8 mA/cm<sup>2</sup> using a "Semidry"-Blot device in the presence of Transblot-SD buffer. Following transfer proteins were stained with Ponceau S (2 g/l in 2% TCA) in order to visualize and mark standard protein bands. The membrane was destained in water.

#### 2.4.8 Immunoblot detection

After electroblotting the transferred proteins are bound to the surface of the nitrocellulose membrane, providing access for reaction with immunodetection reagents. Remaining binding sites were blocked by immersing the membrane in 1x NET, 0.25% gelatin for at least 4 h. The membrane was then probed with primary antibody (typically overnight). Antibodies were diluted 1:500 to 1:2000 in NET, 0.25% gelatin. The membrane was washed 3x 20 min in 1x NET, 0.25% gelatin, incubated for 1 h with secondary antibody and washed again as before. Antibody-antigen complexes were identified using horseradish peroxidase coupled to the secondary anti-IgG antibody. Luminescent substrates were used to visualize peroxidase activity. Signals were detected with X-ray films or a digital camera unit. Membranes were stripped of bound antibody by shaking in strip-buffer for 1 h at 50°C. Stripped membranes were blocked and reprobed with different primary antibody to confirm equal protein loading.

### 2.5 Biochemical and cell biological assays

#### 2.5.1 Stimulation of cells

Cells were seeded in cell culture dishes of appropriate size and grown overnight to about 80% confluence. After serum-starvation for 48 h HNSCC cells were treated with inhibitors and agonists as indicated in the figure legends, washed with cold PBS and then lysed for 10 min on ice. In some cases cells were transfected 24 h after seeding and serum-starved one day following transfection before being stimulated as indicated above.

#### 2.5.2 ERK1/2 and Akt/PKB phosphorylation

For determination of ERK1/2 and Akt phosphorylation, approximately 20 µg of whole cell lysate protein/lane was resolved by SDS-PAGE and immunoblotted using rabbit polyclonal phospho-specific ERK/MAPK antibody. Akt phosphorylation was detected by protein immunoblotting using rabbit polyclonal anti-phospho-Akt antibody. Quantitation of ERK1/2 was performed using the Luminescent Image Analysis System (Fuji). After quantitation of ERK1/2 phosphorylation, membranes were stripped of immunoglobulin and reprobed using rabbit polyclonal anti-ERK1/2 or rabbit polyclonal anti-Akt antibody to confirm equal protein loading.

#### 2.5.3 ERK/MAPK activity

HA-ERK2 or endogenous ERK2 were immunoprecipitated from lysates obtained from six-well dishes using 0.5 µg of anti-HA antibody or 0.4 µg of anti-ERK2 antibody, respectively.

Precipitates were washed three times with HNTG buffer, and washed once with kinase buffer (20 mM HEPES, pH 7.5, 10 mM MgCl<sub>2</sub>, 1 mM dithiothreitol, 200 μM sodium orthovanadate). Kinase reactions were performed in 30 μL of kinase buffer supplemented with 0.5 mg/mL myelin basic protein, 50 μM ATP and 1 μCi of [ $\gamma$ -<sup>32</sup>P]ATP for 10 min at room temperature. Reactions were stopped by addition of 30 μL of LaemmLi buffer and subjected to gel electrophoresis on 15% gels. Labeled MBP was quantitated using a Phosphoimager (Fuji).

#### 2.5.4 Gelatin zymography

Conditioned media of SCC-25 cells was analyzed under nonreducing conditions and separated in 10% SDS-polyacrylamide gels co-polymerized with 0.1% (w/v) gelatin to demonstrate gelatinolytic activity (MMP-2 and MMP-9) as described previously (Kleiner and Stetler-Stevenson, 1994). Duplicate gels were incubated as controls in buffer containing 10 mM EDTA to inhibit MMP activity. The gels were stained with Coomassie G250 and dried with a gel drier.

#### 2.5.5 Flow cytometric analysis of cell surface proteins

Was performed as described before (Prenzel et al., 1999). In brief, cells were seeded, grown for 20 h and in some cases retrovirally infected as indicated. Upon serum-starvation for 24 h cells were treated with inhibitors and growth factors as indicated. After collection, cells were stained with ectodomain-specific antibodies against HB-EGF, TGF $\alpha$  or AR for 45 min. After washing with PBS, cells were incubated with FITC-conjugated secondary antibodies for 15 min and washed again with PBS. Cells were analysed on a Becton Dickinson FACScalibur flow cytometer.

#### 2.5.6 AR sandwich-ELISA

**Plate preparation:** An ELISA microtiter plate was coated overnight at RT with an monoclonal anti-AR capture antibody (MAB262, 4.0 μg/mL in PBS, 100 μL/well). Well supernatants were then decanted and plates were washed three times with wash buffer (PBS, 0.05% Tween 20). Wells were blocked with 150 μL/well block buffer (PBS, 0.5 % BSA) overnight at 4°C and washed again three times with wash buffer.

**Assay procedure:** SCC-9 cells were seeded into 12-well plates (3.2 x 10<sup>4</sup> cells per well) and incubated for 18 h. Upon serum deprivation for 24 h, cells were subjected to preincubation with batimastat (10 μM) for 20 min and stimulated as indicated in the figure legends. Cell culture media was collected and, after addition of PMSF (1 mM), precleared by centrifugation (10 min, 13,000 rpm). Samples were transferred to the antibody-coated plate (100 μL/well) and incubated for 2 h at RT with gentle agitation and washed three times with wash buffer. Next, 100 μL of biotinylated, affinity-purified, goat polyclonal, AR-detection antibody (BAF262, 150 ng/mL in dilution buffer: PBS, 0.5% BSA, 0.05% Tween 20; 100 μL/well) was added to each well and incubated for 2 h at RT. The plate was washed three times before the addition of 100 μL HRP-conjugated streptavidin (100 ng/mL in dilution buffer) to each well. Plates were then incubated for 20 min at RT. Free avidin conjugate was washed away (four washes) and 100 μL freshly prepared substrate solution (tetramethyl benzidine, TMB) was added to each well and incubated at RT with gently shaking in the dark. After 15 min the reaction was stopped by addition of 100 μL/well 250 mM HCl. The absorbance at 455 nm was read with a reference wavelength of 650 nm using an ELISA plate reader. AR concentrations for each sample were calculated after generating a standard curve using the dilution series of human recombinant AR protein.

### 2.5.7 Incorporation of $^3\text{H}$ -thymidine into DNA

SCC-9 or SCC-25 cells were seeded into 12-well plates ( $2.5 \times 10^4$  or  $6 \times 10^4$  cells per well, respectively). Upon serum deprivation for 48 h, cells were subjected to preincubation with inhibitors before ligand treatment. After 18 h incubation, cells were pulse-labelled with  $^3\text{H}$ -thymidine ( $1 \mu\text{Ci/mL}$ ) for 4 h, and thymidine incorporation was measured by trichloroacetic acid precipitation and subsequent liquid-scintillation counting.

### 2.5.8 Distribution of cell cycle phases

SCC-25 cells were seeded into 6-well plates ( $1.5 \times 10^4$  cells per well). Upon serum deprivation for 48 h, cells were subjected to 20 min preincubation with either DMSO (control) or batimastat before ligand treatment. After 18 h incubation, cells were collected and incubated in hypotonic buffer containing 0.1% sodium acetate, 0.1% Triton X-100 and  $20 \mu\text{g/mL}$  propidiumiodide for 2 h on ice. Samples were analysed on a Becton Dickinson FACScalibur flow cytometer.

### 2.5.9 *In vitro* wound closure

The assay was performed as previously described (Fishman et al., 2001) with some modifications. Confluent monolayers of SCC-9 cells were wounded with a uniform scratch, the medium was removed and cells were washed twice with PBS. Medium without FCS was added and cells were subjected to 20 min preincubation with either DMSO (control), 250 nM AG1478 or  $10 \mu\text{M}$  batimastat before ligand treatment. Cells were permitted to migrate into the area of clearing for 48 h. Wound closure was monitored by visual examination using a Zeiss microscope.

### 2.5.10 Migration

Analysis of chemotactic directional migration was performed as described before (O-Charoenrat et al., 2000) using a modified Boyden chamber. SCC-9 cells in exponential growth were harvested, washed and suspended in standard medium without FCS. Cells were preincubated with either DMSO (control), 125 nM AG1478 or  $5 \mu\text{M}$  batimastat for 20 min. Preincubation of cells with inhibitors did not affect viability or attachment of cells to membranes (data not shown).  $1 \times 10^5$  cells were seeded into polycarbonate membrane inserts (6.5 mm diameter and  $8 \mu\text{m}$  pore size) in 24-transwell cell culture dishes in the presence or absence of ligand. The lower chamber was filled with  $600 \mu\text{L}$  standard medium without FCS containing  $10 \mu\text{g/mL}$  of fibronectin as a chemoattractant. Cells were permitted to migrate for 36 h. Following incubation, nonmigrated cells were removed from the upper surface of the membranes. The cells that had migrated to the lower surface were fixed and stained with crystal violet. The stained cells were solubilized in 10% acetic acid, absorbance at 570 nm was measured in a micro-plate reader.

## 2.6 Statistical analysis

Student's *t*-test was used to compare data between two groups. Values are expressed as mean  $\pm$  standard deviation (s. d.) of at least triplicate samples.  $P < 0.05$  was considered statistically significant.

### 3 RESULTS

#### 3.1 GPCR agonists stimulate EGFR tyrosine phosphorylation via a metalloprotease-dependent pathway in HNSCC.

GPCR-induced EGFR signal transactivation was previously shown to couple G protein activation to the Ras-MAPK pathway in non-transformed cell lines such as Rat-1 fibroblasts, COS-7, HEK-293 and vascular smooth muscle cells (Gschwind et al., 2001). In contrast, little is known about the involvement and the molecular mechanisms of EGFR transactivation in cancer cell pathophysiology. To investigate the functional role of EGFR transactivation in squamous cell carcinoma the HNSCC cell lines SCC-4, SCC-9, SCC-15, SCC-25, FaDu and Detroit-562 were screened for their responsiveness to the GPCR ligands LPA (10  $\mu$ M), thrombin (Thr, 1 U/ml), carbachol (Car, 1 mM) and bradykinin (Bk, 5  $\mu$ M) at physiological concentrations. Following stimulation for three minutes cell lysates were subjected to immunoprecipitation with anti-EGFR antibodies and immunoblotted against phosphotyrosine.

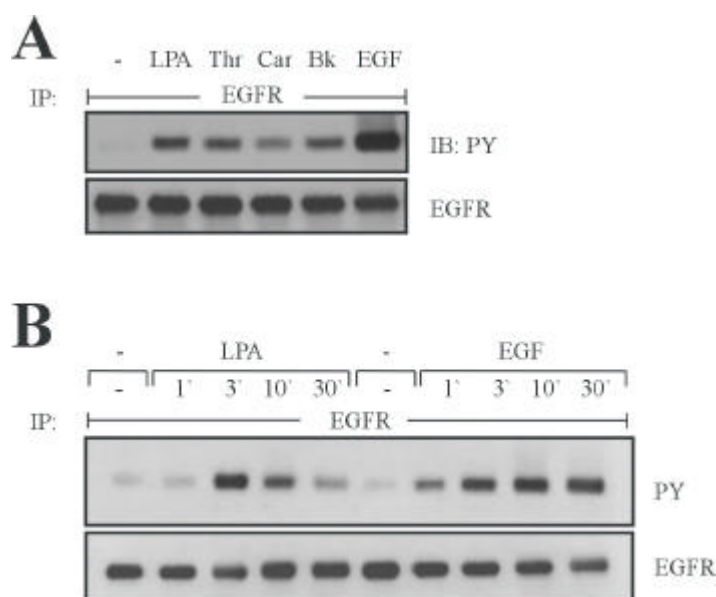


**Figure 4. Diverse GPCR ligands stimulate tyrosine phosphorylation of the EGFR in head and neck squamous cell carcinoma cells.** A) SCC-9 cells were serum-starved for 48 h and treated with 10  $\mu$ M LPA, 1 U/ml thrombin (Thr), 1 mM carbachol (Car), 5  $\mu$ M bradykinin (Bk) or 7.5 ng/ml EGF for 3 min. After lysis, EGFR was immunoprecipitated (IP) using monoclonal anti-EGFR antibody. Tyrosine-phosphorylated EGFR was detected by immunoblotting (IB) with monoclonal anti-phosphotyrosine (PY) antibody, followed by reprobing of the same filter with polyclonal anti-EGFR antibody (EGFR). B) Quiescent SCC-9 cells were treated with 10  $\mu$ M LPA or 7.5 ng/ml EGF for the indicated times. After cell lysis, EGFR tyrosine phosphorylation was detected as described under (A) followed by reprobing of the same filter with anti-EGFR antibody.

While treatment of serum-deprived SCC-4, SCC-9 and FaDu cells with either GPCR agonist or EGF (7.5 ng/ml) resulted in tyrosine phosphorylation of the EGFR (Fig. 4A, representative

data shown for SCC-9) transactivation of the EGFR was induced by LPA and thrombin in SCC-25, by LPA and bradykinin in SCC-15 and by LPA in Detroit-562 (Table 2) demonstrating that cross-talk pathways linking GPCR stimulation with EGFR activation are installed both in HNSCC cells that display low (FaDu, SCC-9) and high EGFR (SCC-15, SCC-4, Detroit-562) expression levels.

**Table 2** Tyrosine phosphorylation of the EGFR by GPCR agonists in HNSCC cell lines

Cell line	LPA	Thr	Car	Bk	EGF	EGFR <sup>d</sup>
SCC-4	+ <sup>a</sup>	+	+	+	+	++++
SCC-9	+	+	+	+	+	+
FaDu	+	+	+	+	+	+
SCC-25	+	+	- <sup>b</sup>	-	+	++
SCC-15	+	-	-	+	+	+++
Detroit-562	+	ND <sup>c</sup>	ND	ND	+	+++++

<sup>a</sup>(Trans)activation of the EGFR by immunoblot analysis

<sup>b</sup>Transactivation of the EGFR not detectable

<sup>c</sup>ND, not determined

<sup>d</sup>Relative expression levels of the EGFR by immunoblot (Azemar et al., 2000; O-Charoenrat et al., 2000)

In time-course experiments (Fig. 4B, representative data shown for LPA in SCC-9 cells) the transactivation signal was detectable as early as three minutes after LPA treatment. Moreover, LPA-induced EGFR tyrosine phosphorylation was slightly slower and more transient when compared to EGF stimulation (7.5 ng/ml). Together, these findings suggested a role for the EGFR as a convergence point for signaling by diverse GPCR agonists and demonstrated that HNSCC cells may be targets for stimulation by multiple ligands. The finding that LPA was the predominant stimulus of EGFR activation among several GPCR ligands in all cell lines examined (Table 2) led the further investigations focus on LPA-induced signal transactivation in HNSCC.

To examine which GPCRs are involved in LPA signaling in head and neck cancer cells, micro-array analysis of cDNA prepared from SCC-9, SCC-15 and SCC-25 cells was performed. Besides the EGFR, HER2 and HER3, all three known LPA receptor genes (EDG2, EDG4 and EDG7) were found to be expressed in SCC-9 and SCC-15 while expression of EDG2 and EDG7 was detected in SCC-25 cells (Fig. 5). The three LPA receptors are known to display cell type-specific coupling properties for heterotrimeric G proteins.

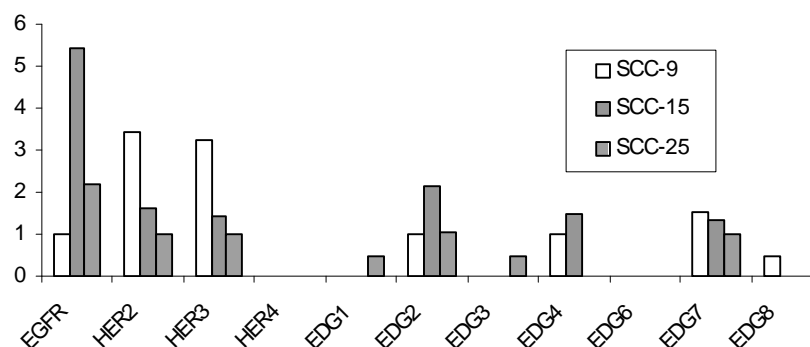


**Figure 5. Expression pattern of EGFR- and EDG receptor family members by cDNA micro-array analysis.** cDNA prepared from SCC-9, SCC-15 and SCC-25 cells was labelled with  $\alpha$ [ $^{33}$ P]dATP and hybridized on array filters as described under *Materials and Methods*. Data represent relative hybridization signals for individual genes.

Therefore, the effect of pertussis toxin (PTX) which inactivates  $G\alpha$  subunits of the  $G_i/o$  family of G proteins on LPA-induced EGFR tyrosine phosphorylation was examined. As shown in Figure 6A, pre-incubation of head and neck cancer cells with PTX (100 ng/ml) strongly attenuated the EGFR transactivation signal upon LPA stimulation whereas carbachol-, EGF- and pervanadate-induced EGFR tyrosine phosphorylation remained unaffected. (Pervanadate is a potent tyrosine phosphatase inhibitor which increases the tyrosine phosphorylation content of many intracellular proteins (Huyer et al., 1997)). These findings suggested that a predominantly PTX-sensitive cross-talk pathway links agonist-treated LPA receptors with the EGFR in HNSCC cells.

Recently, Prenzel et al. have demonstrated that GPCR-induced EGFR transactivation in COS-7 and HEK-293 cells requires proteolytic cleavage of the membrane-anchored growth factor precursor proHB-EGF (Prenzel et al., 1999). To address the question whether a metalloprotease-dependent mechanism is involved in EGFR transactivation in HNSCC cells the effect of broad-spectrum metalloprotease inhibitors on GPCR-triggered EGFR signal activation in head and neck cancer cells was investigated. As shown in Figure 6A, the hydroxamic acid derivatives batimastat (BB94, 10  $\mu$ M) and marimastat (BB2516, 10  $\mu$ M), as well as the peptide-based metalloprotease inhibitor FN-439 (100  $\mu$ M), completely blocked LPA- and carbachol-induced EGFR tyrosine phosphorylation in SCC-9 cells while these compounds did not interfere with EGF or pervanadate stimulated EGFR activation (Fig. 6A, representative data shown for BB94). Similar results were obtained in SCC-4, SCC-15, SCC-25, FaDu and Detroit-562 cells. Under these experimental settings, serine-protease inhibitors such as PMSF (10  $\mu$ M) and aprotinin (100 ng/ml) did not influence the GPCR-induced transactivation signal (data not shown).

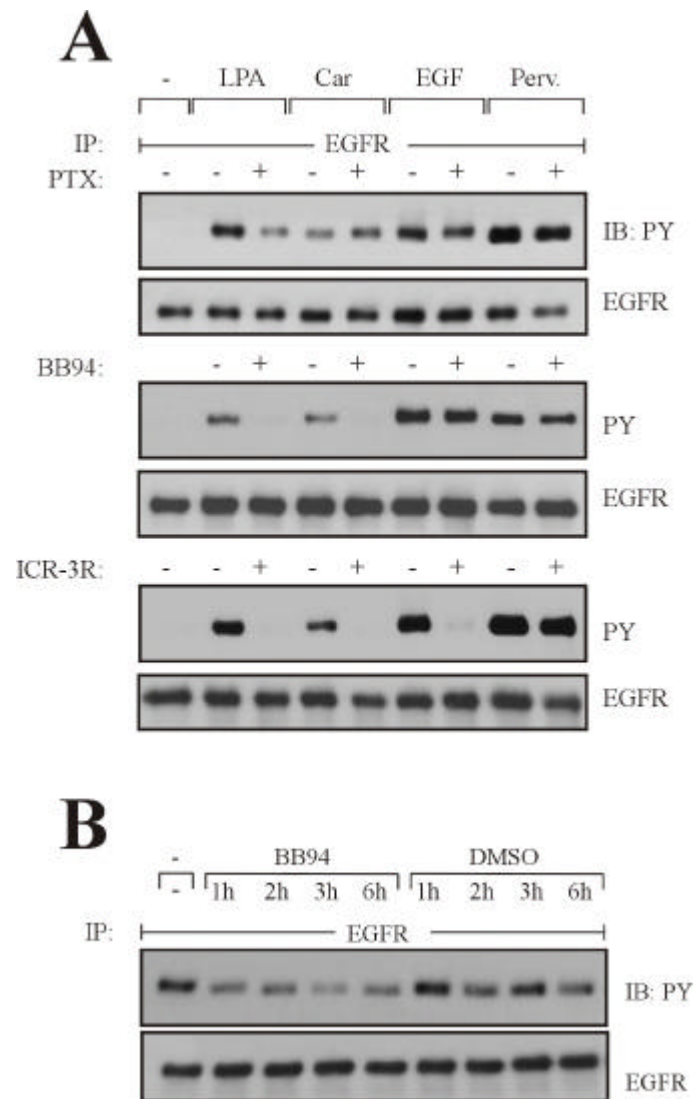


**Figure 6. Both, GPCR-induced and constitutive EGFR tyrosine phosphorylation, depend on metalloprotease activity.** A) Quiescent SCC-9 cells were pretreated with PTX (100 ng/ml; 18 h), batimastat (BB94, 10  $\mu$ M; 20 min), anti-EGFR blocking antibody ICR-3R (20  $\mu$ g/ml; 60 min) or an equal volume of vehicle, and stimulated for 3 min with 10  $\mu$ M LPA or 7.5 ng/ml EGF. Cell lysates were analyzed as described under *Figure 4*. B) SCC-25 cells were seeded at  $3 \times 10^5$  cells in 6-Well dishes in standard medium and incubated for 18 h. Cells were washed with PBS and incubated with medium without FCS in the presence of batimastat (BB94, 10  $\mu$ M) or vehicle (DMSO) for the indicated period of time. Cell lysates were analyzed as described under *Figure 4*.

Next, the effect of the EGFR-specific blocking antibody ICR-3R on EGFR phosphotyrosine content upon stimulation with GPCR ligands was examined. ICR-3R targets the extracellular domain of the EGFR and prevents binding of EGF-like ligands to the receptor (Mateo et al., 1997). Interestingly, preincubation of head and neck cancer cells with ICR-3R (20  $\mu$ g/ml) completely abrogated the EGFR transactivation signal and EGF-induced EGFR tyrosine phosphorylation whereas the antibody did not interfere with pervanadate-induced responses (Fig. 6A, representative data shown for SCC-9).

In addition to its effect on the EGFR transactivation signal upon acute GPCR stimulation, batimastat drastically reduced basal tyrosine phosphorylation levels of the EGFR in SCC-25

cells during a period of six hours after serum withdrawal (Fig. 6B) suggesting the critical involvement of metalloproteases in autocrine growth factor precursor shedding in HNSCC presumably by regulating basal EGFR ligand availability. Together, these experiments demonstrated that a variety of physiologically relevant GPCR agonists are capable of inducing rapid EGFR activation in head and neck cancer cells via a pathway that involves both PTX-sensitive and PTX-insensitive G proteins, metalloprotease activity and the extracellular ligand-binding domain of the EGFR. Moreover, metalloproteases are required for constitutive EGFR tyrosine phosphorylation in HNSCC.

### 3.2 Transactivation of HER2/neu is dependent on metalloprotease function and EGFR tyrosine kinase activity.

Since the oncoprotein HER2/neu, which serves as a prognostic marker in HNSCC (Quon et al., 2001), has been reported to be transactivated by agonist-treated GPCRs in Rat-1 fibroblasts (Daub et al., 1996) and since HER2/neu is expressed in SCC-9, SCC-15 and SCC-25 cells (Fig. 5) the question was raised whether HER2/neu is activated in response to LPA in this tumor type. The experiment presented in Figure 7 demonstrated that LPA (20  $\mu$ M) dramatically increased tyrosine phosphorylation of HER2/neu in SCC-9 cells and that transactivation of HER2/neu was sensitive to batimastat.

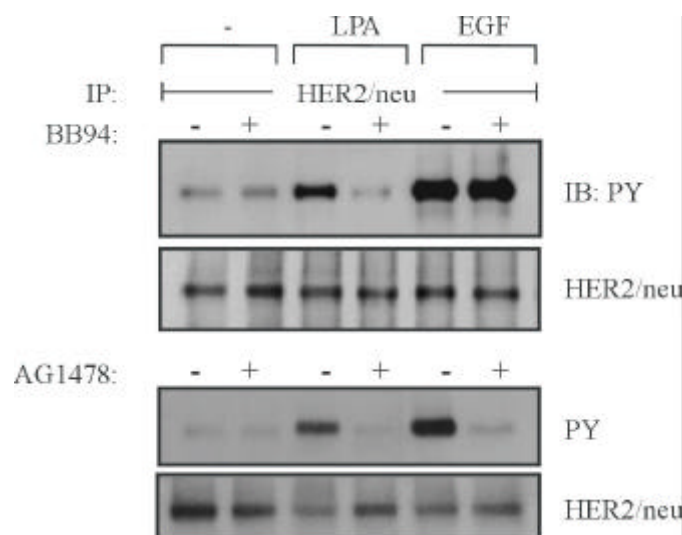


**Figure 7. Effect of metalloprotease and EGFR inhibition on LPA-induced transactivation of HER2/neu.** Quiescent SCC-9 cells were pretreated with batimastat (BB94, 10  $\mu$ M), AG1478 (250 nM) or an equal volume of vehicle (DMSO) for 20 min, and stimulated for 3 min with 20  $\mu$ M LPA or 10 ng/ml EGF. After cell lysis, HER2/neu was immunoprecipitated using polyclonal anti-HER2/neu antibody. Tyrosine-phosphorylated HER2/neu was detected by immunoblotting with monoclonal anti-phosphotyrosine antibody, followed by reprobing of the same filter with polyclonal anti-HER2/neu antibody.

In addition, tyrosine phosphorylation of HER2/neu following LPA or EGF treatment was abolished by the EGFR inhibitor AG1478 (250 nM). Phosphorylation of HER2/neu therefore appears to result from EGFR transphosphorylation. The above results implicate that the regulation of metalloproteases and the intrinsic EGFR tyrosine kinase activity are critical for LPA-induced transactivation of HER2/neu in HNSCC cells.

### 3.3 EGFR association and tyrosine phosphorylation of SHC and Gab1 upon LPA treatment is metalloprotease-dependent.

One key downstream event in the transmission of mitogenic signals by the activated EGFR is the association and subsequent tyrosine phosphorylation of adaptor proteins (Prenzel et al., 2001). Furthermore, SHC and Gab1 phosphorylation represent important regulatory steps in mitogenic GPCR signaling (Chen et al., 1996; Daub et al., 1997). To address the role of the EGFR and metalloproteases in LPA-induced adaptor protein recruitment, SHC was immunoprecipitated from SCC-9 lysates and immunoblotted against phosphotyrosine. As demonstrated in Figure 8, LPA stimulation lead to increased tyrosine phosphorylation of SHC and two proteins of 170 kDa and 116 kDa which co-immunoprecipitated with activated SHC.

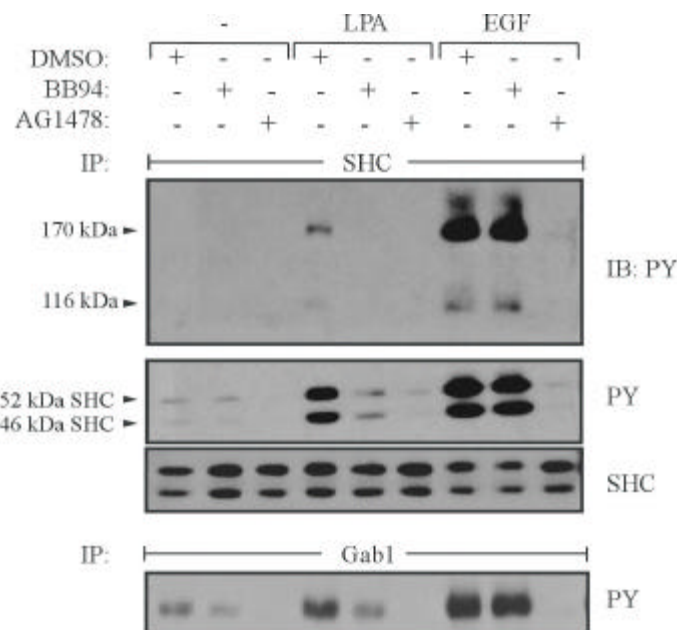


**Figure 8. LPA-stimulated SHC and Gab1 tyrosine phosphorylation requires both EGFR and metalloprotease activities.** Quiescent SCC-9 cells were preincubated with inhibitors as described under *Figure 7* and stimulated for 5 min with 10  $\mu$ M LPA or 7.5 ng/ml EGF. After cell lysis, SHC and Gab1 were immunoprecipitated using polyclonal anti-SHC and anti-Gab1 antibody, respectively. Tyrosine-phosphorylated proteins were detected by immunoblotting with monoclonal anti-phosphotyrosine antibody, followed by reprobing of the same filter with monoclonal anti-SHC antibody.

The 170 kDa protein showed immunoreactivity with anti-EGFR antibodies (data not shown) whereas in agreement with earlier reports the faint 116 kDa band could be identified as the adaptor protein Gab1 (Daub et al., 1997; Murasawa et al., 1998). Moreover, pre-treatment of SCC-9 cells with batimastat or AG1478 completely prevented LPA-induced tyrosine phosphorylation of SHC and of the co-immunoprecipitated EGFR and Gab1. As shown by immunoblot analysis, the increased Gab1 phosphotyrosine content in response to LPA treatment was sensitive to batimastat and AG1478 (Fig. 8). Moreover, batimastat did not alter EGF stimulated SHC and Gab1 tyrosine phosphorylation. Together, these data demonstrate that LPA mobilizes the docking proteins SHC and Gab1 by activating the EGFR through a metalloprotease-dependent pathway.

### 3.4 Activation of the ERK/MAPK pathway by LPA requires both EGFR function and metalloprotease activity.

Activation of the ERK/MAPK pathway is a key step in the regulation of important cellular responses such as cell proliferation. Therefore, the effect of LPA and EGF stimulation on MAPK activity in head and neck cancer cells was investigated by immunoblotting cell lysates with phospho-specific MAPK antibodies. In time-course experiments LPA (10  $\mu$ M) and EGF (5 ng/ml)-induced ERK/MAPK activation was detectable as early as three min following stimulation and peaked within 15 min in both SCC-9 and SCC-25 cells (Fig. 9, representative data shown for SCC-25).

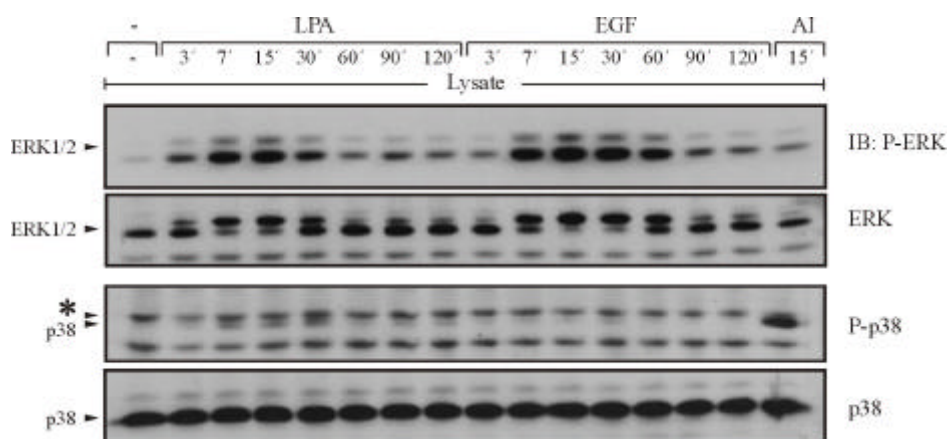


**Figure 9. Time-course of ERK and p38/MAPK activation.** Quiescent SCC-25 cells were treated with 10  $\mu$ M LPA, 5 ng/ml EGF or 5  $\mu$ g/ml anisomycin (AI) for the indicated times. After lysis, activated ERK1/2 and p38 was detected by immunoblotting of total lysates with polyclonal anti-phospho-ERK (*P-ERK*) or anti-phospho-p38 (*P-p38*) antibody, followed by reprobing of the same filter with monoclonal anti-ERK (*ERK*) and monoclonal anti-p38 (p38) antibody. \*, unspecific signal.

Furthermore, LPA-induced ERK activation was slightly more transient when compared to EGF stimulation. In contrast to ERK1/2, LPA and EGF only led to low-level activation of the stress-responsive MAPK p38, while anisomycin stimulation (5  $\mu\text{g/ml}$ ) served as a positive control.

Based on these findings, the functional role of the EGFR in activation of the MAPK ERK2 evoked by LPA was assessed in HNSCC cells. Previously, expression of a dominant-negative EGFR mutant has been shown to block EGFR-specific downstream signaling events (Daub et al., 1997). Therefore, hemagglutinin (HA)-tagged ERK2 (HA-ERK2) was co-expressed together with the EGFR mutant HER-CD533 in SCC-9 cells. HA-ERK2 activity was measured *in vitro* with an immunocomplex assay using myelin basic protein (MBP) as a substrate. As shown in Figure 10, LPA (10  $\mu\text{M}$ ) and EGF (5 ng/ml) lead to an eight-fold increase of HA-ERK2 activity in cells transfected with empty vector while in the presence of different amounts of HER-CD533, activation of HA-ERK2 was inhibited up to 75%. As specificity controls, expression of HER-CD533 did not influence PDGF stimulated HA-ERK2 activation and the dominant-negative  $\beta\text{PDGFR-CD504}$  mutant had no significant effect on HA-ERK2 activation by LPA. Interestingly,  $\beta\text{PDGFR-CD504}$  attenuated HA-ERK2 stimulation upon EGF treatment by 50%, pointing towards an additional cross-talk mechanism between these two RTKs as suggested before (Bagowski et al., 1999; He et al., 2001).

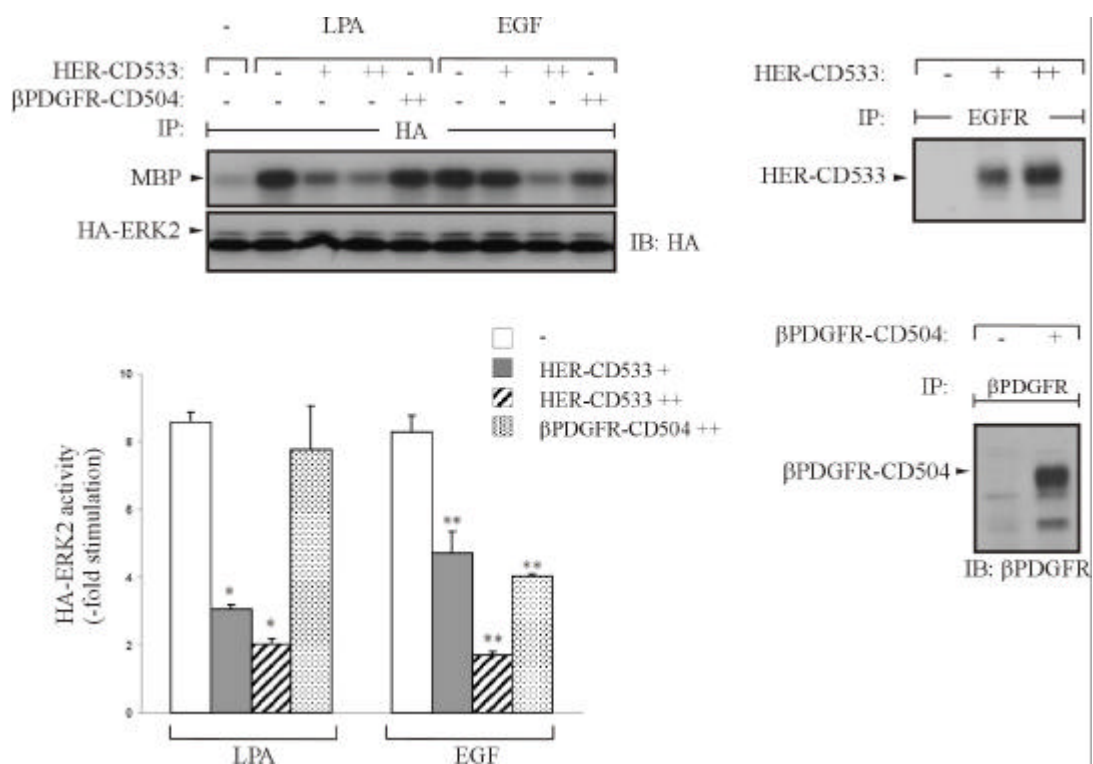


**Figure 10. Inhibition of ERK/MAPK activation by expression of dominant-negative EGFR HER-CD533.** SCC-9 cells were transiently transfected with an expression plasmid encoding HA-ERK2 (250 ng/well). Where indicated, a plasmid encoding HER-CD533 (+: 150 ng/well, ++: 450 ng/well) or  $\beta$ PDGFR-CD504 (+: 450 ng/well) were co-transfected. Following serum starvation for 24 h, cells were treated for 7 min with LPA (10  $\mu$ M) or EGF (5 ng/ml), lysed and HA-ERK2 activity was determined using MBP as substrate as described in *Materials and Methods*. Phosphorylated MBP was visualized by autoradiography after gel electrophoresis and HA-ERK2 was immunoblotted in parallel using monoclonal anti-HA antibody. Quantitative analysis of HA-ERK2 activation from three independent experiments (mean  $\pm$  s.d.). \*,  $P < 0.001$  for the difference between control + LPA and HER-CD533 + LPA; \*\*,  $P < 0.005$  for control + EGF versus HER-CD533 + EGF and  $\beta$ PDGFR-CD504. For expression control of HER-CD533, transfected cells were labeled with [ $^{35}$ S]methionine and lysates were subjected to immunoprecipitation with monoclonal anti-EGFR antibody followed by autoradiography. Expression of  $\beta$ PDGFR-CD504 was detected by subjecting lysates to immunoprecipitation with anti- $\beta$ PDGFR 128D4C10 antibody and by immunoblotting with monoclonal anti- $\beta$ PDGFR antibody.

To extend the results obtained with ectopically expressed ERK in SCC-9 cells, the requirement of EGFR and metalloprotease activities for activation of endogenous ERK/MAPK in response to LPA was investigated. AG1478 treatment completely abrogated ERK2 activation upon LPA and EGF stimulation in SCC-9 and SCC-25 cancer cells (Fig. 11).

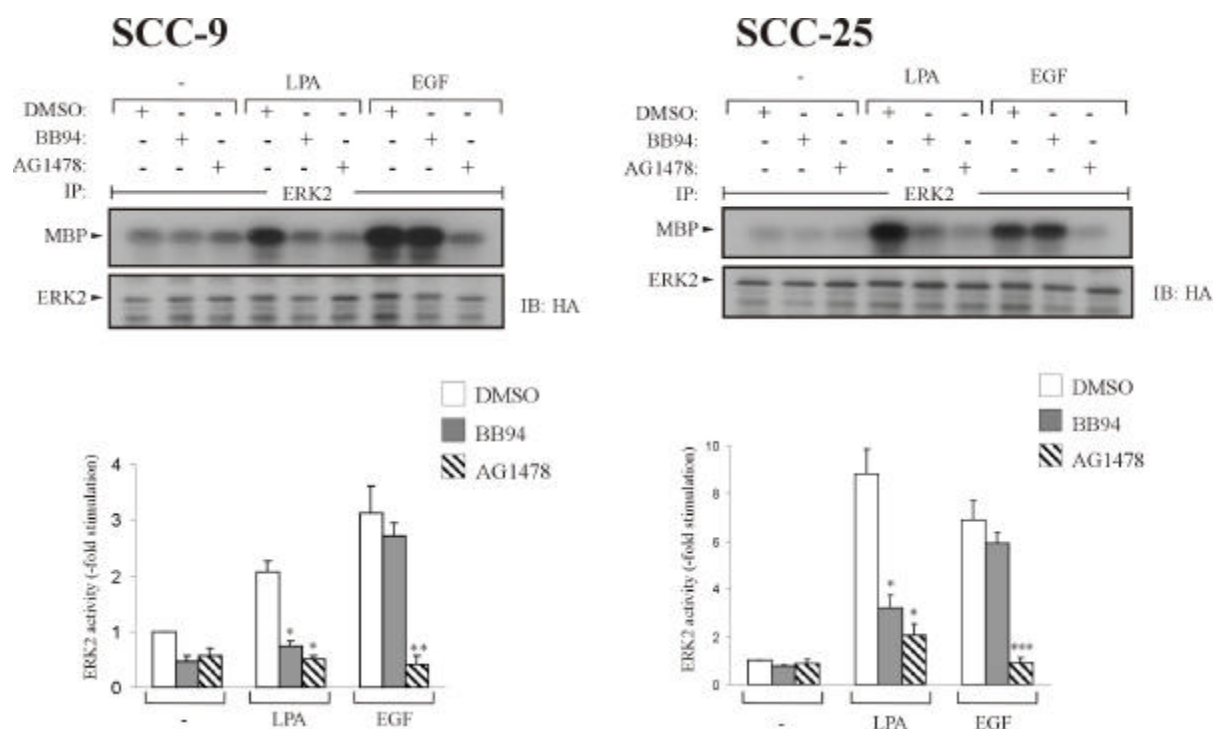


**Figure 11. Inhibition of endogenous ERK/MAPK activation by interfering with EGFR signal transmission.** Quiescent SCC-9 and SCC-25 cells were preincubated with batimastat (10  $\mu$ M), AG1478 (250 nM) or vehicle (DMSO) for 20 min, and stimulated for 7 min with 10  $\mu$ M LPA or 5 ng/ml EGF. After cell lysis, endogenous ERK2 was immunoprecipitated using polyclonal anti-ERK2 antibody and ERK2 activity was determined using MBP as substrate and ERK2 was immunoblotted in parallel using polyclonal anti-ERK2 antibody. Quantitative analysis of endogenous ERK2 activation from three independent experiments (mean  $\pm$  s.d.). \*,  $P < 0.005$  for the difference between DMSO + LPA versus BB94 + LPA and AG1478 + LPA; \*\*,  $P < 0.01$  for DMSO + EGF versus AG1478 + EGF (SCC-9). \*\*\*,  $P < 0.05$  for DMSO + EGF versus AG1478 + EGF (SCC-25).

Furthermore, LPA-triggered ERK2 activation was almost completely inhibited by batimastat whereas ERK2 activation by exogenous EGF was minimally affected. Taken together, these data demonstrate a critical role for metalloprotease-mediated transactivation of the EGFR in promotion of the ERK/MAPK pathway in HNSCC cells.

Recently, the NRTK Src was shown to be a critical mediator of GPCR-induced ERK/MAPK activation that can either act upstream (Luttrell et al., 1997) or downstream (Daub et al., 1997) of the transactivated EGFR. To address the role of Src in the EGFR transactivation pathway in HNSCC the effect of the Src inhibitor PP1 on GPCR-triggered EGFR and ERK activation was investigated. The results showed that PP1 did not affect LPA-induced EGFR tyrosine phosphorylation (Fig. 12A) whereas ERK activation by LPA was completely abrogated (Fig. 12B). These data suggested the involvement of Src in ERK activation by LPA downstream of the EGFR in HNSCC cells.

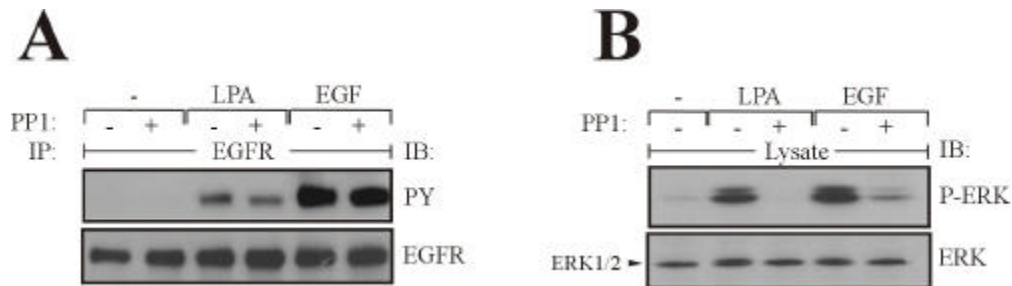


**Figure 12. Effect of the Src inhibitor PP1 on LPA-triggered EGFR tyrosine phosphorylation and ERK/MAPK activation.** Quiescent SCC-9 cells were preincubated with PP1 (20  $\mu$ M, 30 min) or vehicle and stimulated with LPA (10  $\mu$ M) or EGF (7.5 ng/ml) for 3 min. Tyrosine-phosphorylated EGFR (A) and activated ERK (B) were identified as described above.

### 3.5 Metalloprotease-dependent transactivation of the EGFR is required for LPA-induced DNA synthesis and S-phase progression.

Since it has been observed that batimastat reduces basal tyrosine phosphorylation levels of the EGFR in SCC-25 cells (Fig. 6B), it was next investigated whether metalloprotease- or EGFR inhibition influences proliferation of HNSCC cells under normal growth conditions in the presence of 10% FCS. As shown in Figure 13A, batimastat and AG1478 completely blocked growth of SCC-25 cells demonstrating that metalloprotease and EGFR activities are required for growth of HNSCC cells.

For further quantification of mitogenic signaling in response to LPA, the rate of DNA synthesis was measured by an  $^3$ H-thymidine incorporation assay. In SCC-9 and SCC-25 cells that express low and medium levels of EGFR, respectively, AG1478 blocked DNA synthesis in response to LPA or EGF stimulation (Fig. 13B). Furthermore, batimastat reduced the rate

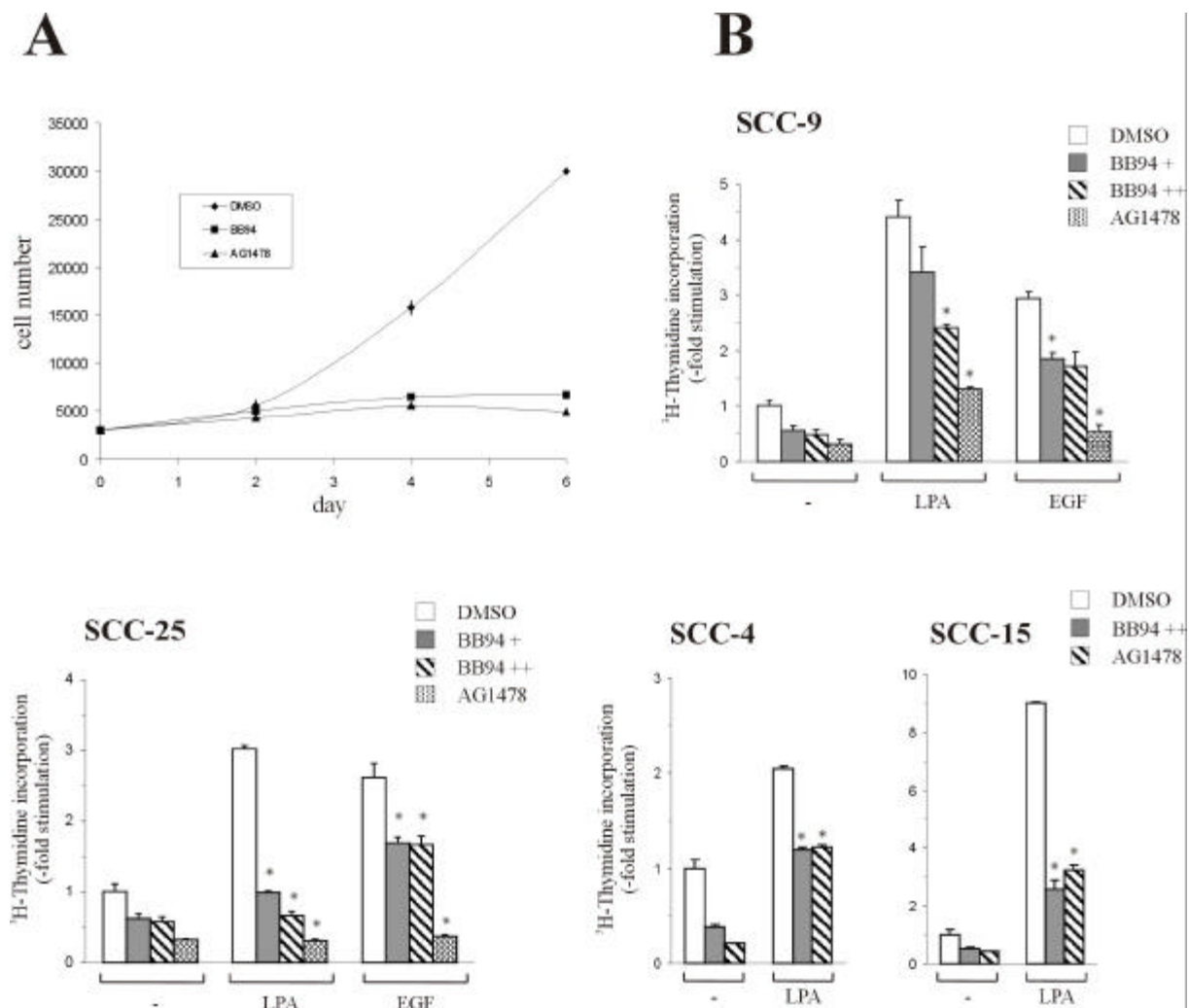


**Figure 13. Batimastat and the EGFR-specific tyrosphostin AG1478 inhibit general and LPA-induced cell proliferation and DNA synthesis.** A) Direct determination of cell proliferation: SCC-25 cells were grown in standard media containing 10% FCS in the presence of batimastat (10  $\mu$ M), AG1478 (250 nM) or vehicle (DMSO). Media were changed every two days. Cells were harvested by trypsination and counted by using a Coulter counter. Shown are the results of triplicate wells  $\pm$  s.d.. B)  $^3$ H-thymidine incorporation into DNA. Quiescent HNSCC cells were preincubated with batimastat (+: 5  $\mu$ M, ++: 10  $\mu$ M), AG1478 (250 nM) or vehicle (DMSO) for 20 min and incubated in the absence or presence of ligands (LPA, 10  $\mu$ M; EGF, 25 ng/ml) for 18 h. Cells were then pulse-labelled with  $^3$ H-thymidine and thymidine incorporation was measured by liquid-scintillation counting. Quantitative analysis from three independent experiments (mean  $\pm$  s.d.). \*,  $P < 0.025$  for the difference between control versus inhibitor-treated samples.

of DNA synthesis by LPA in a dose-dependent fashion up to 45% (10  $\mu$ M batimastat) in SCC-9, while in SCC-25 cells complete inhibition of DNA synthesis by batimastat was observed already at 5  $\mu$ M. This difference in batimastat-sensitivity indicates variations in the dependence of HNSCC cells on the TMPS pathway. Interestingly, DNA synthesis induction by exogenous EGF was also reduced by batimastat by 40% in SCC-9 cells and 35% in SCC-25 cells suggesting that EGF stimulation results in enhanced shedding of endogenous EGFR ligands. These findings are consistent with reports showing that HNSCC cell lines and tumors are mitogenically stimulated by EGF-like autocrine systems (O-Charoenrat et al., 2000b). In

addition, the MEK inhibitor PD98059 (5  $\mu$ M) completely inhibited basal, as well as, LPA- and EGF- induced DNA synthesis in SCC-9 and SCC-25 cells (data not shown), underscoring the importance of the Ras/MAPK pathway in the regulation of cell proliferation in response to growth factor stimulation. In the EGFR over-expressing cell lines SCC-4 and SCC-15 LPA was also able to stimulate thymidine incorporation in a batimastat- and AG1478-dependent manner (Fig. 13B) suggesting that cross-talk pathways between GPCRs and the EGFR are also relevant for head and neck cancer cell proliferation with high EGFR background.

To extend the results on proliferative responses upon GPCR stimulation growth factor-induced cell cycle progression of serum-deprived SCC-25 cells was investigated by flow cytometric analysis. As shown in Table 3, the accumulation of a S-phase cell population in response to LPA (25  $\mu$ M) was sensitive to metalloprotease inhibition. Complete abolishment of LPA-induced S-phase progression was observed in the presence of 5  $\mu$ M batimastat (Fig. 14). Under these experimental conditions, EGF (50 ng/ml) stimulated S-phase entry was reduced by 50% which, as mentioned above, indicates an involvement of metalloprotease-dependent growth factor precursor cleavage in the EGF action on these cells.

**Table 3** *LPA-induced S-phase progression is blocked by the metalloprotease inhibitor batimastat in SCC-25 cells*

Stimulus	Batimastat	< G1	G1	S	G2/M
-	-	5 <sup>a</sup>	75	9	11
LPA	-	3	65	19	13
	0.2 $\mu$ M	4	66	16	14
	1 $\mu$ M	5	71	12	12
	5 $\mu$ M	8	69	9	14
EGF	-	5	64	19	12
	0.2 $\mu$ M	8	61	19	12
	1 $\mu$ M	5	66	18	11
	5 $\mu$ M	6	69	14	11

<sup>a</sup>Flow cytometric analysis of SCC-25 cell cycle (% of cells). Quiescent SCC-25 cells were preincubated with batimastat or vehicle (DMSO) for 20 min and incubated in the absence or presence of ligands (LPA, 25  $\mu$ M; EGF, 50 ng/ml) for 18 h. Representative data of one of three experiments are shown.

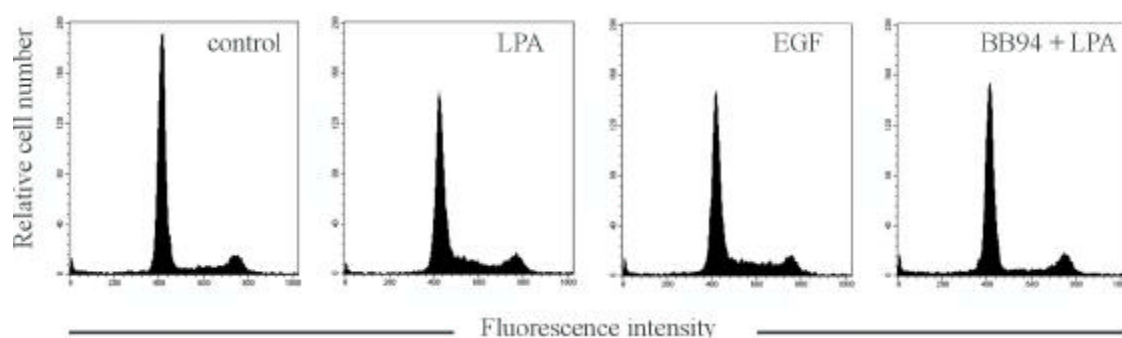


**Figure 14. Effect of metalloprotease inhibition on S-phase progression.** Quiescent SCC-25 cells were preincubated with batimastat (5  $\mu$ M) or vehicle (DMSO) for 20 min and incubated in the absence or presence of ligands (LPA, 25  $\mu$ M; EGF, 50 ng/ml) for 18 h. Cells were harvested and analysed by flow cytometry.

Together, these data emphasize the biological significance of metalloprotease-dependent EGFR signal transactivation in LPA-induced mitogenic signaling of head and neck cancer cells.

### 3.6 LPA enhances HNSCC cell motility via transactivation of the EGFR.

Besides proliferation, cell motility represents another critical parameter in the pathobiology of cancer. Recent reports demonstrated that EGF-like ligands such as HB-EGF, TGF $\alpha$  and amphiregulin promote invasion of HNSCC cells *in vitro* (O-Charoenrat et al., 2000a) and that LPA stimulation is capable of promoting migration of ovarian cancer cells (Fishman et al., 2001). It was therefore hypothesized that GPCR stimulation, that leads to EGFR transactivation, might influence the migratory behaviour of head and neck cancer cells. First, the effect of LPA on migration of HNSCC keratinocytes was investigated in an *in vitro* wound closure assay. Migration of cells was studied by scraping a wound into a confluent monolayer of SCC-9 or SCC-25 cells and determining the rate of closure. Both LPA (5  $\mu$ M or 20  $\mu$ M) and HB-EGF (20 ng/ml) drastically enhanced closure of the wounded area (Fig. 15A, representative data shown for SCC-9). Furthermore, wound closure in response to LPA was completely blocked by AG1478 or batimastat at selective concentrations. These observations suggested a role of the EGFR transactivation pathway in regulation of the migratory behaviour of head and neck cancer cells.

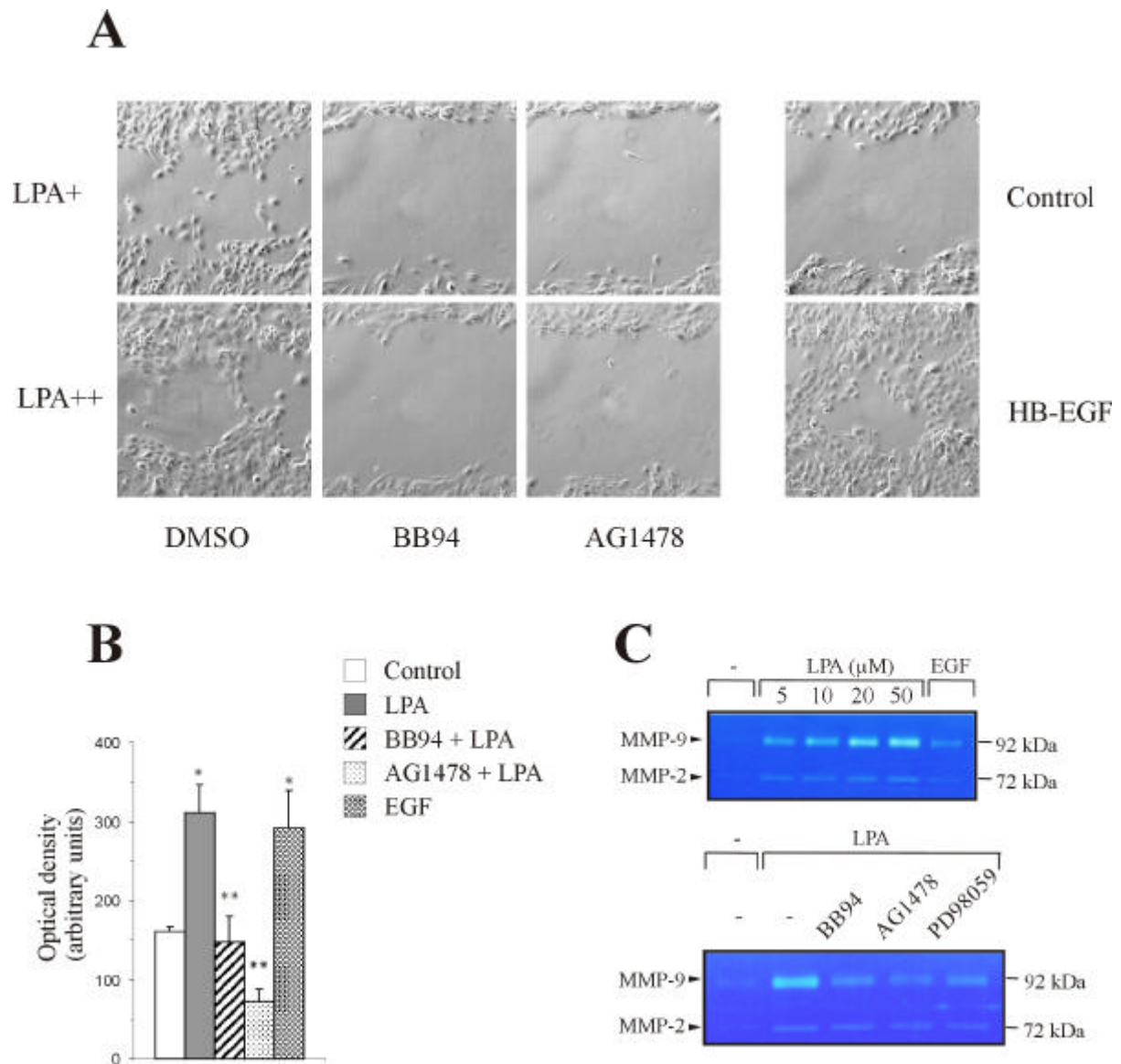


**Figure 15. GPCR stimulated wound closure, migration and expression of MMP-9 require both EGFR and metalloprotease activities.** **A)** *In vitro* wound closure assay. SCC-9 cells were seeded into 6-Well plates and grown to confluence for a classical wounding assay. Cells were scraped with a plastic tip, the medium was removed and cells were rinsed twice with PBS. Medium without FCS was added and cells were preincubated with either DMSO (control), 250 nM AG1478 or 10  $\mu$ M batimastat. Cells were stimulated with LPA (+: 5  $\mu$ M, ++: 20  $\mu$ M) or HB-EGF (20 ng/ml) and permitted to migrate for 48 h. The dishes were monitored microscopically (20x). **B)** Chemotactic migration toward fibronectin. SCC-9 cells were preincubated with either DMSO (control), 125 nM AG1478 or 5  $\mu$ M batimastat. Cells were seeded into membrane inserts of transwell dishes in the presence or absence of ligands (LPA, 50  $\mu$ M; EGF, 25 ng/ml) and were permitted to migrate for 36 h toward fibronectin as a chemoattractant. Nonmigrated cells were removed from the upper surface of the membrane, while the cells that had migrated to the lower surface were fixed and stained with crystal violet. Absorbance of solubilized cells was measured with a micro-plate reader. Each bar is the average of quadruplicate values (mean  $\pm$  s.d.). \*,  $P < 0.005$  for the difference between control versus LPA and EGF. \*\*,  $P < 0.001$  between LPA versus BB94 + LPA and AG1478 + LPA. **C)** Zymography of conditioned media from SCC-25 cells. Quiescent SCC-25 cells were stimulated with the indicated concentration of LPA and 25 ng/ml EGF, respectively, for 2 d (*upper panel*) or stimulated with 10  $\mu$ M LPA in the presence of 10  $\mu$ M batimastat, 250 nM AG1478, 10  $\mu$ M PD98059 or vehicle (*lower panel*). Gelatinolytic activity of MMP-2 and MMP-9 was visualized by staining gels with Coomassie G250.

Secondly, the chemotactic motility of HNSCC cells in response to growth factor stimulation was assessed in a modified Boyden chamber assay. Similar to the results obtained in the induction of wound closure, chemotactic migration of SCC-9 cells toward fibronectin was strongly potentiated by LPA or EGF stimulation (Fig. 15B). Moreover, inhibition of EGFR or metalloprotease activity prevented LPA-triggered migration of SCC-9 cells.

Besides high EGFR expression levels, over-expression of certain matrix metalloproteinases (MMPs) has been associated with increased invasive potential of HNSCC tumors and poor prognosis. Recently, it has been demonstrated that direct EGFR stimulation with EGF-like ligands upregulates the expression of MMP-9 in HNSCC cell lines (O-Charoenrat et al., 2000a). Therefore, the effect of LPA on the expression of MMP-2 and MMP-9 in SCC-25 cells was determined by gelatin zymography. As shown in Figure 15C, LPA drastically induced the expression of MMP-9 in a concentration-dependent manner, while the expression of MMP-2 was only weakly affected. Moreover, LPA-induced MMP-9 expression was significantly inhibited by batimastat, AG1478 and the MEK inhibitor PD98059, suggesting a direct role of the TMPS pathway and downstream ERK activation in the regulation of MMP-9 expression in head and neck cancer cells.

Altogether, these data substantiate the importance of EGFR and metalloprotease function in GPCR stimulated motility of head and neck cancer cells.

### **3.7 LPA promotes cell-surface ectodomain processing and release of AR.**

It has been reported previously that LPA stimulation leads to the metalloproteolytic processing of the growth factor precursor HB-EGF in COS-7 and VeroH cells (Hirata et al., 2001; Prenzel et al., 1999; Umata et al., 2001). To gain further insight into the molecular mechanisms of EGFR signal transactivation in head and neck cancer, the question was addressed whether HB-EGF or other EGF-like growth factors are cleaved upon GPCR stimulation in HNSCC. By cDNA micro-array analysis expression of HB-EGF, TGF $\alpha$  and AR mRNAs was found in SCC-9, SCC-15 and SCC-25 cells (Fig. 16). Expression on the protein level, as well as, cell-surface localization of these ligands were confirmed by flow cytometry using ectodomain specific antibodies (Fig. 17A). Interestingly, and in contrast to the results in COS-7 cells, treatment of SCC-9 and SCC-15 cancer cells with LPA (10  $\mu$ M) or the phorbol ester TPA (1 mM) dramatically reduced the cell surface content of endogenous proAR (Fig. 17B).

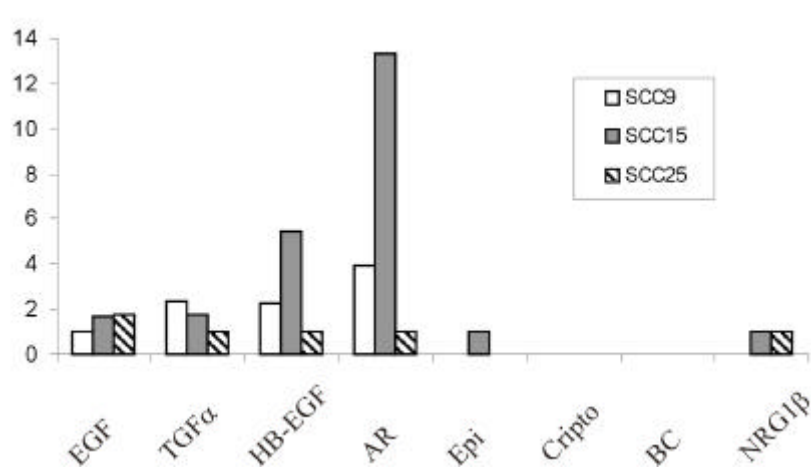


**Figure 16. Expression pattern of EGF-like growth factor precursors by cDNA micro-array analysis.** cDNA prepared from SCC-9, SCC-15 and SCC-25 cells was labelled with  $\alpha$ [ $^{33}$ P]dATP and hybridized on array filters as described under *Materials and Methods*. Data represent relative hybridization signals for individual genes.

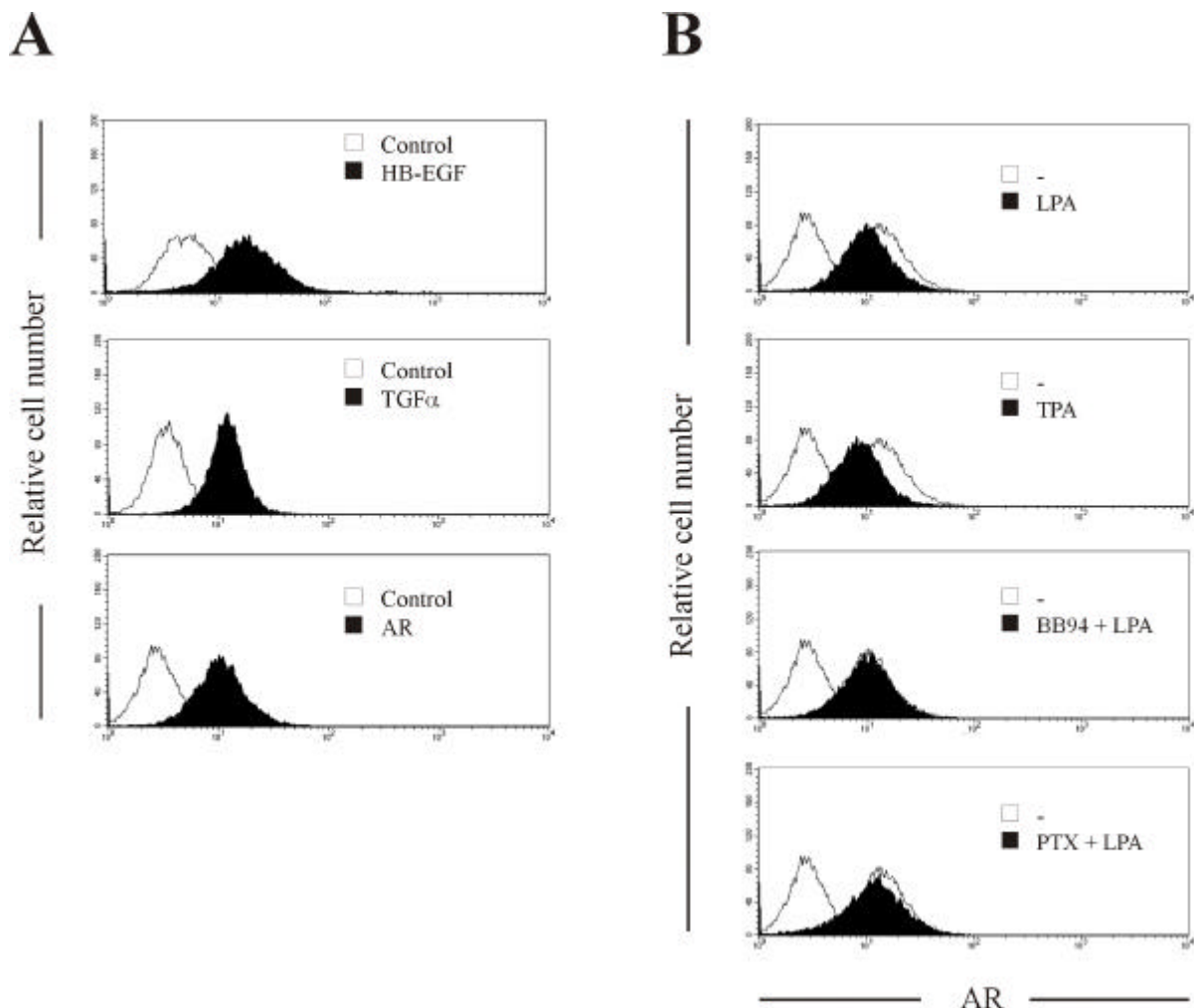


**Figure 17. Flow cytometric analysis of EGF-like precursor expression and LPA-induced proteolytic processing of proAR.** A) Quiescent SCC-9 cells were collected and stained for surface HB-EGF, TGF $\alpha$  or AR and analysed by flow cytometry. Control cells were labelled with FITC-conjugated secondary antibody alone. B) SCC-9 cells were serum-starved for 24 h, incubated for the last 18 h with PTX (100 ng/ml) or for 20 min with batimastat (10  $\mu$ M) and stimulated for 5 min with LPA (10  $\mu$ M) or TPA (1  $\mu$ M). Control cells were labelled with FITC-conjugated secondary antibody alone. Cells were collected and analysed for cell surface AR density by flow cytometry.

However, in this cellular context, LPA was not able to induce the proteolytic cleavage of proTGF $\alpha$  or proHB-EGF, while TPA stimulation resulted in shedding of both EGF-like growth factor precursors (data not shown). These findings suggested that LPA stimulation selectively induces shedding of proAR in HNSCC. AR is widely expressed in normal human tissues (Plowman et al., 1990) and represents the major autocrine growth factor for keratinocytes in the process of wound healing (Cook et al., 1991; Schelfhout et al., 2002). Interestingly, enhanced expression of AR has been detected in epidermal biopsies derived from psoriatic lesions as well as in colon and stomach carcinomas (Cook et al., 1992). Moreover, AR has been shown to act as an autocrine growth factor for normal and transformed mammary epithelial and colon carcinoma cells (Johnson et al., 1992; Li et al., 1992; Normanno et al., 1994). In agreement with the previous findings demonstrating an involvement of predominantly PTX-sensitive G proteins in EGFR transactivation (Fig. 6A), PTX (100 ng/ml) partially inhibited proAR shedding at the cell-surface of SCC-9 cells (Fig. 17B). In addition, batimastat (BB94, 10  $\mu$ M) completely abolished LPA-induced ectodomain cleavage of proAR (Fig. 17B). This result confirmed the requirement of metalloprotease activity for proAR shedding in response to GPCR stimulation mediated by PTX-sensitive and, to lesser extent, PTX-insensitive G proteins.

In addition to the decrease in the amount of cell-surface proAR (17B), LPA stimulation resulted in the accumulation of mature AR in cell culture medium as determined by sandwich-ELISA (Fig. 18).

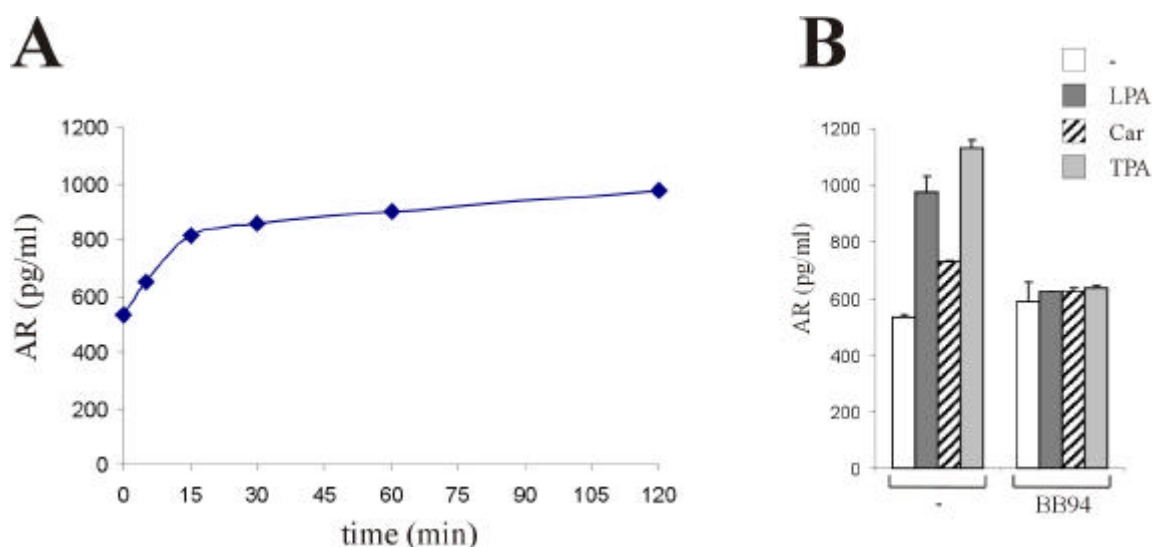


**Figure 18. GPCR-induced proteolytic release of AR by sandwich-ELISA.** A) Quiescent SCC-9 cells were stimulated with 10  $\mu$ M LPA as indicated. Conditioned medium was collected and analyzed for total amount of AR by ELISA. Each point is the average of duplicate values. B) Quiescent SCC-9 cells were preincubated with batimastat (10 mM) or vehicle for 20 min followed by stimulation with 10  $\mu$ M LPA, 1 mM carbachol, 1 mM TPA for 120 min and analyzed as described under A). Each bar is the average of triplicate values (mean  $\pm$  s.d.).

The amount of free AR increased from 533 pg/ml to 975 pg/ml within 120 min after LPA stimulation, while half-maximal AR-release was observed already after about 10 min (Fig. 18A). AR release in response to carbachol was substantially lower compared to LPA stimulation (Fig. 18B) suggesting a direct correlation between the amount of released AR and the EGFR tyrosine phosphorylation content in response to GPCR ligands (see Fig. 4A, 6A). Moreover, pre-incubation with batimastat completely prevented GPCR- and TPA-induced accumulation of AR in cell culture medium (Fig. 18B), demonstrating metalloprotease-dependency of AR release.

In conclusion, stimulation of head and neck cancer cells with the GPCR ligands LPA and carbachol results in the rapid activation of a metalloprotease activity that specifically cleaves proAR at the cell surface, subsequently leading to release of the mature growth factor.

### **3.8 LPA-induced EGFR signal transactivation and downstream events depend on AR.**

To gain insight into the functional role of AR precursor processing in the EGFR transactivation pathway the effect of anti-AR neutralizing antibodies on EGFR-tyrosine-phosphorylation by LPA in SCC-9 cells was examined. Pre-treatment with either polyclonal goat (50 µg/ml) or monoclonal mouse (25 µg/ml) antibodies raised against the ectodomain of human AR inhibited the EGFR transactivation signal while EGFR activation upon EGF stimulation remained unaffected (Fig. 19A). Similar results were obtained upon stimulation of SCC-9 cells with carbachol (data not shown). In contrast, inhibition of HB-EGF by using the diphtheria toxin mutant CRM197 or anti-HB-EGF neutralizing antibodies showed no effect on LPA- or carbachol-induced EGFR transactivation (data not shown). Since it has been observed that the glycosaminoglycan heparin abrogates thrombin-induced EGFR transactivation in vascular smooth muscle cells by blocking HB-EGF function (Kalmes et al., 2000) and both HB-EGF and AR belong to the family of heparin-binding growth factors the question was raised whether heparin treatment of SCC-9 cells would affect the EGFR transactivation signal.



### 3.9 ProAR processing is required for ERK/MAPK activation and Akt/PKB phosphorylation in response to LPA.

To define whether AR participates in LPA stimulated ERK/MAPK activation in HNSCC cells, the effect of AR inhibition on ERK1/2 activation was studied.

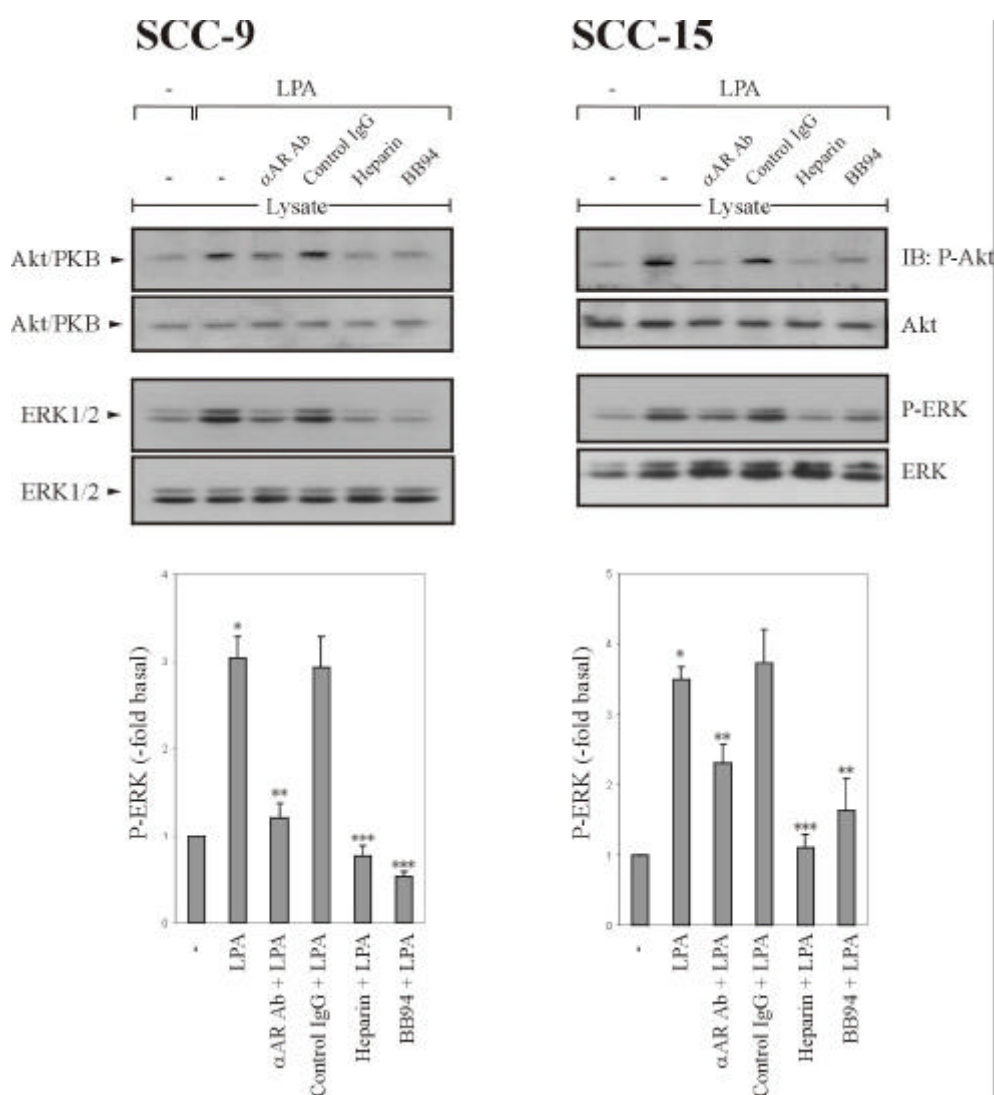


**Figure 20. AR is required for GPCR-induced ERK/MAPK activation and Akt/PKB phosphorylation.**

Quiescent SCC-9 or SCC-15 cells were pretreated with anti-AR neutralizing antibodies ( $\alpha$ AR Ab, 50  $\mu$ g/ml), control IgG (50  $\mu$ g/ml), heparin (100 ng/ml) or batimastat (10  $\mu$ M), and stimulated for 7 min with 10  $\mu$ M LPA or 7.5 ng/ml EGF. Phosphorylated ERK1/2 was detected by immunoblotting of total lysates with anti-phospho-ERK antibodies (P-ERK). The same filters were reprobed with anti-ERK antibodies (ERK). Quantitative analysis of ERK phosphorylation from three independent experiments (mean  $\pm$  s.d.). SCC-9: \*,  $P < 0.05$  for the difference between unstimulated control versus LPA; \*\*,  $P < 0.001$  for LPA vs.  $\alpha$ AR Ab + LPA; \*\*\*,  $P < 0.025$  for LPA vs. Heparin + LPA and BB94 + LPA. SCC-15: \*,  $P < 0.025$  for the difference between unstimulated control versus LPA; \*\*,  $P < 0.05$  for LPA vs.  $\alpha$ AR Ab + LPA and BB94 + LPA; \*\*\*,  $P < 0.001$  for LPA vs. Heparin + LPA. Stimulation of Akt/PKB. Quiescent SCC-9 or SCC-15 cells were processed as described above and whole cell lysates were immunoblotted with anti-phospho-Akt/PKB antibodies (P-Akt/PKB). The same filters were reprobed with anti-Akt/PKB antibodies (Akt/PKB).

As shown on Figure 20, anti-AR neutralizing antibodies, heparin and batimastat completely prevented LPA-induced ERK activation in SCC-9 cells as determined by immunoblotting of lysates with anti-phospho-ERK antibody and subsequent quantification.

In SCC-15, AR blocking antibodies reduced ERK phosphorylation in response to LPA by 50%, heparin by 95% and batimastat by 75%, respectively. These findings suggested that LPA signaling to ERK1/2 in oral squamous cell carcinoma occurs via both an AR- and metalloprotease-dependent pathway.

In addition to its mitogenic effect, several investigations have revealed that LPA acts as a survival factor by activating both the ERK/MAPK pathway and the PI-3K-dependent phosphorylation of Akt/PKB in diverse cell types (Fang et al., 2002; Sautin et al., 2001; Yart et al., 2002). Therefore, the question was raised whether GPCR stimulation induces phosphorylation of Akt/PKB in head and neck cancer cells. The results indicated that LPA drastically increased phosphorylation of Akt/PKB at Ser-473 in SCC-9 and SCC-15 cells (Fig. 20) and that Akt/PKB phosphorylation was substantially inhibited by AR-blockade or batimastat treatment. Moreover, Akt/PKB phosphorylation by LPA and carbachol was prevented by AG1478 and sensitive to PI-3K inhibition by wortmannin (100 nM) and LY294002 (100  $\mu$ M; Fig. 21).

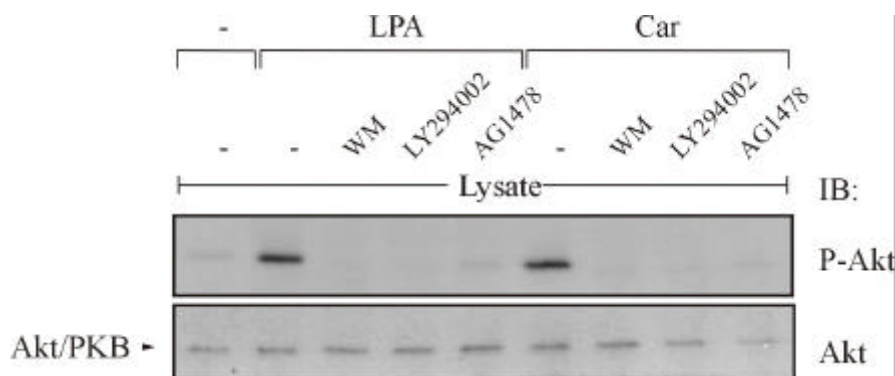


**Figure 21. PI3K and EGFR are required for GPCR-induced Akt/PKB phosphorylation.** Quiescent SCC-9 cells were pre-treated with wortmannin (WM, 100 nM), LY294002 (100  $\mu$ M), AG1478 (250 nM) or vehicle for 30 min and stimulated with 10  $\mu$ M LPA or 1 mM carbachol (*Car*) for 15 min. After lysis, activated Akt/PKB was detected by immunoblotting of total lysates with polyclonal anti-phospho-Akt/PKB (*P-Akt*) antibody, followed by reprobing of the same filter with polyclonal anti-Akt/PKB (*Akt*) antibody.

Together, these findings demonstrated that metalloprotease-dependent processing of the heparin-binding growth factor proAR is a crucial step in LPA-induced ERK/MAPK activation and phosphorylation of Akt/PKB in HNSCC cells.

### 3.10 AR bioactivity is involved in LPA stimulated DNA synthesis and cell motility.

To further extend the studies on AR function for growth-promoting GPCR signaling the effect of AR inhibition on LPA-induced DNA synthesis was examined in an  $^3\text{H}$ -thymidine incorporation assay. As shown in Figure 22A, HNSCC cells displayed a significant reduction in the rate of DNA synthesis triggered by LPA upon AR inhibition by 50% (AR neutralizing antibody + LPA or heparin + LPA) suggesting that a full proliferative response triggered by LPA requires AR. Moreover, batimastat and the EGFR-specific inhibitor tyrphostin AG1478 decreased DNA synthesis by LPA to below basal level.

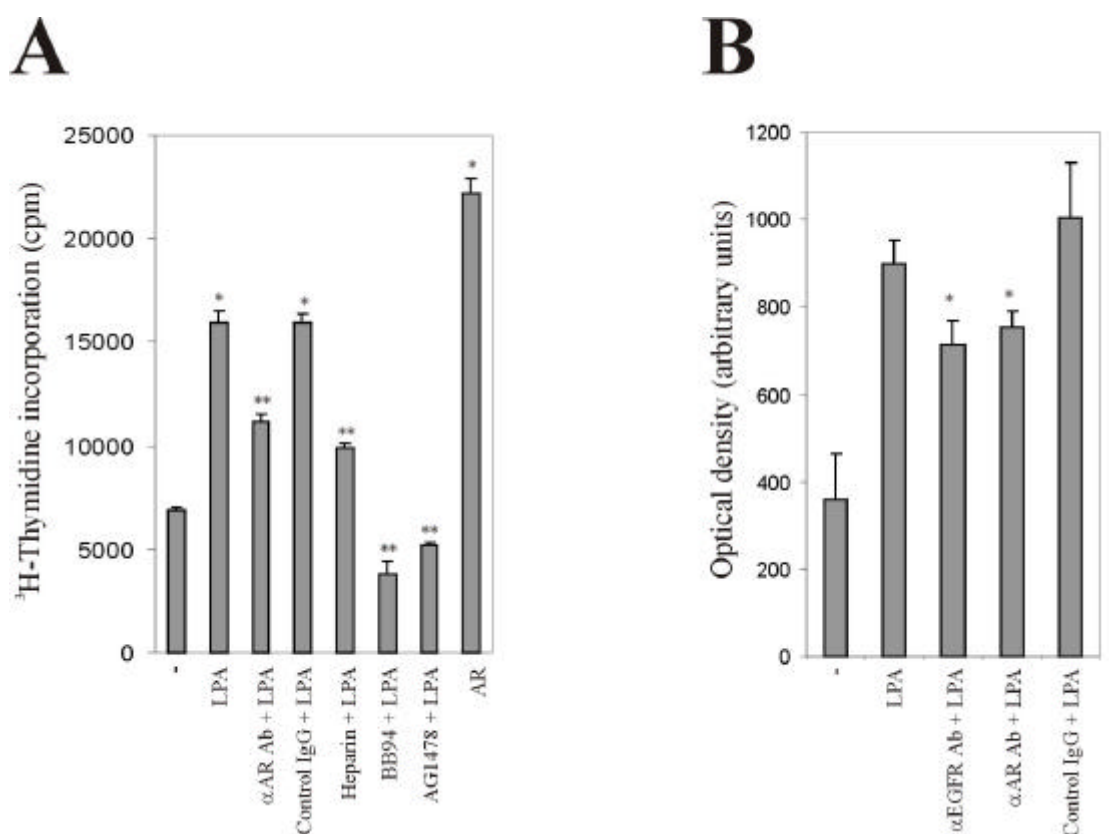


**Figure 22. Effect of AR inhibition on LPA-induced DNA synthesis and migration.** A)  $^3\text{H}$ -thymidine incorporation into DNA. Quiescent SCC-15 cells were pre-incubated with AR neutralizing antibodies ( $\alpha\text{AR Ab}$ , 50  $\mu\text{g/ml}$ ), control IgG (50  $\mu\text{g/ml}$ ), 100 ng/ml heparin, batimastat (10  $\mu\text{M}$ ) or AG1478 (250 nM) and incubated in the absence or presence of ligands (LPA, 10  $\mu\text{M}$ ; AR, 10 ng/ml) for 18 h. Cells were then pulse-labelled with  $^3\text{H}$ -thymidine and thymidine incorporation was measured by liquid-scintillation counting. Quantitative analysis from three independent experiments (mean  $\pm$  s.d.). \*,  $P < 0.001$  for the difference between unstimulated control vs. LPA, control IgG + LPA and AR; \*\*,  $P < 0.001$  for LPA vs.  $\alpha\text{AR Ab} + \text{LPA}$ , Heparin + LPA, BB94 + LPA and AG1478 + LPA. B) Chemotactic migration toward fibronectin. Quiescent SCC-9 cells were preincubated with anti-EGFR neutralizing antibody ICR-3R ( $\alpha\text{EGFR Ab}$ , 20  $\mu\text{g/ml}$ ), AR neutralizing antibody ( $\alpha\text{AR Ab}$ , 50  $\mu\text{g/ml}$ ) or control IgG (50  $\mu\text{g/ml}$ ) in the absence or presence of LPA (50  $\mu\text{M}$ ). Migration of cells was analyzed as described under Figure 15. Each bar is the average of quadruplicate values (mean  $\pm$  s.d.). \*,  $P < 0.025$  for the difference between LPA versus LPA + blocking antibody-treated samples.

Since LPA has been identified as a potent stimulus of cell migration in head and neck cancer cells (see Fig. 15) the effect of AR inhibition on chemotactic motility was studied. The results show that AR and EGFR neutralizing antibodies inhibited LPA-induced tumor cell migration by 16% and 21%, respectively, while control IgG had no effect (Fig. 22B). The results presented here, demonstrating specific involvement of AR function in LPA- and carbachol-induced EGFR tyrosine phosphorylation and motility of HNSCC cells (3.8-3.10) were independently verified by studies conducted in collaboration with S. Hart (this department, MPI of Biochemistry) using RNA interference technology (S. Hart, personal communication; Gschwind, A. *et al.*, submitted, 2002).

In summary, these data further substantiate the importance of AR function as a key element in mitogenic and motility-promoting LPA signaling in head and neck cancer.

### **3.11 TACE is required for proAR shedding and EGFR signal transactivation by LPA and carbachol in HNSCC cells.**

Recent observations have suggested a role of the metalloprotease-disintegrin TACE/ADAM17 in shedding of proAR and other EGF-like growth factor precursors in murine fibroblasts (Peschon *et al.*, 1998; Sunnarborg *et al.*, 2002). Moreover, the proteolytic activity of TACE has been shown to be inhibited by the tissue inhibitor of metalloprotease-3 (Timp-3) but not Timp-1 *in vitro* (Amour *et al.*, 1998). Since TACE and also other ADAMs were found to be widely expressed in HNSCC cell lines on the mRNA (Fig. 23A) and protein level (Fig. 23B) the effect of Timp-1 and Timp-3 on the EGFR transactivation signal was investigated.

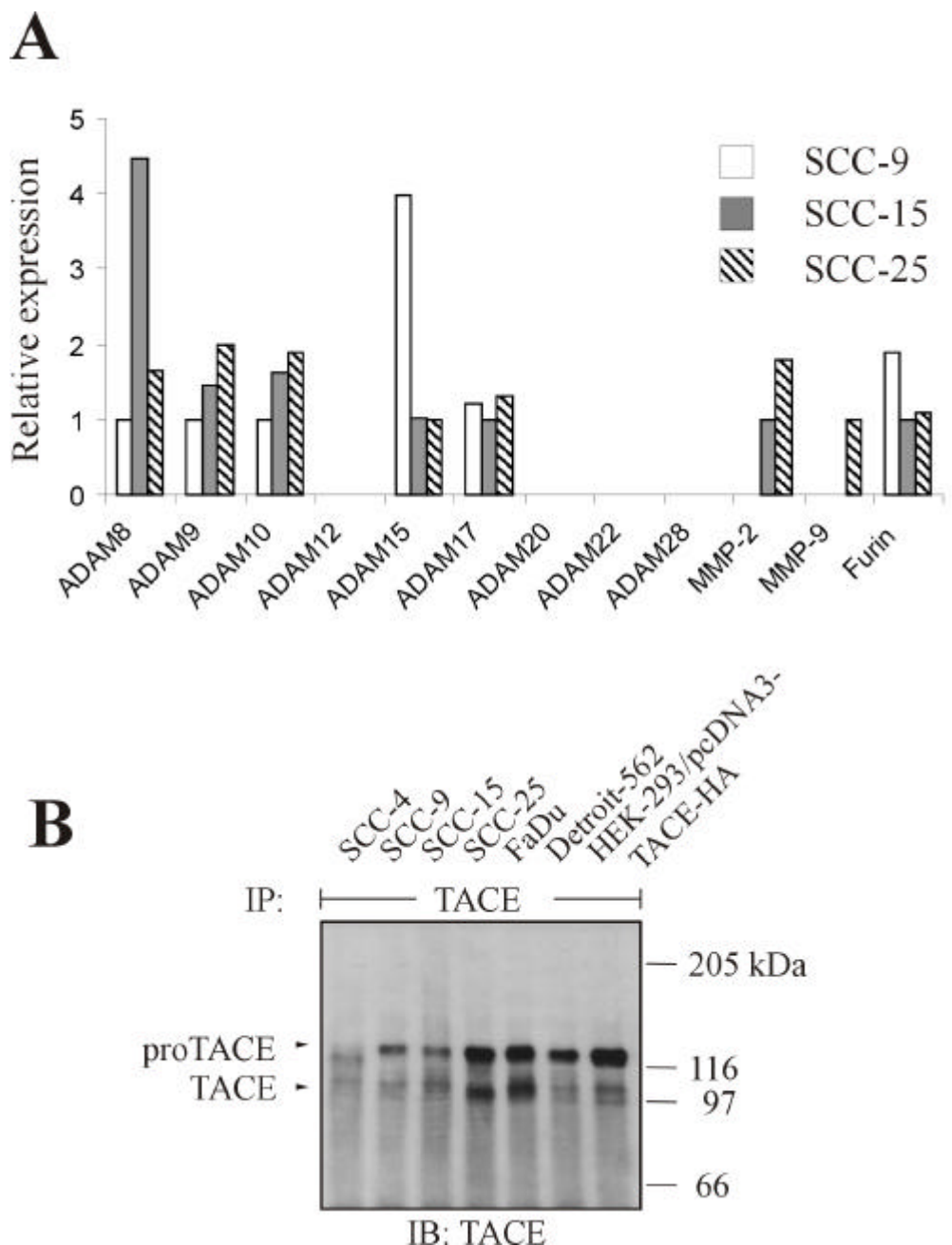


**Figure 23. Expression of TACE and other metalloproteases by cDNA micro-array and Western blot analysis (only TACE) in HNSCC cell lines.** A) cDNA prepared from SCC-9, SCC-15 and SCC-25 cells was labelled with  $\alpha^{32}\text{P}$ dATP and hybridized on array filters as described under *Materials and Methods*. Data represent relative hybridization signals for individual genes. Although ADAM12 did not show an hybridisation signal under this experimental conditions, expression of ADAM12 was observed by RT-PCR analysis in SCC-9 cells (S. Hart, personal communication). B) TACE was immunoprecipitated from lysates with monoclonal anti-TACE antibody. HEK-293 cells transfected with human TACE cDNA served as a positive control.

Indeed, ectopic expression of Timp-3 but not Timp-1 by retroviral transduction significantly inhibited GPCR-induced EGFR tyrosine phosphorylation in SCC-9 cells (Fig. 24A). Expression of Timps carrying a C-terminal VSV-tag was confirmed by immunoblotting total lysates with anti-VSV antibodies (Fig. 24B). These results pointed towards a direct involvement of TACE in the TMPS pathway in HNSCC cells.

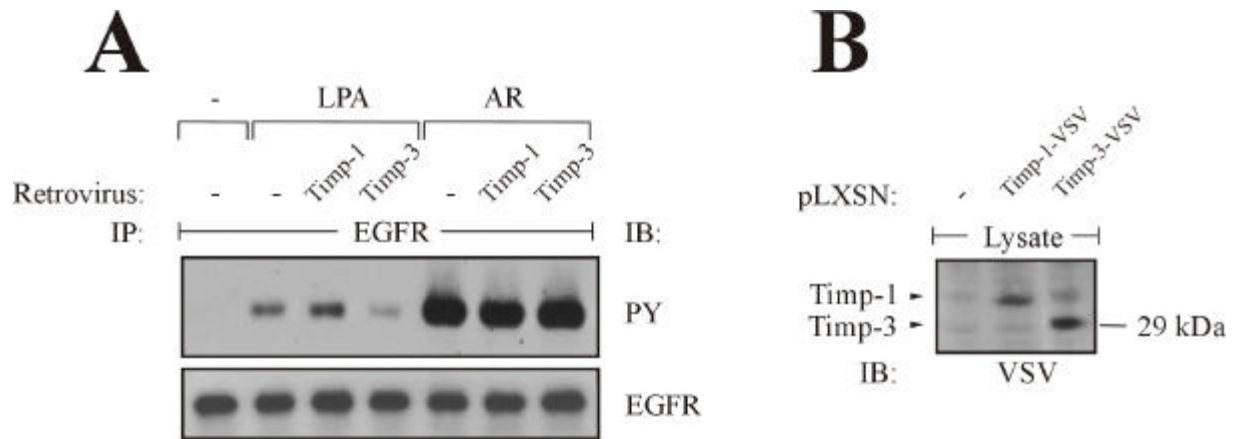


**Figure 24. Timp-3 but not Timp-1 inhibits EGFR signal transactivation in SCC-9 cells.** A) SCC-9 cells were infected with retrovirus encoding human Timp-1 or Timp-3. EGFR activation was determined by immunoblot after stimulation with agonists as indicated. B) Expression of VSV-tagged Timps was confirmed by immunoblotting crude cell lysates with monoclonal anti-VSV antibody.

Therefore, a dominant-negative TACE mutant which lacks the pro- and metalloprotease domain (Solomon et al., 1999) (Fig. 25D) was ectopically expressed in SCC-9 cells. The results showed that this TACE mutant indeed suppressed GPCR-induced proAR cleavage (Fig. 25A), release of mature AR (Fig. 25B) and EGFR signal transactivation (Fig. 25C).

In contrast, neither dominant-negative mutants of ADAM10 (Lemjabbar and Basbaum, 2002) and ADAM12 (Asakura et al., 2002) which have been shown to be involved in GPCR-triggered proHB-EGF processing nor an analogous ADAM15 mutant affected the GPCR-induced responses (Fig. 25C, Fig. 26). In addition, the specific involvement of TACE in LPA- and carbachol-induced EGFR tyrosine phosphorylation in HNSCC cells was corroborated and extended to downstream mitogenic and motility-promoting signaling events by studies using RNA interference (S. Hart, personal communication; Gschwind, A. *et al.*, submitted, 2002).

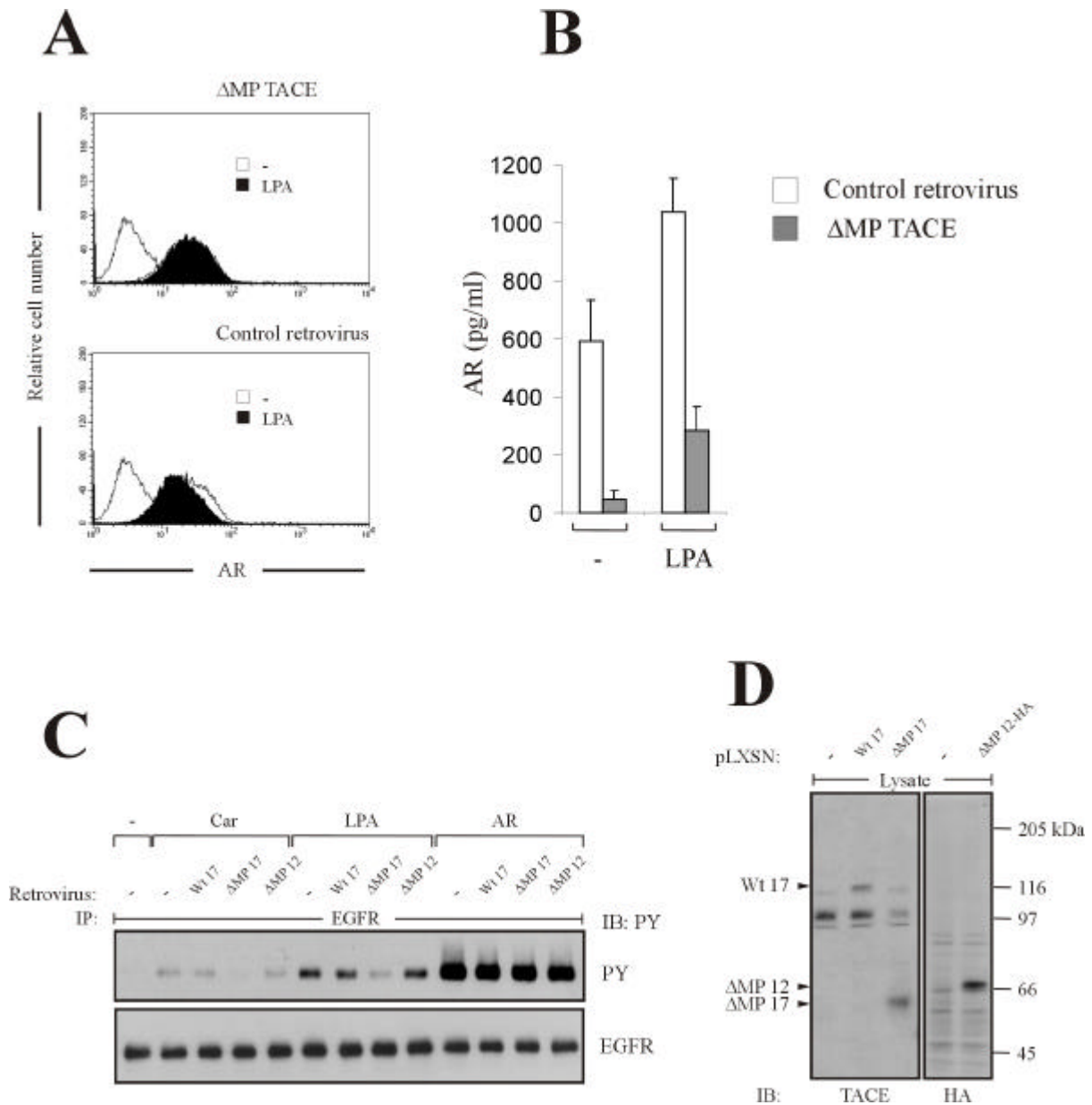


**Figure 25. Dominant-negative TACE suppresses GPCR-induced AR release and EGFR signal transactivation.** SCC-9 cells were infected with retrovirus encoding a TACE mutant that lacks the pro- and metalloprotease domain ( $\Delta$ MP TACE) or with control retrovirus. ProAR ectodomain shedding (A) and AR release into cell culture medium (B) was analyzed by flow cytometry and AR-ELISA, respectively. C) SCC-9 cells were infected with retrovirus encoding wild-type TACE (Wt 17), dominant-negative TACE ( $\Delta$ MP TACE), dominant negative ADAM12 ( $\Delta$ MP 12) or control retrovirus. EGFR tyrosine phosphorylation was determined by immunoblot after stimulation with agonists as indicated. D) Expression of protease constructs was confirmed by immunoblotting crude cell lysates with polyclonal anti-TACE and monoclonal anti-HA antibody, respectively.

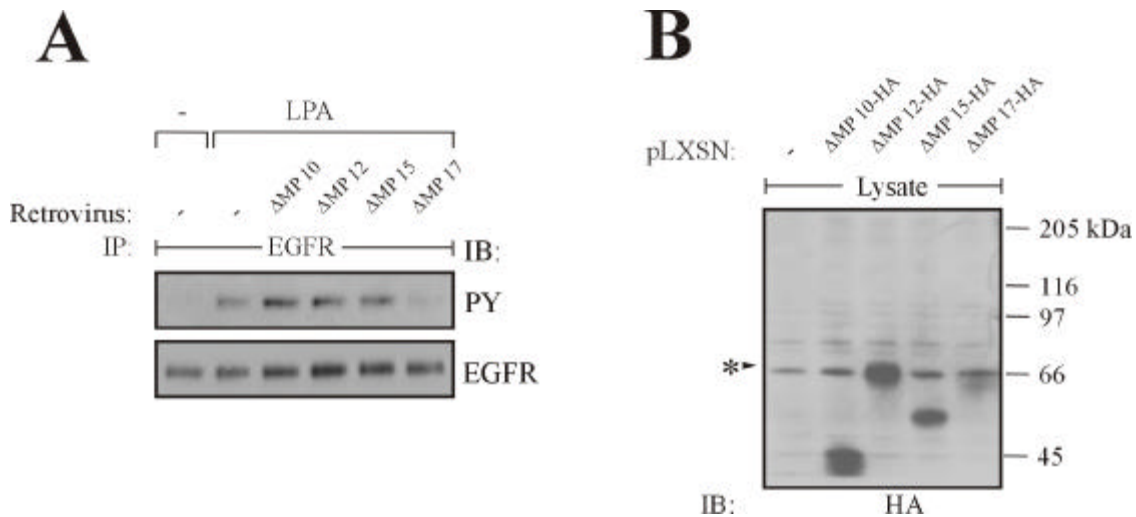


**Figure 26. Specificity of dominant-negative TACE for LPA-induced EGFR signal transactivation in HNSCC.** A) SCC-9 cells were infected with retrovirus encoding deletion mutants of ADAM10 ( $\Delta$ AMP 10), ADAM12 ( $\Delta$ AMP 12), ADAM15 ( $\Delta$ AMP 15) or TACE ( $\Delta$ AMP 17) lacking the pro- and metalloprotease domain. EGFR tyrosine phosphorylation was determined by immunoblot after stimulation with LPA. B) Expression of HA-tagged protease mutants was confirmed by immunoblotting crude cell lysates with monoclonal anti-HA antibody. \*, unspecific signal.

Collectively, these data suggested that TACE is involved in proAR cleavage and EGFR signal transactivation by LPA and carbachol in HNSCC cells.

### 3.12 TACE is involved in carbachol stimulated proHB-EGF shedding and EGFR signal transactivation in COS-7 cells.

Analysis of the phenotype resulting from targeted disruption of the TACE genes in mice suggested a role for TACE in ectodomain shedding of a variety of EGF-like growth factor precursors, including proHB-EGF (Peschon et al., 1998; Sunnarborg et al., 2002). To determine whether TACE can also be involved in proHB-EGF cleavage in response to GPCR stimulation, endogenous proHB-EGF ectodomain shedding in TACE-deficient murine fibroblasts was investigated. The fibroblast cell line *tace* <sup>$\Delta$ Zn/ $\Delta$ Zn</sup> EC-2 expresses an inactive, truncated mutant of TACE lacking the Zn<sup>2+</sup>-binding motif in the active site of the enzyme (Peschon et al., 1998; Reddy et al., 2000). Both TACE-deficient (EC-2) and wild-type murine fibroblasts (EC-4) were infected with retrovirus encoding human, muscarinic acetylcholine receptor-1 (M1R) and, following stimulation with the M1R agonist carbachol or with TPA, the cell-surface content of proHB-EGF was determined by FACS analysis. The results showed that both carbachol and TPA induced cell-surface ectodomain shedding of proHB-EGF in a batimastat-sensitive fashion in EC-4 wild-type fibroblasts (Fig. 27, left panel). In contrast, proHB-EGF shedding was deficient in *tace* <sup>$\Delta$ Zn/ $\Delta$ Zn</sup> EC-2 cells (Fig. 27, right panel). Nevertheless, carbachol and TPA were about equally efficient in activating ERK1/2 in EC-2

and EC-4 cells demonstrating that both cell lines were responsive to these stimuli (Fig. 28). Interestingly, co-infection of murine TACE together with M1R partially restored carbachol- and TPA-induced proHB-EGF shedding in *tace* <sup>$\Delta$ Zn/ $\Delta$ Zn</sup> EC-2 fibroblasts (Fig. 27, right panel). Together, these data demonstrated that TACE is required for carbachol- and TPA-triggered proHB-EGF shedding in murine fibroblasts.

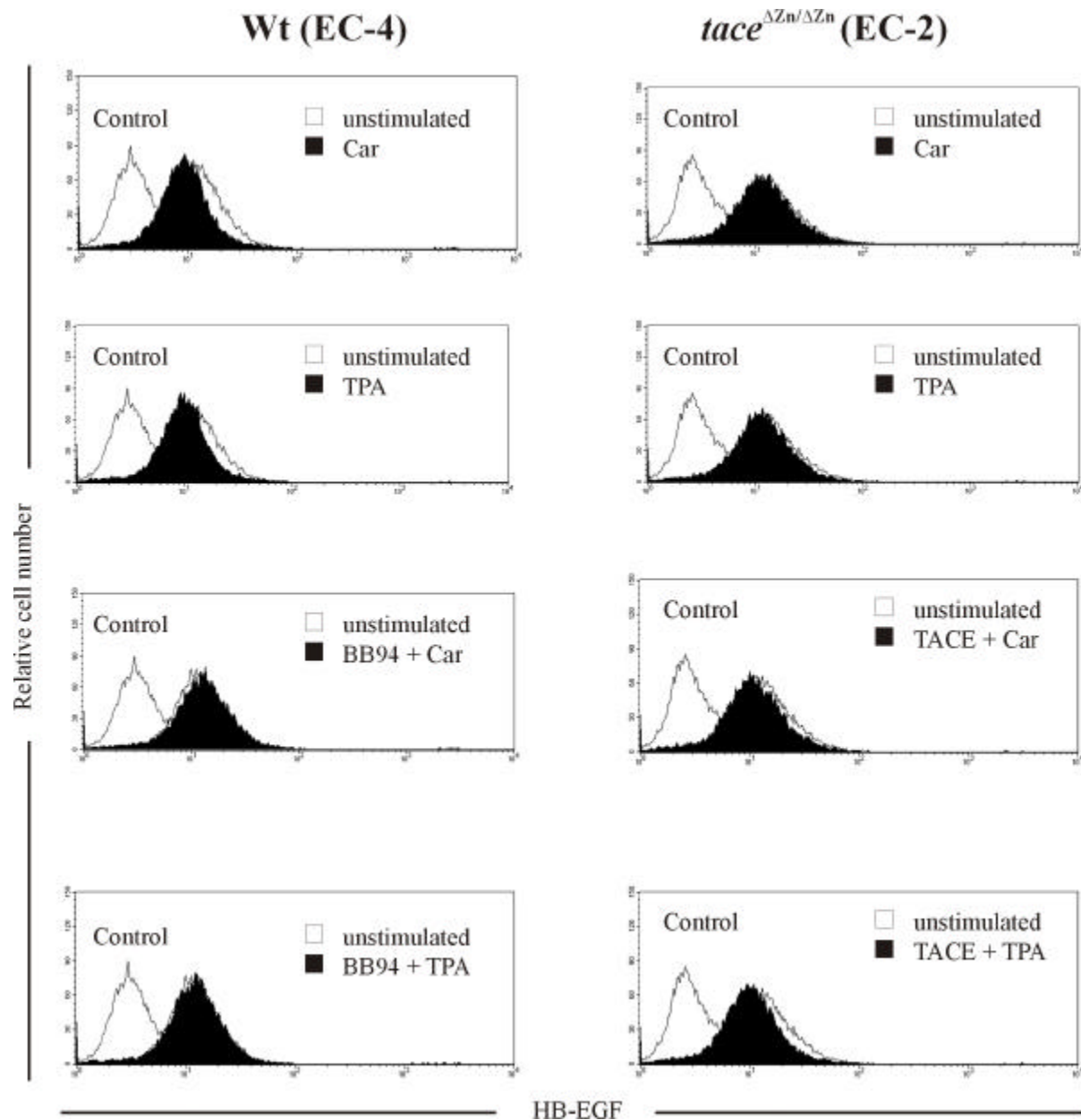


**Figure 27. Flow cytometric analysis of carbachol- and TPA-induced proteolytic processing of proHB-EGF in murine fibroblasts.** TACE-deficient *tace* <sup>$\Delta$ Zn/ $\Delta$ Zn</sup> (EC-2, right panel) and wild-type murine fibroblasts (Wt, EC-4, left panel) were infected with retrovirus encoding M1R. Where indicated, *tace* <sup>$\Delta$ Zn/ $\Delta$ Zn</sup> EC-2 cells were co-infected with retrovirus encoding murine TACE to reconstitute TACE function. After stimulation with carbachol (Car, 1 mM) for 20 min or TPA (1 mM) for 10 min cells were collected and stained for surface proHB-EGF and analysed by flow cytometry. Control cells were labelled with FITC-conjugated secondary antibody alone.

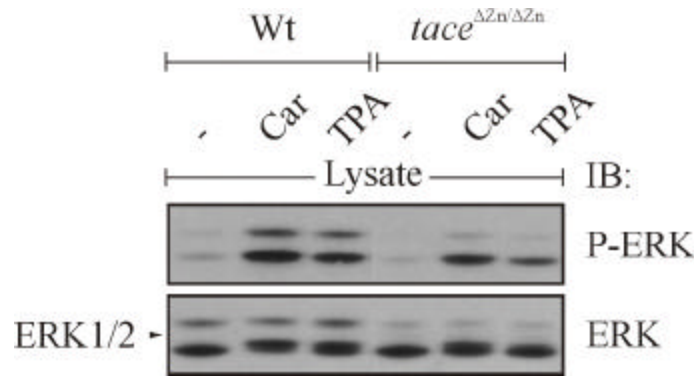


**Figure 28. Activation of ERK/MAPK in murine fibroblasts.** TACE-deficient  $tace^{\Delta Zn/\Delta Zn}$  (EC-2) and wild-type murine fibroblasts (*Wt*, EC-4) were infected with retrovirus encoding M1R. After stimulation with carbachol (Car, 1 mM) or TPA (1 mM) for 10 min cells were lysed and activation of ERK was determined by immunoblotting cell lysates with polyclonal anti-phospho-ERK antibody followed by reprobing of the same filter with polyclonal anti-ERK antibody to confirm equal protein loading.

Since Prenzel and colleagues have recently shown that proHB-EGF shedding links agonist-treated GPCRs with activation of the EGFR in COS-7 cells (Prenzel et al., 1999) it was hypothesized that blockade of TACE function might affect GPCR-induced proteolytic cleavage of proHB-EGF in this cell system.

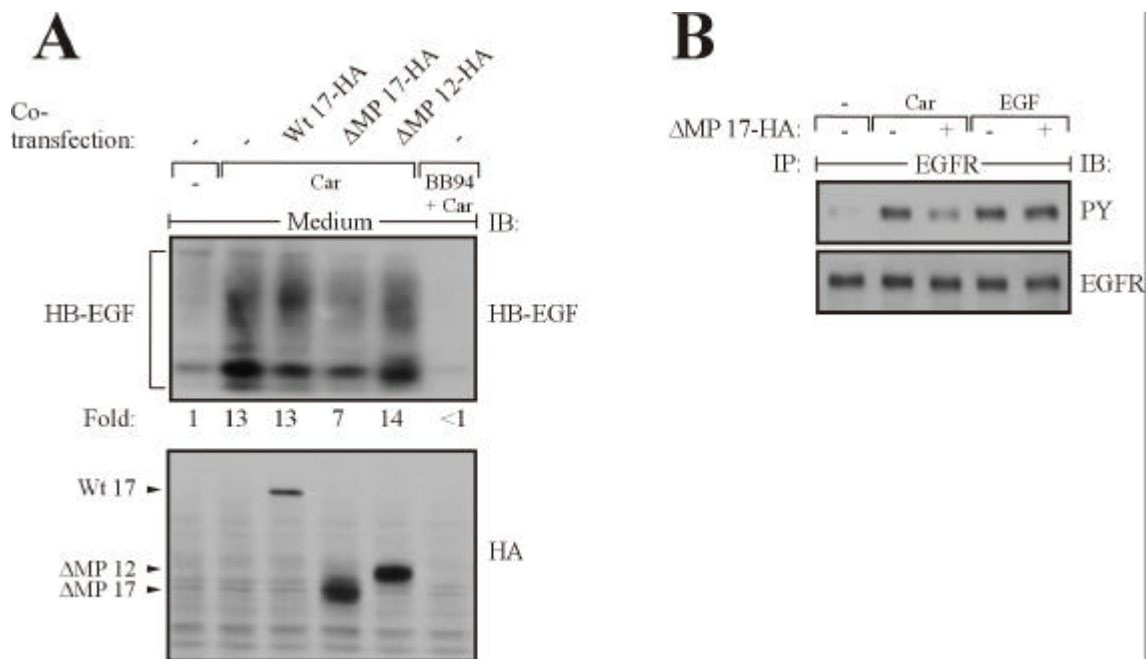


**Figure 29. Dominant-negative TACE attenuates carbachol stimulated proHB-EGF shedding and EGFR transactivation in COS-7 cells.** A) COS-7 cells were transiently transfected with pcDNA3-proHB-EGF-VSV, pcDNA3-M1R and expression construct encoding wild-type TACE (Wt 17-HA), dominant-negative TACE ( $\Delta$ AMP 17-HA), dominant-negative ADAM12 ( $\Delta$ AMP 12-HA) as indicated. Transfected cells were pre-incubated  $\pm$  BB94 (10  $\mu$ M) for 20 min and stimulated with carbachol (1 mM) for 20 min. Total protein in conditioned medium was precipitated with TCA and analysed by Western blot. Mature HB-EGF was identified with polyclonal anti-HB-EGF antibody (upper panel). Expression of HA-tagged protease constructs was confirmed by immunoblotting crude cell lysates with monoclonal anti-HA antibody (lower panel). B) COS-7 cells were transfected with pcDNA3-M1R  $\pm$  pcDNA3- $\Delta$ AMP-TACE-HA. EGFR tyrosine phosphorylation upon carbachol (1 mM, 3 min) stimulation was analysed by immunoblot.

In fact, co-transfection of dominant-negative TACE with M1R and proHB-EGF inhibited carbachol-induced HB-EGF release into cell culture medium by 50%, while an analogous ADAM12 mutant or wild-type TACE showed no effect (Fig. 29A, upper panel). In addition, pre-incubation of cells with batimastat completely prevented HB-EGF release. Interestingly, dominant-negative TACE also significantly inhibited carbachol-induced EGFR transactivation (Fig. 29B) suggesting the involvement of TACE in proHB-EGF shedding and EGFR signal transactivation by carbachol in COS-7 cells.

### 3.13 The cytoplasmic domain of proHB-EGF is dispensible for carbachol and TPA stimulated proHB-EGF shedding in COS-7 cells.

Finally, it was investigated whether the cytoplasmic domain of proHB-EGF is required for stimulus-induced processing of proHB-EGF. The results showed that similar to wild type proHB-EGF (Prenzel et al., 1999), a deletion mutant of proHB-EGF lacking the cytoplasmic tail was indeed proteolytically processed in response to carbachol or TPA but not EGF in COS-7 cells (Fig. 30).

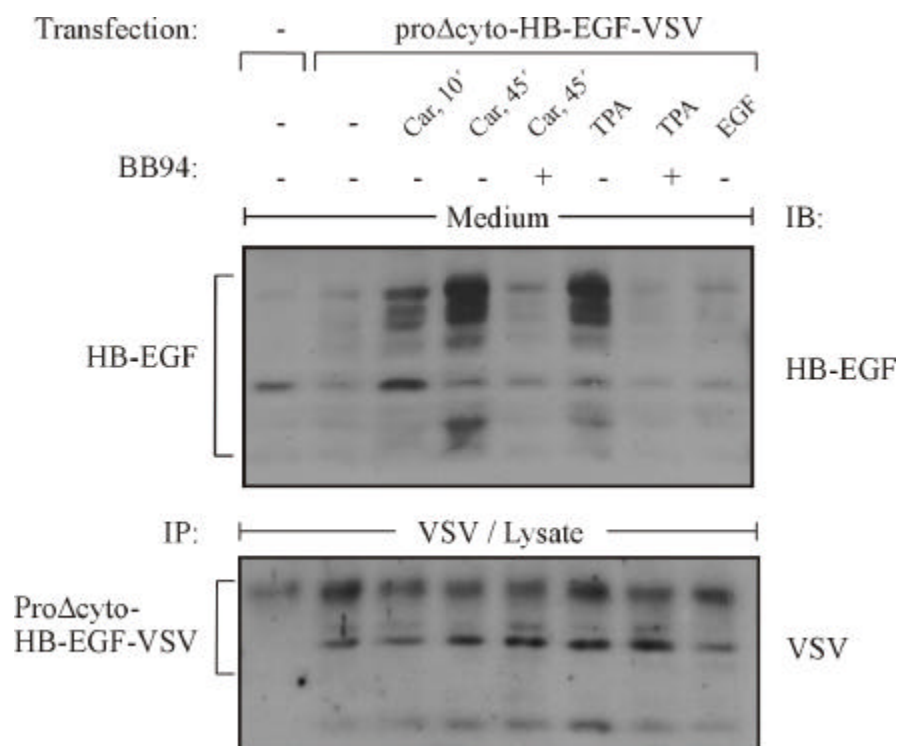


**Figure 30. The cytoplasmic domain of proHB-EGF is dispensible for carbachol-induced shedding.** COS-7 cells were transiently transfected with pcDNA3-M1R and pcDNA3-pro $\Delta$ cyto-HB-EGF-VSV. Transfected cells were pre-incubated  $\pm$  BB94 (10  $\mu$ M) for 20 min and stimulated with carbachol (1 mM) or TPA (1 mM) as indicated. Total protein in conditioned medium was precipitated with TCA. Mature HB-EGF was identified by Western blot analysis with polyclonal anti-HB-EGF antibody (upper panel). Expression of pro $\Delta$ cyto-HB-EGF-VSV was analyzed by immunoprecipitation/immunoblot with monoclonal anti-VSV antibody (lower panel).

In addition, HB-EGF release by carbachol and TPA was sensitive to batimastat. Together, these data demonstrated that the cytoplasmic domain of proHB-EGF is dispensable for carbachol- and TPA-triggered proHB-EGF shedding.

## 4 DISCUSSION

Deregulated signaling through EGFR family members is frequently involved in cancer development due to overexpression, activating mutations or autocrine stimulation of the receptors by EGF-like growth factors (Zwick et al., 2001). In different forms of squamous cell carcinoma EGFR expression serves as an early marker of neoplastic transformation (Rusch et al., 1995) and is closely related to the malignant potential of tumors (Almadori et al., 1999; Grandis et al., 1998; Kersemaekers et al., 1999). In addition, GPCRs have been implicated in the etiology of hyperproliferative diseases because of activating mutations or when locally exposed to an excess of agonist (Marinissen and Gutkind, 2001). Given the significance of both heptahelical receptor-mediated and direct EGFR signaling in tumor cell biology this study investigates the pathophysiological significance and the molecular mechanisms of EGFR signal transactivation in head and neck cancer cells.

### **4.1 Transactivation of the EGFR and HER2/neu by GPCR agonists involves a ligand-dependent mechanism in HNSCC cells.**

The data presented here provide evidence that treatment of HNSCC cells with bradykinin, carbachol, thrombin or LPA results in rapid EGFR activation (Fig. 4; Table 2). Previously, bradykinin stimulation of HNSCC cell lines has been reported to cause elevation of intracellular calcium levels while calcium influx inhibitors blocked proliferation and migration of head and neck cancer cells (Wu et al., 1997). Moreover, it has been shown that the thrombin receptor PAR1 is widely expressed in oral squamous cell carcinoma and that thrombin enhances growth of metastatic HNSCC cells (Liu et al., 2001). The experimental finding that the LPA receptor-EGFR cross-talk is established in all six head and neck cancer cell lines examined in this study (Table 2) suggests that the EGFR signal transactivation pathway in response to LPA is a major hallmark of this type of cancer. EGFR tyrosine phosphorylation upon stimulation with LPA has been reported in several cell lines including Rat-1 (Daub et al., 1996), HEK-293 (Della Rocca et al., 1999), PC-12 (Kim et al., 2000), Swiss 3T3 (Gohla et al., 1998), HaCaT and COS-7 (Daub et al., 1997) with kinetics similar to those found in squamous cancer cells (Fig. 4B). Since all three known LPA receptors which display differences in G protein coupling are expressed in HNSCC (Fig. 5) and the EGFR transactivation signal was significantly inhibited by PTX (Fig. 6A) it can be concluded that, in

this cell type, predominantly PTX-sensitive G proteins mediate EGFR transactivation following LPA treatment. In COS-7, PTX attenuates LPA-evoked EGFR tyrosine phosphorylation to a lesser extent (Daub et al., 1997) than observed in head and neck cancer cells (Fig. 6A). Moreover, Gohla *et al.* reported that EGFR-dependent stress fiber formation by LPA in Swiss 3T3 was exclusively mediated by G<sub>13</sub> proteins (Gohla et al., 1998). Together, these experimental findings suggest that LPA-induced EGFR activation is mediated by different G protein subtypes in a cell type-specific manner.

In light of the finding that besides LPA several other GPCR agonists are inducers of the transactivation signal (Fig. 4; Table 2) the EGFR may function as a central integrator of signaling by diverse, cancer-promoting GPCR ligands in HNSCC. Expression of a variety of pathophysiologically significant GPCRs and the role of the EGFR as a convergence point for heptahelical receptor stimulation provides a rational explanation for the enhanced sensitivity of head and neck cancer cells towards motility- and growth-promoting stimuli. Further investigations are to be conducted, however, to determine whether the observed GPCR expression patterns are prerequisite to or the consequence of neoplastic transformation in HNSCC.

Originally, a ligand-independent, intracellular pathway of EGFR transactivation had been proposed (Carpenter, 1999; Hackel et al., 1999; Luttrell et al., 1999) which was supported by the rapid kinetics of EGFR tyrosine phosphorylation in response to GPCR agonists and the fact that soluble EGF-like growth factors could not be detected in cell culture medium. Later, it was demonstrated that in COS-7, HEK-293 and Rat-1 cells EGFR transactivation is critically dependent on cell surface processing of the EGF-like growth factor precursor proHB-EGF through an unknown metalloprotease which is sensitive to the inhibitor batimastat (Prenzel et al., 1999). The experimental results presented here show that in analogy to the COS-7 system in head and neck cancer cells (Fig. 6A) a batimastat-sensitive shedding activity is induced upon GPCR stimulation that results in the release of soluble EGFR ligands which subsequently bind to the ectodomain of the EGFR. The finding that in SCC-9 HNSCC cells LPA treatment also leads to tyrosine phosphorylation of the oncoprotein HER2/neu (Fig. 7), confirms a previous observations in Rat-1 fibroblasts (Daub et al., 1996) and further expands the significance of the TMPS pathway. A critical role for EGFR-HER2/neu heterodimers in the etiology of HNSCC has been recently suggested by the finding that EGFR and HER2/neu are specifically co-expressed in neoplastic epithelium of tumors when compared to normal tissue (Bei et al., 2001). Our findings that transactivation of both the EGFR and HER2/neu required metalloprotease activity (Fig. 6-7) and that the EGFR-specific

inhibitor AG1478 completely prevented tyrosine phosphorylation of HER2/neu by LPA (Fig. 7) establish the LPA receptors and possibly other GPCRs as new upstream regulators of EGFR and HER2/neu signals. It remains to be further examined whether HER3 which is also expressed in HNSCC cell lines (Fig. 5) contributes to serpentine receptor signal transmission in these cells.

#### **4.2 Regulation of the proliferative and migratory behavior of HNSCC cells by GPCRs requires EGFR function and metalloprotease activity.**

When the role of EGFR transactivation in LPA-induced mitogenic signaling was investigated, it was found that inhibition of EGFR function or metalloprotease activity by small chemical compounds blocked EGFR association and phosphorylation of the tyrosine kinase substrates SHC and Gab1 upon LPA treatment (Fig. 8). Furthermore, it was observed that expression of a dominant-negative EGFR mutant abrogated ERK/MAPK activation by LPA in SCC-9 cells (Fig. 10). Similarly, endogenous ERK2 activation by LPA was blocked by AG1478 in SCC-9 and SCC-25 (Fig. 11). These experimental data indicate that the EGFR is instrumental in transducing mitogenic signals in response to LPA in head and neck cancer cells as previously described for several model systems such as Rat-1 (Daub et al., 1996), COS-7 (Daub et al., 1997), PC-12 (Kim et al., 2000) and HEK-293 (Della Rocca et al., 1999). Interestingly, Albanell *et al.* have reported that immunostaining of activated ERK1/2 was associated with high EGFR and HER2/neu expression levels in head and neck tumor biopsies (Albanell et al., 2001). Moreover, anti-EGFR therapy with Cetuximab (C225) resulted in lower ERK activation and decreased keratinocyte proliferation in HNSCC patients (Albanell et al., 2001). Combined with the data of this study, GPCR-induced activation of the EGFR in head and neck cancer cells might lead to enhanced ERK/MAPK activity and proliferation *in vivo*. Besides the EGFR-dependency of MAPK activation by LPA in HNSCC, studies with the metalloprotease inhibitor batimastat suggested the critical involvement of a shedding activity in the stimulation of ERK (Fig. 11). These observations agree with previous reports on the ligand-dependency of ERK activation in vascular smooth muscle cells (Eguchi et al., 2001; Kalmes et al., 2000), MDA-MB-231 (Filardo et al., 2000) and COS-7 cells (Pierce et al., 2001). Recently, it was demonstrated that specific interference with the EGFR kinase activity reduced the rate of DNA synthesis in Rat-1 fibroblast and Swiss 3T3 cells in response to LPA and other GPCR agonists (Daub et al., 1996; Santiskulvong et al., 2001). The current results

further indicate that LPA-induced DNA synthesis and S-phase cell cycle progression requires EGFR and metalloprotease activity in HNSCC with both low and high EGFR expression levels (Fig. 13-14, Table 3). Since LPA treatment of Detroit-562 cells did not result in further stimulation of cell proliferation (data not shown) EGFR activity may not be significantly enhanced by GPCR ligands in cancer cells with the highest EGFR over-expression.

A further important aspect of these findings is that, in addition to the proliferative responses, EGFR signal transactivation plays a direct role in the regulation of the migratory behavior of head and neck cancer cells. It has been reported before that wound stimuli induce metalloprotease-dependent shedding of EGF-like ligands in keratinocytes (Tokumaru et al., 2000) and that LPA enhances wound closure and invasion of ovarian cancer cells (Fishman et al., 2001). Interestingly, it is shown here that LPA treatment drastically increased the rate of wound closure and chemotactic migration in an EGFR and metalloprotease-dependent manner (Fig. 15) providing a mechanistic explanation for GPCR-triggered wound healing and migration via transactivation of the EGFR in HNSCC. Finally, studies using pharmacological inhibitors against individual elements of the TMPS pathway suggested a critical role for the EGFR and MEK in LPA-induced expression of the matrix metalloprotease MMP-9, an important regulator of angiogenesis and tumor progression (O-Chaoenrat et al., 2000a; O-Chaoenrat et al., 2000b).

### **4.3 ProAR ectodomain cleavage is a prerequisite to EGFR activation by GPCR agonists in HNSCC cells.**

Several observations have supported the concept of a ligand-dependent mechanism of EGFR transactivation (Gschwind et al., 2001). In diverse cell systems, EGFR signal transmission in response to LPA and other GPCR ligands requires metalloprotease activity and HB-EGF. However, although SCC-9, SCC-15 and SCC-25 cells express proTGF $\alpha$  and proAR in addition to proHB-EGF (Fig. 16, 17A), LPA selectively induced rapid shedding of endogenous proAR (Fig. 17B) and subsequent release of the mature ligand (Fig. 18). This is the first demonstration that agonist-treated GPCRs induce ectodomain cleavage of this EGF-like growth factor precursor. Previously, Brown *et al.* have provided evidence for metalloprotease-dependent shedding of proAR in Madin-Darby canine kidney cells by several non-physiological stimuli such as TPA, pervanadate or calcium ionophore (Brown et al., 2001).

Furthermore, it was demonstrated here that proAR cleavage in head and neck cancer cells following LPA treatment was attenuated by PTX and completely blocked by batimastat (Fig. 17B). A similar result was obtained on the level of EGFR tyrosine phosphorylation (Fig. 6A) suggesting that GPCR-mediated proAR shedding may be directly involved in the EGFR transactivation pathway. This hypothesis was further supported by the finding that function-perturbing anti-AR antibodies and heparin abrogated the EGFR transactivation signal and downstream mitogenic responses by LPA (Fig 19-22), while the potential involvement of HB-EGF was excluded. These growth-promoting signaling events are accompanied by phosphorylation of the survival mediator Akt/PKB via PI-3K downstream of the EGFR (Fig. 20-21). Recently, AR was shown to be a potent inhibitor of apoptosis induced by serum deprivation in non-small cell lung cancer cell lines (Hurbin et al., 2002) suggesting that AR can provide survival signals for cancer cells derived from different form of squamous cell carcinoma. In the current experiments using anti-AR neutralizing antibodies and heparin, however, no complete blockade of LPA-induced ERK/MAPK activation, DNA synthesis and transwell migration was observed. This could be due to limitations in inhibitor potency or due to limited access of the inhibitors to the growth factor embedded in the heparan sulfate proteoglycan matrix.

Despite the expression of a variety of EGFR ligands in HNSCC cells (Fig. 16, 17A) and some functional redundancy within the EGFR ligand family in developmental processes, the results of this study demonstrated that AR is specifically required for LPA- and carbachol-induced EGFR transactivation and downstream signaling events (see 3.7-3.10). However, what is the (patho-)physiological function of proHB-EGF and proTGF $\alpha$  in head and neck cancer cells? The observations of this study and by Eccles and co-workers (O-Charoenrat et al., 2002) that basal levels of EGFR tyrosine phosphorylation (Fig. 5B), ERK1/2 activity (Fig. 11) and cell proliferation (Fig. 13) were significantly reduced by batimastat and AG1478, however, strongly argued for the existence of autocrine EGFR activation loops that require metalloprotease activity for EGFR ligand shedding. Furthermore, anti-TGF $\alpha$  neutralizing antibodies reduced proliferation of SCC-9 and FaDu cells (Solorzano et al., 1997) and TGF $\alpha$  antisense therapy has recently been shown to inhibit HNSCC tumor growth in nude mice (Endo et al., 2000). Collectively, these studies demonstrate a critical role for TGF $\alpha$  in autocrine stimulation of the EGFR resulting in sustained proliferation of HNSCC cells while our current data establish a function of AR in GPCR-induced cellular responses.

#### 4.4 TACE is the proAR sheddase in HNSCC cells.

The enzymes implicated in shedding of EGF-like growth factor precursors belong to the ADAM family of zinc-dependent proteinases which are widely expressed in many tissues and also in HNSCC cell lines (Fig. 23). The finding that the EGFR transactivation signal in HNSCC cells is sensitive to Timp-3 but not Timp-1 (Fig. 24) is in accordance with the published inhibitor spectrum of recombinant TACE *in vitro* (Amour et al., 1998). Moreover, Sunnarborg *et al.* have recently proposed a role for TACE in constitutive ectodomain cleavage of proAR, proHB-EGF and proTGF $\alpha$  (Sunnarborg et al., 2002). Remarkably, they showed that reintroduction of TACE into *tace* <sup>$\Delta$ Zn/ $\Delta$ Zn</sup> EC-2 fibroblasts resulted in increased basal shedding of the co-transfected growth factor precursors.

The current data identify a novel biological function for the metalloprotease TACE in GPCR signalling, since expression of a dominant-negative TACE mutant blocked cell-surface proAR cleavage, release of mature AR and EGFR tyrosine phosphorylation by LPA and carbachol (Fig. 25). Although recent reports have implicated ADAM10 (Lemjabbar and Basbaum, 2002; Yan et al., 2002) and ADAM12 (Asakura et al., 2002) in HB-EGF-dependent TMPS pathways (Table 4) the involvement of these metalloproteases in EGFR signal transactivation in HNSCC cells was excluded (Fig. 26). How TACE is activated by heterotrimeric G proteins is currently not known. Although ERK has been shown to bind to and phosphorylate the cytoplasmic domain of TACE at threonine 735 in response to TPA stimulation (Diaz-Rodriguez et al., 2002), GPCR-induced AR release and EGFR tyrosine phosphorylation is insensitive to MEK inhibitors in HNSCC cells (unpublished observation) suggesting ERK1/2 not to be involved upstream of the EGFR. Another report demonstrated that TACE must be expressed with its membrane-anchoring domain for TPA stimulated shedding of TNF, p75 TNFR, and IL-1R-II, but that the cytoplasmic domain of TACE is not required for the shedding of these substrates (Reddy et al., 2000). Future studies will therefore have to focus on the question whether the cytoplasmic domain of TACE and other ADAM proteases are involved in GPCR-induced shedding of EGF-like ligands.

In summary, the results of this study indicate that treatment of head and neck squamous cell carcinoma cells with GPCR ligands such as LPA and carbachol leads to the rapid and specific cleavage of proAR at the cell-surface by TACE (Fig. 31). Moreover, release of mature AR is a prerequisite to EGFR stimulation, subsequent SHC and Grb2 adaptor protein recruitment and downstream activation of ERK1/2 and PI-3K-dependent phosphorylation of Akt/PKB. Finally, this triple-membrane-passing signal (TMPS) mechanism of EGFR transactivation

provides a molecular explanation for the question of how GPCR ligands regulate the proliferative and migratory behavior of HNSCC cells.

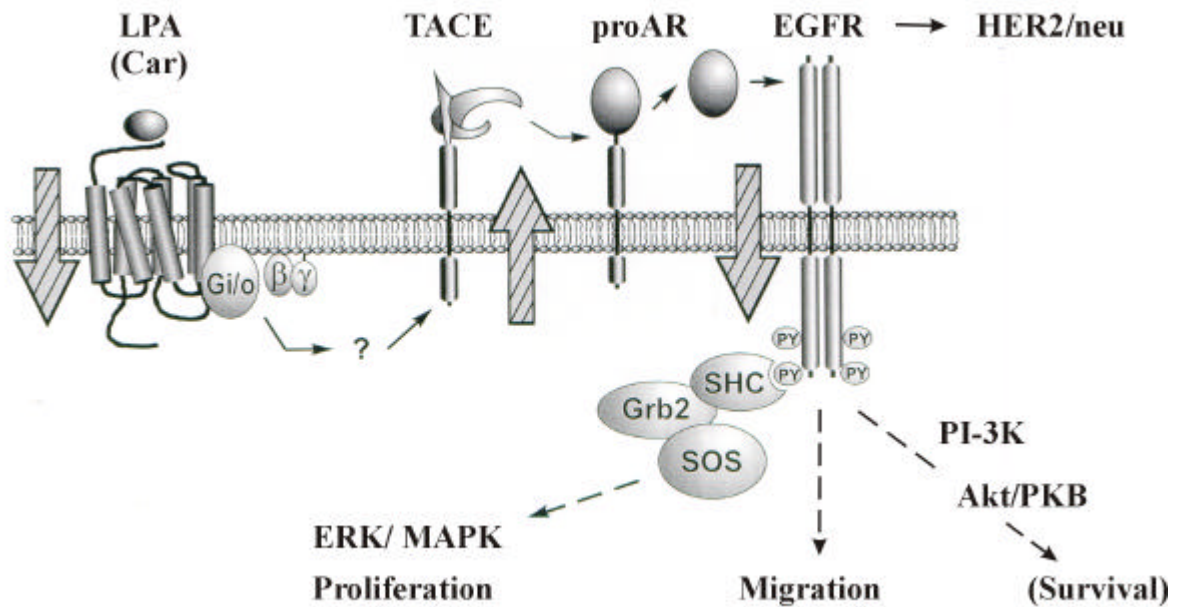


**Figure 31. Triple-membrane-passing signal (TMPS) mechanism of EGFR transactivation in HNSCC cells.** Activation of TACE by the GPCR agonists LPA and carbachol results in cell-surface ectodomain cleavage of proAR. Upon release of mature AR the EGFR and HER2/neu are activated leading to an EGFR-characteristic intracellular signal. GPCR ligands regulate the proliferative and migratory behavior of head and neck cancer cells via the TMPS pathway. Adapted from (Gschwind et al., 2001).

#### 4.4 TACE is involved in carbachol-induced proHB-EGF ectodomain processing in murine fibroblasts and COS-7 cells.

Besides its role in proAR cleavage in HNSCC cells, TACE was shown to be involved in proHB-EGF processing in murine fibroblasts (Fig. 27) and COS-7 cells (Fig. 29) in response to carbachol stimulation. These findings are in contrast to recent observations showing that a dominant-negative mutant of ADAM10 significantly attenuates bombesin-induced shedding of proHB-EGF and EGFR tyrosine phosphorylation in COS-7 cells (Yan et al., 2002). In both studies, however, no complete inhibition of proHB-EGF cleavage was achieved. It therefore remains to be investigated, whether ADAM10 and TACE cooperate in proHB-EGF cleavage and EGFR stimulation in this cell system or whether carbachol and bombesin specifically trigger the activation of two different metalloproteases.

Further studies on ectodomain shedding in COS-7 cells using a C-terminal deletion mutant of proHB-EGF showed that the cytoplasmic domain of proHB-EGF is dispensable for carbachol-

and TPA-induced processing (Fig. 30). These findings are in agreement with recent observations that ionomycin-induced proHB-EGF cleavage is not dependent on the presence of the proHB-EGF cytoplasmic tail segment in rat NbMC-2 prostate epithelial cells (Dethlefsen et al., 1998). Collectively, these data suggest that GPCR-induced ectodomain shedding of proHB-EGF is most likely regulated on the metalloprotease level.

## 4.6 Perspectives

Recent reports identified TGF $\alpha$  as an element in signal transmission from GPCRs to the EGFR in gastric epithelia (Pai et al., 2002) and T-84 cells (McCole et al., 2002) suggesting that at least three, HB-EGF, AR and TGF $\alpha$  of the eight known EGF-like growth factors can be mediators of EGFR signal transactivation (Table 4). Although TACE-deficient murine fibroblasts show partial defects in constitutive and 4-aminophenylmercuric acetate (APMA)-induced TGF $\alpha$  release (Merlos-Suarez et al., 2001; Peschon et al., 1998; Sunnarborg et al., 2002), the identity of the ADAM(s) responsible for proTGF $\alpha$  cleavage by GPCR ligands in the cell systems mentioned above remains to be determined.

There is an increasing body of evidence that, in addition to the potential involvement of several EGF-like ligands in TMPS pathways, one individual growth factor precursor such as proHB-EGF can be cleaved by several ADAMs: ADAM9, ADAM10, ADAM12 and TACE have been shown to be proHB-EGF sheddases in living cells (Table 4 and 4.5).

Cell line, Tissue	Stimulus	GPCR	Protease	EGF-like ligand	Biological response	Reference
Lung epithelia, NCI-H292	gram+ lipoteichoic acid (LTA)	platelet-activating factor receptor (PAFR)	ADAM10	HB-EGF	Ras, mucin synthesis	(Lemjabbar and Basbaum, 2002)
Rat neonatal cardiomyocytes	phenylephrine (PE), AngII, ET-1	AngR, ETR	ADAM12	HB-EGF	cardiac hypertrophy	(Asakura et al., 2002)
COS-7, PC3	bombesin	BombR	ADAM10	HB-EGF	SHC, Gab1, ERK	(Yan et al., 2002)
Vero-H	TPA	-	ADAM9	HB-EGF	proHB-EGF shedding	(Izumi et al., 1998)
Gastric epithelia, colon cancer	prostaglandin E2	-	?	TGF $\alpha$	ERK, c-fos, proliferation	(Pai et al., 2002)
T-84	carbachol	muscarinic AChR	?	TGF $\alpha$	ERK, inhibition of chloride secretion	(McCole et al., 2002)
HNSCC cell lines	LPA, carbachol	EDG, muscarinic AChR	TACE	AR	ERK, proliferation, migration	This study
Murine fibroblasts; COS-7	carbachol	MIR	TACE	HB-EGF	proHB-EGF shedding; EGFR transactivation	This study

**Table 4: Critical elements of EGFR signal transactivation pathways.**

Another level of complexity is added to the mechanisms of growth factor precursor cleavage by the observation that, for example, in Vero-H cells TPA induces proHB-EGF shedding via ADAM9 (Izumi et al., 1998) while LPA-induced proHB-EGF cleavage in the same cell system is independent of ADAM9 (Umata et al., 2001). These data suggest that different stimuli can induce proteolytic cleavage of an individual growth factor precursor via different metalloproteases in one cell line. Therefore, an important issue of future studies will be to determine what defines the choice of EGFR ligands in signal transmission of GPCRs to the EGFR and the physiological significance of either TGF $\alpha$ , ADAM10/HB-EGF, ADAM12/HB-EGF or TACE/AR in different cell-types. Signal specificity may in part be achieved by localizing these modules to discrete regions in the cell membrane. Interestingly, co-immunoprecipitation studies by Maudsley and colleagues demonstrated that the  $\beta$ 2-adrenergic receptor physically interacts with the "transactivated" EGFR in COS-7 cells (Maudsley et al., 2000) suggesting the formation of a macromolecular signaling complex which is likely to contain other elements of the TMPS pathway.

Metalloprotease-mediated ectodomain shedding of growth factor precursors *in vivo* is as yet only poorly understood. The severe phenotype of mice lacking TACE suggests an essential role for soluble TGF $\alpha$  in normal development and emphasizes the importance of protein ectodomain shedding *in vivo*. In addition, absence of functional TACE results in impaired basal solubilisation of a variety of other EGF-like ligands such as AR and HB-EGF (Merlos-Suarez et al., 2001; Sunnarborg et al., 2002; Fig. 27, this study). ADAM10-deficient mice

have been reported to die very early in embryogenesis with multiple defects of the developing central nervous system, somites, and cardiovascular system (Hartmann et al., 2002). It is not known, however, whether these developmental defects are due to impaired growth factor precursor shedding. On the other hand, mice lacking ADAM9 have no evident major abnormalities during development or adult life (Weskamp et al., 2002). Moreover, proHB-EGF processing is comparable in embryonic fibroblasts isolated from ADAM9(-/-) and wild-type mice, arguing against an essential role of ADAM9 in proHB-EGF shedding in these cells.

Further investigations *in vivo* will also have to focus on the relevance of TMPS pathways for both normal and pathophysiological processes. Remarkably, recent data derived from animal models have implicated GPCR-EGFR cross-talk pathways in abnormal ERK1/2 signaling in vascular smooth muscle cells from hypertensive rats (Touyz et al., 2002), in cardiac hypertrophy (Asakura et al., 2002) and ischemic preconditioning (Krieg et al., 2002). Finally, this and other studies have demonstrated that GPCR-induced and autocrine activation of the EGFR appears to be critical for the growth of HNSCC. Elucidation of the molecular mechanisms underlying deregulated EGFR signaling may ultimately lead to pharmaceutical intervention in HNSCC and other human cancers.

## 5 SUMMARY

Transactivation of the EGFR represents the paradigm for cross-talk between G protein-coupled receptors (GPCRs) and receptor tyrosine kinase signaling pathways. The molecular mechanisms and the pathophysiological significance of GPCR-induced EGFR signal transactivation, however, is only poorly understood. In a variety of squamous cell carcinoma cell lines of the head and neck (HNSCCs), it was found that treatment with the GPCR agonists LPA, bradykinin, thrombin and carbachol results in rapid tyrosine phosphorylation of the EGFR. In these tumor cells, signal transactivation of the EGFR and the oncoprotein HER2/neu is critically dependent on metalloprotease activity. Using the metalloprotease inhibitors batimastat and marimastat, the EGFR-specific tyrosine kinase inhibitor AG1478, and a dominant-negative EGFR mutant, it was shown that EGFR tyrosine phosphorylation, recruitment of the adaptor proteins SHC and Gab1, and activation of the ERK/MAPK pathway in response to LPA depend both on metalloprotease function and EGFR tyrosine kinase activity. Most importantly, critical characteristics of HNSCC cell lines such as DNA synthesis, cell cycle progression and tumor cell migration are stimulated by LPA and can be abrogated by interfering with EGFR signal transmission suggesting that highly abundant GPCR ligands such as LPA may function as tumor promoters and determinants of HNSCC progression.

Previous investigations revealed that EGFR signal transactivation often involves cell-surface proteolysis of the growth factor precursor proHB-EGF in non-transformed cells. Stimulation of squamous cell carcinoma cells with LPA or carbachol, however, results in metalloprotease-dependent cleavage and release of the EGFR ligand amphiregulin (AR). Moreover, inhibition of AR biological activity by neutralizing antibodies or heparin prevents GPCR-induced EGFR tyrosine phosphorylation, downstream mitogenic signaling events, activation of Akt/PKB, cell proliferation and migration. Recent studies supported a role for the metalloprotease-disintegrin TACE/ADAM17 in ectodomain shedding of EGFR ligands. Interestingly, evidence was provided here that blockade of TACE by expression of the tissue inhibitor of metalloprotease (TIMP)-3 or of a dominant-negative TACE mutant suppresses GPCR stimulated AR release and tyrosine phosphorylation of the EGFR.

Together, these data substantiate the importance of a mechanism that promotes head and neck cancer cell proliferation and motility by GPCR ligands involving EGFR transactivation. Finally, these findings demonstrate that proAR cleavage by TACE is required for GPCR-induced EGFR activation implying that TACE can function as an effector of GPCR signaling that regulates receptor cross-talk in human cancer cells.

## 6 REFERENCES

- Adomeit, A., Graness, A., Gross, S., Seedorf, K., Wetzker, R. and Liebmann, C. (1999) Bradykinin B(2) receptor-mediated mitogen-activated protein kinase activation in COS-7 cells requires dual signaling via both protein kinase C pathway and epidermal growth factor receptor transactivation. *Mol Cell Biol*, **19**, 5289-97.
- Albanell, J., Codony-Servat, J., Rojo, F., Del Campo, J.M., Sauleda, S., Anido, J., Raspall, G., Giralt, J., Rosello, J., Nicholson, R.I., Mendelsohn, J. and Baselga, J. (2001) Activated extracellular signal-regulated kinases: association with epidermal growth factor receptor/transforming growth factor alpha expression in head and neck squamous carcinoma and inhibition by anti-epidermal growth factor receptor treatments. *Cancer Res*, **61**, 6500-10.
- Almadori, G., Cadoni, G., Galli, J., Ferrandina, G., Scambia, G., Exarchakos, G., Paludetti, G. and Ottaviani, F. (1999) Epidermal growth factor receptor expression in primary laryngeal cancer: an independent prognostic factor of neck node relapse. *Int J Cancer*, **84**, 188-91.
- Alroy, I. and Yarden, Y. (1997) The ErbB signaling network in embryogenesis and oncogenesis: signal diversification through combinatorial ligand-receptor interactions. *FEBS Lett*, **410**, 83-6.
- Amour, A., Slocombe, P.M., Webster, A., Butler, M., Knight, C.G., Smith, B.J., Stephens, P.E., Shelley, C., Hutton, M., Knauper, V., Docherty, A.J. and Murphy, G. (1998) TNF-alpha converting enzyme (TACE) is inhibited by TIMP-3. *FEBS Lett*, **435**, 39-44.
- Asakura, M., Kitakaze, M., Takashima, S., Liao, Y., Ishikura, F., Yoshinaka, T., Ohmoto, H., Node, K., Yoshino, K., Ishiguro, H., Asanuma, H., Sanada, S., Matsumura, Y., Takeda, H., Beppu, S., Tada, M., Hori, M. and Higashiyama, S. (2002) Cardiac hypertrophy is inhibited by antagonism of ADAM12 processing of HB-EGF: metalloproteinase inhibitors as a new therapy. *Nat Med*, **8**, 35-40.
- Azemar, M., Schmidt, M., Arlt, F., Kennel, P., Brandt, B., Papadimitriou, A., Groner, B. and Wels, W. (2000) Recombinant antibody toxins specific for ErbB2 and EGF receptor inhibit the in vitro growth of human head and neck cancer cells and cause rapid tumor regression in vivo. *Int J Cancer*, **86**, 269-75.
- Bagowski, C.P., Stein-Gerlach, M., Choidas, A. and Ullrich, A. (1999) Cell-type specific phosphorylation of threonines T654 and T669 by PKD defines the signal capacity of the EGF receptor. *Embo J*, **18**, 5567-76.
- Bei, R., Pompa, G., Vitolo, D., Moriconi, E., Ciocci, L., Quaranta, M., Frati, L., Kraus, M.H. and Muraro, R. (2001) Co-localization of multiple ErbB receptors in stratified epithelium of oral squamous cell carcinoma. *J Pathol*, **195**, 343-8.
- Belcheva, M.M., Haas, P.D., Tan, Y., Heaton, V.M. and Coscia, C.J. (2002) The Fibroblast Growth Factor Receptor Is at the Site of Convergence between  $\mu$ -Opioid

- Receptor and Growth Factor Signaling Pathways in Rat C6 Glioma Cells. *J Pharmacol Exp Ther*, **303**, 909-918.
- Black, R.A. (2002) Tumor necrosis factor-alpha converting enzyme. *Int J Biochem Cell Biol*, **34**, 1-5.
- Black, R.A., Rauch, C.T., Kozlosky, C.J., Peschon, J.J., Slack, J.L., Wolfson, M.F., Castner, B.J., Stocking, K.L., Reddy, P., Srinivasan, S., Nelson, N., Boiani, N., Schooley, K.A., Gerhart, M., Davis, R., Fitzner, J.N., Johnson, R.S., Paxton, R.J., March, C.J. and Cerretti, D.P. (1997) A metalloproteinase disintegrin that releases tumour-necrosis factor-alpha from cells. *Nature*, **385**, 729-33.
- Blume-Jensen, P. and Hunter, T. (2001) Oncogenic kinase signalling. *Nature*, **411**, 355-65.
- Bode, W., Gomis-Ruth, F.X. and Stockler, W. (1993) Astacins, serralyisins, snake venom and matrix metalloproteinases exhibit identical zinc-binding environments (HEXXHXXGXXH and Met-turn) and topologies and should be grouped into a common family, the 'metzincins'. *FEBS Lett*, **331**, 134-40.
- Brachmann, R., Lindquist, P.B., Nagashima, M., Kohr, W., Lipari, T., Napier, M. and Derynck, R. (1989) Transmembrane TGF-alpha precursors activate EGF/TGF-alpha receptors. *Cell*, **56**, 691-700.
- Brinckerhoff, C.E. and Matrisian, L.M. (2002) Matrix metalloproteinases: a tail of a frog that became a prince. *Nat Rev Mol Cell Biol*, **3**, 207-14.
- Brown, C.L., Coffey, R.J. and Dempsey, P.J. (2001) The proamphiregulin cytoplasmic domain is required for basolateral sorting, but is not essential for constitutive or stimulus-induced processing in polarized Madin-Darby canine kidney cells. *J Biol Chem*, **276**, 29538-49.
- Carpenter, G. (1999) Employment of the epidermal growth factor receptor in growth factor-independent signaling pathways. *J Cell Biol*, **146**, 697-702.
- Castagliuolo, I., Valenick, L., Liu, J. and Pothoulakis, C. (2000) Epidermal growth factor receptor transactivation mediates substance P-induced mitogenic responses in U-373 MG cells. *J Biol Chem*, **275**, 26545-50.
- Chen, C. and Okayama, H. (1987) High-efficiency transformation of mammalian cells by plasmid DNA. *Mol Cell Biol*, **7**, 2745-52.
- Chen, Y., Grall, D., Salcini, A.E., Pelicci, P.G., Pouyssegur, J. and Van Obberghen-Schilling, E. (1996) Shc adaptor proteins are key transducers of mitogenic signaling mediated by the G protein-coupled thrombin receptor. *Embo J*, **15**, 1037-44.
- Chung, C.T. and Miller, R.H. (1988) A rapid and convenient method for the preparation and storage of competent bacterial cells. *Nucleic Acids Res*, **16**, 3580.
- Cohen, P. (2002) The origins of protein phosphorylation. *Nat Cell Biol*, **4**, E127-30.

- Cook, P.W., Pittelkow, M.R., Keeble, W.W., Graves-Deal, R., Coffey, R.J., Jr. and Shipley, G.D. (1992) Amphiregulin messenger RNA is elevated in psoriatic epidermis and gastrointestinal carcinomas. *Cancer Res*, **52**, 3224-7.
- Cunnick, J.M., Dorsey, J.F., Standley, T., Turkson, J., Kraker, A.J., Fry, D.W., Jove, R. and Wu, J. (1998) Role of tyrosine kinase activity of epidermal growth factor receptor in the lysophosphatidic acid-stimulated mitogen-activated protein kinase pathway. *J Biol Chem*, **273**, 14468-75.
- Daub, H., Wallasch, C., Lankenau, A., Herrlich, A. and Ullrich, A. (1997) Signal characteristics of G protein-transactivated EGF receptor. *Embo J*, **16**, 7032-44.
- Daub, H., Weiss, F.U., Wallasch, C. and Ullrich, A. (1996) Role of transactivation of the EGF receptor in signalling by G-protein-coupled receptors. *Nature*, **379**, 557-60.
- Della Rocca, G.J., Maudsley, S., Daaka, Y., Lefkowitz, R.J. and Luttrell, L.M. (1999) Pleiotropic coupling of G protein-coupled receptors to the mitogen-activated protein kinase cascade. Role of focal adhesions and receptor tyrosine kinases. *J Biol Chem*, **274**, 13978-84.
- Dethlefsen, S.M., Raab, G., Moses, M.A., Adam, R.M., Klagsbrun, M. and Freeman, M.R. (1998) Extracellular calcium influx stimulates metalloproteinase cleavage and secretion of heparin-binding EGF-like growth factor independently of protein kinase C. *J Cell Biochem*, **69**, 143-53.
- Diaz-Rodriguez, E., Montero, J.C., Esparis-Ogando, A., Yuste, L. and Pandiella, A. (2002) Extracellular Signal-regulated Kinase Phosphorylates Tumor Necrosis Factor alpha-converting Enzyme at Threonine 735: A Potential Role in Regulated Shedding. *Mol Biol Cell*, **13**, 2031-44.
- Doedens, J.R. and Black, R.A. (2000) Stimulation-induced down-regulation of tumor necrosis factor-alpha converting enzyme. *J Biol Chem*, **275**, 14598-607.
- Downward, J. (2001) The ins and outs of signalling. *Nature*, **411**, 759-62.
- Eguchi, S., Dempsey, P.J., Frank, G.D., Motley, E.D. and Inagami, T. (2001) Activation of MAPKs by angiotensin II in vascular smooth muscle cells. Metalloprotease-dependent EGF receptor activation is required for activation of ERK and p38 MAPK but not for JNK. *J Biol Chem*, **276**, 7957-62.
- Eguchi, S., Numaguchi, K., Iwasaki, H., Matsumoto, T., Yamakawa, T., Utsunomiya, H., Motley, E.D., Kawakatsu, H., Owada, K.M., Hirata, Y., Marumo, F. and Inagami, T. (1998) Calcium-dependent epidermal growth factor receptor transactivation mediates the angiotensin II-induced mitogen-activated protein kinase activation in vascular smooth muscle cells. *J Biol Chem*, **273**, 8890-6.
- Endo, A., Nagashima, K., Kurose, H., Mochizuki, S., Matsuda, M. and Mochizuki, N. (2002) Sphingosine 1-phosphate induces membrane ruffling and increases motility of human umbilical vein endothelial cells via vascular endothelial growth factor receptor and CrkII. *J Biol Chem*, **277**, 23747-54.

- Fang, X., Gaudette, D., Furui, T., Mao, M., Estrella, V., Eder, A., Pustilnik, T., Sasagawa, T., Lapushin, R., Yu, S., Jaffe, R.B., Wiener, J.R., Erickson, J.R. and Mills, G.B. (2000a) Lysophospholipid growth factors in the initiation, progression, metastases, and management of ovarian cancer. *Ann N Y Acad Sci*, **905**, 188-208.
- Fang, X., Yu, S., LaPushin, R., Lu, Y., Furui, T., Penn, L.Z., Stokoe, D., Erickson, J.R., Bast, R.C., Jr. and Mills, G.B. (2000b) Lysophosphatidic acid prevents apoptosis in fibroblasts via G(i)-protein-mediated activation of mitogen-activated protein kinase. *Biochem J*, **352**, 135-43.
- Fang, X., Yu, S., Tanyi, J.L., Lu, Y., Woodgett, J.R. and Mills, G.B. (2002) Convergence of multiple signaling cascades at glycogen synthase kinase 3: Edg receptor-mediated phosphorylation and inactivation by lysophosphatidic acid through a protein kinase C-dependent intracellular pathway. *Mol Cell Biol*, **22**, 2099-110.
- Faure, M., Voyno-Yasenetskaya, T.A. and Bourne, H.R. (1994) cAMP and beta gamma subunits of heterotrimeric G proteins stimulate the mitogen-activated protein kinase pathway in COS-7 cells. *J Biol Chem*, **269**, 7851-4.
- Filardo, E.J., Quinn, J.A., Bland, K.I. and Frackelton, A.R., Jr. (2000) Estrogen-induced activation of Erk-1 and Erk-2 requires the G protein-coupled receptor homolog, GPR30, and occurs via trans-activation of the epidermal growth factor receptor through release of HB-EGF. *Mol Endocrinol*, **14**, 1649-60.
- Fishman, D.A., Liu, Y., Ellerbroek, S.M. and Stack, M.S. (2001) Lysophosphatidic acid promotes matrix metalloproteinase (MMP) activation and MMP-dependent invasion in ovarian cancer cells. *Cancer Res*, **61**, 3194-9.
- Fukuhara, S., Chikumi, H. and Gutkind, J.S. (2001) RGS-containing RhoGEFs: the missing link between transforming G proteins and Rho? *Oncogene*, **20**, 1661-8.
- Garrett, T., McKern, N., Lou, M., Elleman, T., Adams, T., Lovrecz, G., Zhu, H., Walker, F., Frenkel, M., Hoyne, P., Jorissen, R., Nice, E., Burgess, A. and Ward, C. (2002) Crystal Structure of a Truncated Epidermal Growth Factor Receptor Extracellular Domain Bound to Transforming Growth Factor alpha. *Cell*, **110**, 763-73.
- Gershoni, J.M. and Palade, G.E. (1982) Electrophoretic transfer of proteins from sodium dodecyl sulfate-polyacrylamide gels to a positively charged membrane filter. *Anal Biochem*, **124**, 396-405.
- Gether, U. and Kobilka, B.K. (1998) G protein-coupled receptors. II. Mechanism of agonist activation. *J Biol Chem*, **273**, 17979-82.
- Gohla, A., Harhammer, R. and Schultz, G. (1998) The G-protein G13 but not G12 mediates signaling from lysophosphatidic acid receptor via epidermal growth factor receptor to Rho. *J Biol Chem*, **273**, 4653-9.
- Gohla, A., Offermanns, S., Wilkie, T.M. and Schultz, G. (1999) Differential involvement of Galpha12 and Galpha13 in receptor-mediated stress fiber formation. *J Biol Chem*, **274**, 17901-7.

- Grandis, J.R., Melhem, M.F., Gooding, W.E., Day, R., Holst, V.A., Wagener, M.M., Drenning, S.D. and Twardy, D.J. (1998) Levels of TGF- $\alpha$  and EGFR protein in head and neck squamous cell carcinoma and patient survival. *J Natl Cancer Inst*, **90**, 824-32.
- Greenlee, R.T., Hill-Harmon, M.B., Murray, T. and Thun, M. (2001) Cancer statistics, 2001. *CA Cancer J Clin*, **51**, 15-36.
- Grosse, R., Roelle, S., Herrlich, A., Hohn, J. and Gudermann, T. (2000) Epidermal growth factor receptor tyrosine kinase mediates Ras activation by gonadotropin-releasing hormone. *J Biol Chem*, **275**, 12251-60.
- Gschwind, A., Zwick, E., Prenzel, N., Leserer, M. and Ullrich, A. (2001) Cell communication networks: epidermal growth factor receptor transactivation as the paradigm for interreceptor signal transmission. *Oncogene*, **20**, 1594-600.
- Gutkind, J.S. (2000) Regulation of mitogen-activated protein kinase signaling networks by G protein-coupled receptors. *Sci STKE*, **2000**, RE1.
- Hackel, P.O., Zwick, E., Prenzel, N. and Ullrich, A. (1999) Epidermal growth factor receptors: critical mediators of multiple receptor pathways. *Curr Opin Cell Biol*, **11**, 184-9.
- Hanahan, D. and Weinberg, R.A. (2000) The hallmarks of cancer. *Cell*, **100**, 57-70.
- Hartmann, D., de Strooper, B., Serneels, L., Craessaerts, K., Herreman, A., Annaert, W., Umans, L., Lubke, T., Lena Illert, A., von Figura, K. and Saftig, P. (2002) The disintegrin/metalloprotease ADAM 10 is essential for Notch signalling but not for alpha-secretase activity in fibroblasts. *Hum Mol Genet*, **11**, 2615-24.
- He, H., Levitzki, A., Zhu, H.J., Walker, F., Burgess, A. and Maruta, H. (2001) Platelet-derived growth factor requires epidermal growth factor receptor to activate p21-activated kinase family kinases. *J Biol Chem*, **276**, 26741-4.
- Herrlich, A., Daub, H., Knebel, A., Herrlich, P., Ullrich, A., Schultz, G. and Gudermann, T. (1998) Ligand-independent activation of platelet-derived growth factor receptor is a necessary intermediate in lysophosphatidic, acid-stimulated mitogenic activity in L cells. *Proc Natl Acad Sci U S A*, **95**, 8985-90.
- Hirata, M., Umata, T., Takahashi, T., Ohnuma, M., Miura, Y., Iwamoto, R. and Mekada, E. (2001) Identification of serum factor inducing ectodomain shedding of proHB-EGF and studies of noncleavable mutants of proHB-EGF. *Biochem Biophys Res Commun*, **283**, 915-22.
- Hooper, N.M. (1994) Families of zinc metalloproteases. *FEBS Lett*, **354**, 1-6.
- Hubbard, S.R. and Till, J.H. (2000) Protein tyrosine kinase structure and function. *Annu Rev Biochem*, **69**, 373-98.
- Hunter, T. (2000) Signaling 2000 and beyond. *Cell*, **100**, 113-27.

- Hurbin, A., Dubrez, L., Coll, J.L. and Favrot, M.C. (2002) Inhibition of apoptosis by Amphiregulin via an insulin-like growth factor-1 receptor dependent pathway in non-small cell lung cancer cell lines. *J Biol Chem*, **277**, 49127-33.
- Huyer, G., Liu, S., Kelly, J., Moffat, J., Payette, P., Kennedy, B., Tsaprailis, G., Gresser, M.J. and Ramachandran, C. (1997) Mechanism of inhibition of protein-tyrosine phosphatases by vanadate and pervanadate. *J Biol Chem*, **272**, 843-51.
- Imamura, F., Horai, T., Mukai, M., Shinkai, K., Sawada, M. and Akedo, H. (1993) Induction of in vitro tumor cell invasion of cellular monolayers by lysophosphatidic acid or phospholipase D. *Biochem Biophys Res Commun*, **193**, 497-503.
- Iwasaki, H., Eguchi, S., Ueno, H., Marumo, F. and Hirata, Y. (1999) Endothelin-mediated vascular growth requires p42/p44 mitogen-activated protein kinase and p70 S6 kinase cascades via transactivation of epidermal growth factor receptor. *Endocrinology*, **140**, 4659-68.
- Izumi, Y., Hirata, M., Hasuwa, H., Iwamoto, R., Umata, T., Miyado, K., Tamai, Y., Kurisaki, T., Sehara-Fujisawa, A., Ohno, S. and Mekada, E. (1998) A metalloprotease-disintegrin, MDC9/meltrin-gamma/ADAM9 and PKCdelta are involved in TPA-induced ectodomain shedding of membrane-anchored heparin-binding EGF-like growth factor. *Embo J*, **17**, 7260-72.
- Ji, T.H., Grossmann, M. and Ji, I. (1998) G protein-coupled receptors. I. Diversity of receptor-ligand interactions. *J Biol Chem*, **273**, 17299-302.
- Johnson, G.R., Saeki, T., Gordon, A.W., Shoyab, M., Salomon, D.S. and Stromberg, K. (1992) Autocrine action of amphiregulin in a colon carcinoma cell line and immunocytochemical localization of amphiregulin in human colon. *J Cell Biol*, **118**, 741-51.
- Kalmes, A., Vesti, B.R., Daum, G., Abraham, J.A. and Clowes, A.W. (2000) Heparin blockade of thrombin-induced smooth muscle cell migration involves inhibition of epidermal growth factor (EGF) receptor transactivation by heparin-binding EGF-like growth factor. *Circ Res*, **87**, 92-8.
- Keely, S.J., Calandrella, S.O. and Barrett, K.E. (2000) Carbachol-stimulated transactivation of epidermal growth factor receptor and mitogen-activated protein kinase in T(84) cells is mediated by intracellular  $Ca^{2+}$ , PYK-2, and p60(src). *J Biol Chem*, **275**, 12619-25.
- Keely, S.J., Uribe, J.M. and Barrett, K.E. (1998) Carbachol stimulates transactivation of epidermal growth factor receptor and mitogen-activated protein kinase in T84 cells. Implications for carbachol-stimulated chloride secretion. *J Biol Chem*, **273**, 27111-7.
- Kersemaekers, A.M., Fleuren, G.J., Kenter, G.G., Van den Broek, L.J., Uljee, S.M., Hermans, J. and Van de Vijver, M.J. (1999) Oncogene alterations in carcinomas of the uterine cervix: overexpression of the epidermal growth factor receptor is associated with poor prognosis. *Clin Cancer Res*, **5**, 577-86.

- Kim, S.N., Park, J.G., Lee, E.B., Kim, S.S. and Yoo, Y.S. (2000) Characterization of epidermal growth factor receptor function in lysophosphatidic acid signaling in PC12 cells. *J Cell Biochem*, **76**, 386-93.
- Kleiner, D.E. and Stetler-Stevenson, W.G. (1994) Quantitative zymography: detection of picogram quantities of gelatinases. *Anal Biochem*, **218**, 325-9.
- Kranenburg, O. and Moolenaar, W.H. (2001) Ras-MAP kinase signaling by lysophosphatidic acid and other G protein-coupled receptor agonists. *Oncogene*, **20**, 1540-6.
- Krieg, T., Qin, Q., McIntosh, E.C., Cohen, M.V. and Downey, J.M. (2002) Acetylcholine and Adenosine Activate PI3-Kinase in Rabbit Hearts Through Transactivation of Receptor Tyrosine Kinases. *Am J Physiol Heart Circ Physiol*, **283**, H2322-30.
- Kunkel, T.A. (1985) Rapid and efficient site-specific mutagenesis without phenotypic selection. *Proc Natl Acad Sci U S A*, **82**, 488-92.
- Lee, S.Y. and Rasheed, S. (1990) A simple procedure for maximum yield of high-quality plasmid DNA. *Biotechniques*, **9**, 676-9.
- Lemjabbar, H. and Basbaum, C. (2002) Platelet-activating factor receptor and ADAM10 mediate responses to Staphylococcus aureus in epithelial cells. *Nat Med*, **8**, 41-6.
- Lemmon, M.A., Bu, Z., Ladbury, J.E., Zhou, M., Pinchasi, D., Lax, I., Engelman, D.M. and Schlessinger, J. (1997) Two EGF molecules contribute additively to stabilization of the EGFR dimer. *Embo J*, **16**, 281-94.
- Li, S., Plowman, G.D., Buckley, S.D. and Shipley, G.D. (1992) Heparin inhibition of autonomous growth implicates amphiregulin as an autocrine growth factor for normal human mammary epithelial cells. *J Cell Physiol*, **153**, 103-11.
- Liu, Y., Gilcrease, M.Z., Henderson, Y., Yuan, X.H., Clayman, G.L. and Chen, Z. (2001) Expression of protease-activated receptor 1 in oral squamous cell carcinoma. *Cancer Lett*, **169**, 173-80.
- Luttrell, L.M., Daaka, Y. and Lefkowitz, R.J. (1999a) Regulation of tyrosine kinase cascades by G-protein-coupled receptors. *Curr Opin Cell Biol*, **11**, 177-83.
- Luttrell, L.M., Della Rocca, G.J., van Biesen, T., Luttrell, D.K. and Lefkowitz, R.J. (1997) Gbetagamma subunits mediate Src-dependent phosphorylation of the epidermal growth factor receptor. A scaffold for G protein-coupled receptor-mediated Ras activation. *J Biol Chem*, **272**, 4637-44.
- Luttrell, L.M., Ferguson, S.S., Daaka, Y., Miller, W.E., Maudsley, S., Della Rocca, G.J., Lin, F., Kawakatsu, H., Owada, K., Luttrell, D.K., Caron, M.G. and Lefkowitz, R.J. (1999b) Beta-arrestin-dependent formation of beta2 adrenergic receptor-Src protein kinase complexes. *Science*, **283**, 655-61.
- Marinissen, M.J. and Gutkind, J.S. (2001) G-protein-coupled receptors and signaling networks: emerging paradigms. *Trends Pharmacol Sci*, **22**, 368-76.

- Massague, J. and Pandiella, A. (1993) Membrane-anchored growth factors. *Annu Rev Biochem*, **62**, 515-41.
- Mateo, C., Moreno, E., Amour, K., Lombardero, J., Harris, W. and Perez, R. (1997) Humanization of a mouse monoclonal antibody that blocks the epidermal growth factor receptor: recovery of antagonistic activity. *Immunotechnology*, **3**, 71-81.
- Maudsley, S., Pierce, K.L., Zamah, A.M., Miller, W.E., Ahn, S., Daaka, Y., Lefkowitz, R.J. and Luttrell, L.M. (2000) The beta(2)-adrenergic receptor mediates extracellular signal-regulated kinase activation via assembly of a multi-receptor complex with the epidermal growth factor receptor. *J Biol Chem*, **275**, 9572-80.
- McCole, D.F., Keely, S.J., Coffey, R.J. and Barrett, K.E. (2002) Transactivation of the epidermal growth factor receptor in colonic epithelial cells by carbachol requires extracellular release of transforming growth factor-alpha. *J Biol Chem*, **277**, 42603-12.
- Merlos-Suarez, A., Ruiz-Paz, S., Baselga, J. and Arribas, J. (2001) Metalloprotease-dependent protransforming growth factor-alpha ectodomain shedding in the absence of tumor necrosis factor-alpha-converting enzyme. *J Biol Chem*, **276**, 48510-7.
- Messing, J. (1983) New M13 vectors for cloning. *Methods Enzymol*, **101**, 20-78.
- Moolenaar, W.H. (1999) Bioactive lysophospholipids and their G protein-coupled receptors. *Exp Cell Res*, **253**, 230-8.
- Moolenaar, W.H., Kranenburg, O., Postma, F.R. and Zondag, G.C. (1997) Lysophosphatidic acid: G-protein signalling and cellular responses. *Curr Opin Cell Biol*, **9**, 168-73.
- Moss, M.L., Jin, S.L., Milla, M.E., Bickett, D.M., Burkhart, W., Carter, H.L., Chen, W.J., Clay, W.C., Didsbury, J.R., Hassler, D., Hoffman, C.R., Kost, T.A., Lambert, M.H., Leesnitzer, M.A., McCauley, P., McGeehan, G., Mitchell, J., Moyer, M., Pahel, G., Rocque, W., Overton, L.K., Schoenen, F., Seaton, T., Su, J.L., Becherer, J.D. and et al. (1997) Cloning of a disintegrin metalloproteinase that processes precursor tumour-necrosis factor-alpha. *Nature*, **385**, 733-6.
- Mullis, K.B. and Faloona, F.A. (1987) Specific synthesis of DNA in vitro via a polymerase-catalyzed chain reaction. *Methods Enzymol*, **155**, 335-50.
- Murasawa, S., Mori, Y., Nozawa, Y., Gotoh, N., Shibuya, M., Masaki, H., Maruyama, K., Tsutsumi, Y., Moriguchi, Y., Shibasaki, Y., Tanaka, Y., Iwasaka, T., Inada, M. and Matsubara, H. (1998) Angiotensin II type 1 receptor-induced extracellular signal-regulated protein kinase activation is mediated by Ca<sup>2+</sup>/calmodulin-dependent transactivation of epidermal growth factor receptor. *Circ Res*, **82**, 1338-48.
- Nagase, H. and Woessner, J.F., Jr. (1999) Matrix metalloproteinases. *J Biol Chem*, **274**, 21491-4.
- Normanno, N., Selvam, M.P., Qi, C.F., Saeki, T., Johnson, G., Kim, N., Ciardiello, F., Shoyab, M., Plowman, G., Brandt, R. and et al. (1994) Amphiregulin as an autocrine growth factor for c-Ha-ras- and c-erbB-2-transformed human mammary epithelial cells. *Proc Natl Acad Sci U S A*, **91**, 2790-4.

- O-Charoenrat, P., Modjtahedi, H., Rhys-Evans, P., Court, W.J., Box, G.M. and Eccles, S.A. (2000a) Epidermal growth factor-like ligands differentially up-regulate matrix metalloproteinase 9 in head and neck squamous carcinoma cells. *Cancer Res*, **60**, 1121-8.
- O-Charoenrat, P., Rhys-Evans, P. and Eccles, S. (2000b) Expression and regulation of c-ERBB ligands in human head and neck squamous carcinoma cells. *Int J Cancer*, **88**, 759-65.
- O-Charoenrat, P., Rhys-Evans, P., Modjtahedi, H., Court, W., Box, G. and Eccles, S. (2000c) Overexpression of epidermal growth factor receptor in human head and neck squamous carcinoma cell lines correlates with matrix metalloproteinase-9 expression and in vitro invasion. *Int J Cancer*, **86**, 307-17
- O-Charoenrat, P., Rhys-Evans, P. and Eccles, S. (2002) A synthetic matrix metalloproteinase inhibitor prevents squamous carcinoma cell proliferation by interfering with epidermal growth factor receptor autocrine loops. *Int J Cancer*, **100**, 527-33.
- Ogiso, H., Ishitani, R., Nureki, O., Fukai, S., Yamanaka, M., Kim, J., Saito, K., Sakamoto, A., Inoue, M., Shirouzu, M. and Yokoyama, S. (2002) Crystal structure of the complex of human epidermal growth factor and receptor extracellular domains. *Cell*, **110**, 775-87.
- Olayioye, M.A., Neve, R.M., Lane, H.A. and Hynes, N.E. (2000) The ErbB signaling network: receptor heterodimerization in development and cancer. *Embo J*, **19**, 3159-67.
- Pai, R., Soreghan, B., Szabo, I.L., Pavelka, M., Baatar, D. and Tarnawski, A.S. (2002) Prostaglandin E2 transactivates EGF receptor: A novel mechanism for promoting colon cancer growth and gastrointestinal hypertrophy. *Nat Med*, **8**, 289-93.
- Pear, W.S., Nolan, G.P., Scott, M.L. and Baltimore, D. (1993) Production of high-titer helper-free retroviruses by transient transfection. *Proc Natl Acad Sci U S A*, **90**, 8392-6.
- Peschon, J.J., Slack, J.L., Reddy, P., Stocking, K.L., Sunnarborg, S.W., Lee, D.C., Russell, W.E., Castner, B.J., Johnson, R.S., Fitzner, J.N., Boyce, R.W., Nelson, N., Kozlosky, C.J., Wolfson, M.F., Rauch, C.T., Cerretti, D.P., Paxton, R.J., March, C.J. and Black, R.A. (1998) An essential role for ectodomain shedding in mammalian development. *Science*, **282**, 1281-4.
- Pierce, K.L., Tohgo, A., Ahn, S., Field, M.E., Luttrell, L.M. and Lefkowitz, R.J. (2001) Epidermal growth factor (EGF) receptor-dependent ERK activation by G protein-coupled receptors: a co-culture system for identifying intermediates upstream and downstream of heparin-binding EGF shedding. *J Biol Chem*, **276**, 23155-60.
- Plowman, G.D., Green, J.M., McDonald, V.L., Neubauer, M.G., Disteché, C.M., Todaro, G.J. and Shoyab, M. (1990) The amphiregulin gene encodes a novel epidermal growth factor-related protein with tumor-inhibitory activity. *Mol Cell Biol*, **10**, 1969-81.

- Prenzel, N., Fischer, O.M., Streit, S., Hart, S. and Ullrich, A. (2001) The epidermal growth factor receptor family as a central element for cellular signal transduction and diversification. *Endocr Relat Cancer*, **8**, 11-31.
- Prenzel, N., Zwick, E., Daub, H., Leserer, M., Abraham, R., Wallasch, C. and Ullrich, A. (1999) EGF receptor transactivation by G-protein-coupled receptors requires metalloproteinase cleavage of proHB-EGF. *Nature*, **402**, 884-8.
- Primakoff, P. and Myles, D.G. (2000) The ADAM gene family: surface proteins with adhesion and protease activity. *Trends Genet*, **16**, 83-7.
- Pyne, S. and Pyne, N.J. (2000) Sphingosine 1-phosphate signalling in mammalian cells. *Biochem J*, **349**, 385-402.
- Quon, H., Liu, F.F. and Cummings, B.J. (2001) Potential molecular prognostic markers in head and neck squamous cell carcinomas. *Head Neck*, **23**, 147-59.
- Reddy, P., Slack, J.L., Davis, R., Cerretti, D.P., Kozlosky, C.J., Blanton, R.A., Shows, D., Peschon, J.J. and Black, R.A. (2000) Functional analysis of the domain structure of tumor necrosis factor-alpha converting enzyme. *J Biol Chem*, **275**, 14608-14.
- Riese, D.J., 2nd and Stern, D.F. (1998) Specificity within the EGF family/ErbB receptor family signaling network. *Bioessays*, **20**, 41-8.
- Rusch, V., Klimstra, D., Linkov, I. and Dmitrovsky, E. (1995) Aberrant expression of p53 or the epidermal growth factor receptor is frequent in early bronchial neoplasia and coexpression precedes squamous cell carcinoma development. *Cancer Res*, **55**, 1365-72.
- Salomon, D.S., Bianco, C. and De Santis, M. (1999) Cripto: a novel epidermal growth factor (EGF)-related peptide in mammary gland development and neoplasia. *Bioessays*, **21**, 61-70.
- Sambrook, J., Fritsch, E.F. und Maniatis, T. (1990) Molecular cloning: a laboratory manual. *Cold Spring Harbor Laboratory Press, New York, USA*.
- Santiskulvong, C., Sinnott-Smith, J. and Rozengurt, E. (2001) EGF receptor function is required in late G(1) for cell cycle progression induced by bombesin and bradykinin. *Am J Physiol Cell Physiol*, **281**, C886-98.
- Sautin, Y.Y., Crawford, J.M. and Svetlov, S.I. (2001) Enhancement of survival by LPA via Erk1/Erk2 and PI 3-kinase/Akt pathways in a murine hepatocyte cell line. *Am J Physiol Cell Physiol*, **281**, C2010-9.
- Schagger, H. and von Jagow, G. (1987) Tricine-sodium dodecyl sulfate-polyacrylamide gel electrophoresis for the separation of proteins in the range from 1 to 100 kDa. *Anal Biochem*, **166**, 368-79.
- Schelfhout, V.R., Coene, E.D., Delaey, B., Waeytens, A.A., De Rycke, L., Deleu, M. and De Potter, C.R. (2002) The role of heregulin-alpha as a motility factor and amphiregulin as a growth factor in wound healing. *J Pathol*, **198**, 523-533.

- Schlessinger, J. (2000) Cell signaling by receptor tyrosine kinases. *Cell*, **103**, 211-25.
- Schlessinger, J. (2002) Ligand-induced, receptor-mediated dimerization and activation of EGF receptor. *Cell*, **110**, 669-72.
- Schlondorff, J. and Blobel, C.P. (1999) Metalloprotease-disintegrins: modular proteins capable of promoting cell-cell interactions and triggering signals by protein-ectodomain shedding. *J Cell Sci*, **112**, 3603-17.
- Shapiro, S.D. (1998) Matrix metalloproteinase degradation of extracellular matrix: biological consequences. *Curr Opin Cell Biol*, **10**, 602-8.
- Shawver, L.K., Slamon, D. and Ullrich, A. (2002) Smart drugs: tyrosine kinase inhibitors in cancer therapy. *Cancer Cell*, **1**, 117-23.
- Shiga, H., Rasmussen, A.A., Johnston, P.G., Langmacher, M., Baylor, A., Lee, M. and Cullen, K.J. (2000) Prognostic value of c-erbB2 and other markers in patients treated with chemotherapy for recurrent head and neck cancer. *Head Neck*, **22**, 599-608.
- Shin, D.M., Donato, N.J., Perez-Soler, R., Shin, H.J., Wu, J.Y., Zhang, P., Lawhorn, K., Khuri, F.R., Glisson, B.S., Myers, J., Clayman, G., Pfister, D., Falcey, J., Waksal, H., Mendelsohn, J. and Hong, W.K. (2001) Epidermal growth factor receptor-targeted therapy with C225 and cisplatin in patients with head and neck cancer. *Clin Cancer Res*, **7**, 1204-13.
- Slack, B.E. (2000) The m3 muscarinic acetylcholine receptor is coupled to mitogen-activated protein kinase via protein kinase C and epidermal growth factor receptor kinase. *Biochem J*, **348**, 381-7.
- Solomon, K.A., Pesti, N., Wu, G. and Newton, R.C. (1999) Cutting edge: a dominant negative form of TNF-alpha converting enzyme inhibits proTNF and TNFRII secretion. *J Immunol*, **163**, 4105-8.
- Soltoff, S.P. (1998) Related adhesion focal tyrosine kinase and the epidermal growth factor receptor mediate the stimulation of mitogen-activated protein kinase by the G-protein-coupled P2Y2 receptor. Phorbol ester or [Ca<sup>2+</sup>]<sub>i</sub> elevation can substitute for receptor activation. *J Biol Chem*, **273**, 23110-7.
- Stocker, W. and Bode, W. (1995) Structural features of a superfamily of zinc-endopeptidases: the metzincins. *Curr Opin Struct Biol*, **5**, 383-90.
- Strachan, L., Murison, J.G., Prestidge, R.L., Sleeman, M.A., Watson, J.D. and Kumble, K.D. (2001) Cloning and biological activity of epigen, a novel member of the epidermal growth factor superfamily. *J Biol Chem*, **276**, 18265-71.
- Sunnarborg, S.W., Hinkle, C.L., Stevenson, M., Russell, W.E., Raska, C.S., Peschon, J.J., Castner, B.J., Gerhart, M.J., Paxton, R.J., Black, R.A. and Lee, D.C. (2002) Tumor necrosis factor-alpha converting enzyme (TACE) regulates epidermal growth factor receptor ligand availability. *J Biol Chem*, **277**, 12838-45.

- Tokumaru, S., Higashiyama, S., Endo, T., Nakagawa, T., Miyagawa, J.I., Yamamori, K., Hanakawa, Y., Ohmoto, H., Yoshino, K., Shirakata, Y., Matsuzawa, Y., Hashimoto, K. and Taniguchi, N. (2000) Ectodomain shedding of epidermal growth factor receptor ligands is required for keratinocyte migration in cutaneous wound healing. *J Cell Biol*, **151**, 209-20.
- Touyz, R.M., Wu, X.H., He, G., Salomon, S. and Schiffrin, E.L. (2002) Increased angiotensin II-mediated Src signaling via epidermal growth factor receptor transactivation is associated with decreased C-terminal Src kinase activity in vascular smooth muscle cells from spontaneously hypertensive rats. *Hypertension*, **39**, 479-85.
- Tsai, W., Morielli, A.D. and Peralta, E.G. (1997) The m1 muscarinic acetylcholine receptor transactivates the EGF receptor to modulate ion channel activity. *Embo J*, **16**, 4597-605.
- Ullrich, A. and Schlessinger, J. (1990) Signal transduction by receptors with tyrosine kinase activity. *Cell*, **61**, 203-12.
- Umata, T., Hirata, M., Takahashi, T., Ryu, F., Shida, S., Takahashi, Y., Tsuneoka, M., Miura, Y., Masuda, M., Horiguchi, Y. and Mekada, E. (2001) A dual signaling cascade that regulates the ectodomain shedding of heparin-binding epidermal growth factor-like growth factor. *J Biol Chem*, **276**, 30475-82.
- van Corven, E.J., Groenink, A., Jalink, K., Eichholtz, T. and Moolenaar, W.H. (1989) Lysophosphatidate-induced cell proliferation: identification and dissection of signaling pathways mediated by G proteins. *Cell*, **59**, 45-54.
- Venkatakrishnan, G., Salgia, R. and Groopman, J.E. (2000) Chemokine receptors CXCR-1/2 activate mitogen-activated protein kinase via the epidermal growth factor receptor in ovarian cancer cells. *J Biol Chem*, **275**, 6868-75.
- Weiss, F.U., Daub, H. and Ullrich, A. (1997) Novel mechanisms of RTK signal generation. *Curr Opin Genet Dev*, **7**, 80-6.
- Werb, Z. and Yan, Y. (1998) A cellular striptease act. *Science*, **282**, 1279-80.
- Weskamp, G., Cai, H., Brodie, T.A., Higashiyama, S., Manova, K., Ludwig, T. and Blobel, C.P. (2002) Mice lacking the metalloprotease-disintegrin MDC9 (ADAM9) have no evident major abnormalities during development or adult life. *Mol Cell Biol*, **22**, 1537-44.
- Wolfsberg, T.G., Primakoff, P., Myles, D.G. and White, J.M. (1995) ADAM, a novel family of membrane proteins containing A Disintegrin And Metalloprotease domain: multipotential functions in cell-cell and cell-matrix interactions. *J Cell Biol*, **131**, 275-8.
- Wong, S.T., Winchell, L.F., McCune, B.K., Earp, H.S., Teixido, J., Massague, J., Herman, B. and Lee, D.C. (1989) The TGF-alpha precursor expressed on the cell surface binds to the EGF receptor on adjacent cells, leading to signal transduction. *Cell*, **56**, 495-506.

- Wu, Y., Palad, A.J., Wasilenko, W.J., Blackmore, P.F., Pincus, W.A., Schechter, G.L., Spoonster, J.R., Kohn, E.C. and Somers, K.D. (1997) Inhibition of head and neck squamous cell carcinoma growth and invasion by the calcium influx inhibitor carboxyamido-triazole. *Clin Cancer Res*, **3**, 1915-21.
- Xu, Y., Gaudette, D.C., Boynton, J.D., Frankel, A., Fang, X.J., Sharma, A., Hurteau, J., Casey, G., Goodbody, A., Mellors, A. and et al. (1995) Characterization of an ovarian cancer activating factor in ascites from ovarian cancer patients. *Clin Cancer Res*, **1**, 1223-32.
- Xu, Y., Shen, Z., Wiper, D.W., Wu, M., Morton, R.E., Elson, P., Kennedy, A.W., Belinson, J., Markman, M. and Casey, G. (1998) Lysophosphatidic acid as a potential biomarker for ovarian and other gynecologic cancers. *Jama*, **280**, 719-23.
- Yan, Y., Shirakabe, K. and Werb, Z. (2002) The metalloprotease Kuzbanian (ADAM10) mediates the transactivation of EGF receptor by G protein-coupled receptors. *J Cell Biol*, **158**, 221-6.
- Yarden, Y. and Sliwkowski, M.X. (2001) Untangling the ErbB signalling network. *Nat Rev Mol Cell Biol*, **2**, 127-37.
- Yart, A., Roche, S., Wetzker, R., Laffargue, M., Tonks, N.K., Mayeux, P., Chap, H. and Raynal, P. (2002) A function for phosphoinositide 3-kinase beta lipid products in coupling beta gamma to Ras activation in response to lysophosphatidic acid. *J Biol Chem*, **277**, 21167-78.
- Zwick, E., Bange, J. and Ullrich, A. (2001) Receptor tyrosine kinase signalling as a target for cancer intervention strategies. *Endocr Relat Cancer*, **8**, 161-73.
- Zwick, E., Daub, H., Aoki, N., Yamaguchi-Aoki, Y., Tinhofer, I., Maly, K. and Ullrich, A. (1997) Critical role of calcium- dependent epidermal growth factor receptor transactivation in PC12 cell membrane depolarization and bradykinin signaling. *J Biol Chem*, **272**, 24767-70.
- Zwick, E., Hackel, P.O., Prenzel, N. and Ullrich, A. (1999a) The EGF receptor as central transducer of heterologous signalling systems. *Trends Pharmacol Sci*, **20**, 408-12.
- Zwick, E., Wallasch, C., Daub, H. and Ullrich, A. (1999b) Distinct calcium-dependent pathways of epidermal growth factor receptor transactivation and PYK2 tyrosine phosphorylation in PC12 cells. *J Biol Chem*, **274**, 20989-96.

## Publications

Leserer, M., Gschwind, A. and Ullrich, A. (2000) Epidermal growth factor receptor signal transactivation. *IUBMB Life*, **49**, 405-9.

Gschwind, A., Zwick, E., Prenzel, N., Leserer, M. and Ullrich, A. (2001) Cell communication networks: epidermal growth factor receptor transactivation as the paradigm for interreceptor signal transmission. *Oncogene*, **20**, 1594-600.

Gschwind, A., Prenzel, N. and Ullrich, A. (2002) Lysophosphatidic Acid-induced Squamous Cell Carcinoma Cell Proliferation and Motility Involves Epidermal Growth Factor Receptor Signal Transactivation. *Cancer Res*, **62**, 6329-6336.

Hart, S., Gschwind, A., Roidl, A. and Ullrich, A. (2003) Transactivation of the Epidermal Growth Factor Receptor by G Protein-Coupled Receptors. *NATO LIFE SCIENCE BOOK SERIES. Kluwer Academic/Plenum Publishers. In press.*

Gschwind, A., Hart, S., Fischer, O. M. and Ullrich, A. (2003) TACE Cleavage of Proamphiregulin Regulates GPCR-induced Proliferation and Motility of Cancer Cells. *Embo J. In press.*

## Poster Presentations

Leserer, M., Gschwind, A., Prenzel, N., Zwick, E. and Ullrich, A. Metalloprotease-Mediated Epidermal Growth Factor Receptor Signal Transactivation. Gordon Research Conference: Proteolytic Enzymes and Inhibitors. Colby Sawyer College, New London, NH, USA. July 9-14, 2000.

Leserer, M., Gschwind, A. and Ullrich, A. Metalloprotease-Mediated Epidermal Growth Factor Receptor Signal Transactivation. 2. Münchner Studentenkongress für Biowissenschaften – BioLog. Munich, 2000.

Gschwind, A., Prenzel, N., Zwick, E., Gensler, M., Hart, S. and Ullrich, A. Epidermal Growth Factor Receptor Transactivation by G Protein-Coupled Receptors Requires Metalloprotease-Mediated Growth Factor Precursor Cleavage. (2000). Fall Meeting of the German Society of Biochemistry and Molecular Biology (GBM). Munich, October 10-13, 2000.

## Patent Applications

EP 02005452, Prof. A. Ullrich, A. Gschwind, B. Schäfer, M. Leserer, O. Fischer, Use of EGFR transactivation inhibitors in human cancer.

Prof. A. Ullrich, A. Gschwind, S. Hart, EGF Receptor Signal Transactivation in Squamous Cell Carcinoma Requires Proamphiregulin Cleavage by TACE/ADAM17.

## 7 ABBREVIATIONS

AA	Amino acid
Ab	Antibody
ADAM	A disintegrin and metalloprotease domain
Amp <sup>r</sup>	Ampicilline resistance
APS	Ammoniumpersulfate
AR	Amphiregulin
ATP	Adenosintriphosphate
bp	Base pairs
BSA	Bovine serum albumin
°C	Degree celsius
cAMP	Cyclic adenosinmonophosphate
Ca <sup>2+</sup>	Calcium Ions
CaM Kinase	Ca <sup>2+</sup> -calmodulin-dependent kinase
cDNA	Complementary DNA
c-fos	Cellular homologue to v-fos ( <u>FBJ</u> murine osteosarcoma viral oncogene)
c-jun	Cellular homologue to v-jun (avian sarcoma virus 17 oncogene)
DAG	Diacylglycerol
DMEM	Dulbecco's modified eagle medium
DN	Dominant negative
DMSO	Dimethylsulfoxide
DNA	Desoxyribonukleic acid
dsDNA	Dooble-stranded DNA
DTT	Dithiothreitol
ECL	Enhanced chemiluminescence
EDTA	Ethlendiamintetraacetate
EGF	Epidermal growth factor
EGFR	Epidermal growth factor receptor
EGTA	<u>E</u> thylene glycol-bis(2-aminoethyl)- <u>N,N,N',N'</u> - <u>t</u> etra <u>a</u> cetic acid
ERK	Extracellular signal-regulated kinase
FAK	Focal adhesion kinase
FCS	Fetal calf serum
FGF	Fibroblast growth factor
FGFR	Fibroblast growth factor receptor
Fig	Figure
g	Gramm
Gab1	Grb2-associated binder-1
Gab2	Grb2-associated binder-2
GDP	Guanosindiphosphate
GPCR	G protein-coupled receptor
Grb2	Growth factor receptor binding protein 2
GST	Glutathion-S-transferase
GTP	Guanosintriphosphate
h	Hour
HA	Hemagglutinin
HB-EGF	Heparin-binding EGF-like growth factor
H <sub>2</sub> O <sub>bidest</sub>	Twice-distilled, deionised Water

HEPES	N-(2-Hydroxyethyl)-piperazin-N'-2-Ethansulfonic acid
HER	Human EGFR-related
HNSCC	Head and neck squamous cell carcinoma
Ig	Immunglobulin
IP	Immunoprecipitation
IP <sub>3</sub>	Inositol-1,4,5-trisphosphate
IPTG	Isopropyl-β-thiogalactopyranoside
JNK	c-Jun N-terminal kinase
kb	Kilobase
kDa	Kilodalton
l	Liter
LPA	Lysophosphatidic acid
μ	Micro
m	Milli
M	Molar
MAP	Mitogen-activated protein
MAPK	MAP kinase
MBP	Myelin basic protein
MEK	MAPK/ERK Kinase
min	Minute
MMP	Matrix metalloprotease
n	Nano
OD	Optical density
p.a.	Per analysis
PBS	Phosphate-buffered saline
PCR	Polymerase chain reaction
PDGF	Platelet-derived growth factor
PEG	Polyethylenglycole
PI 3-Kinase	Phosphatidylinositol 3-kinase
PIP <sub>2</sub>	Phosphatidylinositol-4,5-diphosphate
PKC	Protein kinase C
PLC	Phospholipase C
PMSF	Phenylmethylsulfonyl-fluoride
PNPP	p-Nitrophenyl-phosphate
PTX	Pertussis toxin
PY	Phospho-tyrosine
Raf	Homologue to v-raf (murine sarcoma viral oncogene)
Ras	Homologue to v-ras (rat sarcoma viral oncogene)
RNA	Ribonucleic acid
rpm	Rotations per minute
RT	Room temperature
RTK	Receptor tyrosine kinase
SAPK	Stress-activated protein kinase
S. D.	Standard deviation
SDS	Natriumdodecylsulfate
SDS-PAGE	SDS polyacrylamide gel elektrophoresis
Sek.	Second
SH2, 3 domain	Src homology 2, 3 domain
SHP-2	SH2-containing PTP-2

---

Sos	Son of sevenless
Src	Homologue to v-src (sarcoma viral oncogene)
TACE	TNF $\alpha$ -converting enzyme
TCA	<u>Trichloroacetic acid</u>
TGF $\alpha$	Transforming growth factor alpha
TEMED	N, N, N', N'-Tetramethylethylenediamine
TNF $\alpha$	Tumor necrosis factor alpha
TPA	12-O-Tetradecanoyl-phorbol-13-acetate
Tris	Tris(hydroxymethyl)aminomethan
Tween 20	Polyoxyethylensorbitanmonolaureate
U	Enzymatic activity unit
O/N	Overnight
UV	Ultraviolett
V	Volt
Vol	Volume
Wt	Wild type

## **Acknowledgements**

I am especially grateful to my mentor Prof. Dr. Axel Ullrich for accompanying this project with his scientific interest and support, for helpful discussions, for his patience and endurance when reviewing manuscripts of mine and his generous help with post-doc applications.

I am indebted to Prof. Dr. Horst Domdey for supervising and promoting this doctoral thesis at the Ludwig-Maximilian-Universität München.

I further want to thank the former and present members of our “transactivation group” Esther, Henrik, Norbert, Stefan, Oliver, Michael, Beatrix and Beatrice for excellent collaboration and numerous helpful discussions.

I am grateful to the encouragement, help and friendship given me by my fellow PhD students and lab colleagues Marc, Alex, Jan, Andreas R., Andreas W., Markus, Hans-Jürgen, Anja, Sylvia, Miriam, Lars, Christiane, Jochen, Marta and last but not least Anil. You all filled our scientific every-day life with joy and fun!

I appreciate the critical discussions and comments about this project by Dr. I. Sures and Prof. Dr. L. Hennighausen.

I am thankful to T. Knyazeva for cDNA and to Dr. R. Abraham for his advice with cDNA arrays. I thank Dr. R. Black (Immunex, Inc.) and his laboratory staff for their pioneering collaboration.

Finally, I especially want to thank my sister Sabine and family for being a source of friendship and recreation in all these years.

# CURRICULUM VITAE

## Andreas Gschwind

Birthdate: November 22, 1972  
Birthplace: Straubing  
Citizenship: German  
Address: Passauer Str. 35, D-81369 Munich

## Education

May, 1999- Ph.D. Research  
Max-Planck Institute of Biochemistry  
Department of Molecular Biology  
Laboratory of Prof. Dr. A. Ullrich

1994-1999 Diploma, Biochemistry, 1999  
University of Regensburg  
Lehrstuhl für Biochemie I (Prof. Dr. M. Sumper)  
Thesis title:  
Cell cycle-dependent phosphorylation of  
kinetochor proteins  
Laboratory of Prof. Dr. J. Lechner

1993-1994 Civilian Service  
at Klinikum St. Elisabeth, Straubing

1992 Abitur  
Ludwigsgymnasium, Straubing

## Teaching

2000- Dipoma Student Advisor, MPI of Biochemistry